MODELING LEACHATE BOD AND COD USING LAB-SCALE REACTOR LANDFILLS AND MULTIPLE LINEAR REGRESSION ANALYSIS

by

SAID ALTOUQI

Presented to the Faculty of the Graduate School of

The University of Texas at Arlington in Partial Fulfillment

of the Requirements

for the Degree of

DOCTOR OF PHILOSOPHY

THE UNIVERSITY OF TEXAS AT ARLINGTON

December 2012

In Memory of My Father..

To My Mother..

Acknowledgements

I thank Allah for giving me the patience and the strength to finish this dissertation.

I would like to thank Dr. Melanie Sattler, my supervisor, for giving me the great opportunity to join this research project and for her unlimited support since my first day at UT Arlington. I would also like to thank Dr. Sahadat Hossain, Dr. Victoria Chen, and the rest of my committee members for their generous contributions in this study. I am also very grateful to my project partners, Dr. Richa Karanjekar and Arpita Bhatt, for their enormous dedication to this project and for their continuous support.

November 07, 2012

Abstract

MODELING LEACHATE BOD AND COD USING LAB-SCALE REACTOR LANDFILLS

AND MULTIPLE LINEAR REGRESSION ANALYSIS

Said Altouqi, Ph.D.

The University of Texas at Arlington, 2012

Supervising Professors: Melanie Sattler and Sahadat Hossain

The increasing production of municipal solid waste is a direct consequence of the continuous growth of the world's population and economy. This fact makes protecting the environment against contamination by different kinds of waste a challenging job for engineers and decision makers. Conventional landfilling practices have sometimes failed to protect fresh water resources against leachate contamination as well as the atmosphere against greenhouse gases such as carbon dioxide and methane. Many developed countries have already taken serious steps toward moving to properly engineered, environmental friendly landfills.

Landfill leachate contains organic and inorganic pollutants that have been extensively studied in the last four decades. Biochemical oxygen demand (BOD) and chemical oxygen demand (COD) are the most widely used indicators of leachate organic pollution. These two parameters are monitored regularly during the process of leachate treatment. They can also be used to recognize the solid waste stabilization stage in landfills. Understanding the behavior of BOD and COD throughout the life of a landfill via mathematical models would help in predicting the future extent of leachate organic pollution and, hence, the most efficient way of operating the leachate treatment facility. The main objective of this study was to develop two mathematical relationships for calculating the exponential decay rate constants (k values) for leachate BOD and COD in terms of rainfall rate, temperature and waste composition.

Twenty-seven lab-scale anaerobic reactor landfills were designed and operated under three temperatures (70, 85, and 100 °F) and three rainfall rates (2, 6, and 12 mm/day). The reactors were filled with various proportions of five waste components: food, paper, yard, textile, and inert inorganics. The range of temperatures and rainfall rates were chosen to include average rates for most locations worldwide, with the exception of deserts. Leachate was collected from these reactors and analyzed for BOD and COD content on a biweekly basis. The two models were developed using multiple linear regression analysis.

The peak BOD concentrations in all the reactors ranged between 856 and 46,134 mg/L and peak COD concentrations were between 2,458 and 64,032 mg/L. Leachate from the 85 °F reactors showed higher BOD and COD content than other reactors with the same waste composition but different temperatures. The 2-mm/day reactors showed longer time (180-200 days) in reaching minimum or stable BOD and COD concentrations and BOD:COD ratio than all other reactors. Low moisture content in those reactors led to slow waste stabilization rates. Food waste reactors produced the highest BOD (46,134 mg/L) and COD (64,032 mg/L) leachate and textile waste produced the lowest (BOD_{max}=8,960 mg/L and COD_{max}= 16,054 mg/L).

The two models developed in this study show that increasing rainfall rate and temperature leads to higher BOD and COD content in leachate, which translates into faster waste decomposition. The k_{COD} model suggests that only paper and textile are the types of refuse that contribute to shaping leachate's COD concentration profile. Paper, yard, and food waste components were found to be significant in the k_{BOD} model. The TP interaction term in both models suggests that paper waste decomposes faster at higher temperatures. In future work, the two models will be validated using field data.

Table of Contents

List of Figures

List of Tables

Chapter 1

Introduction

1.1 Background

A direct result of a growing population and economy of any country is growing municipal solid waste (MSW) production. The world produced 2.02 billion tons of MSW in 2006, which had increased 7% since 2003 (UNEP, 2011). The US Environmental Protection Agency collected data on MSW generation rates in the US from 1960 to 2010 (Figure 1-1). The US generated 250 million tons of MSW in 2010, 100 million tons more than it did in 1980 (EPA, 2011). This massive increase in the amount of generated waste makes the design of a feasible, environmental friendly treatment processes more challenging for the people working in the waste management field, not to mention the subsequent increase of the footprint of solid waste dumping sites. Many countries are currently moving from simple, unregulated landfills that have no leachate collection systems, no gas collection system, and no liners to engineered landfills.

Landfill leachate is the liquid that drains out of landfills and originates from rain, melting snow, and/or the waste itself. Leachate can be a threat to the environment, especially to ground and surface waters (Figure 1-2), for decades and even centuries after landfill closure (Johannessen, 1999). Regulations in the US strictly require treatment of leachate before it can be discharged into reservoirs. Treatment of leachate is not an easy task due to the complexity of its constituents and the wide variation of its concentration, which depends on the type of waste, weather conditions, and landfill age.

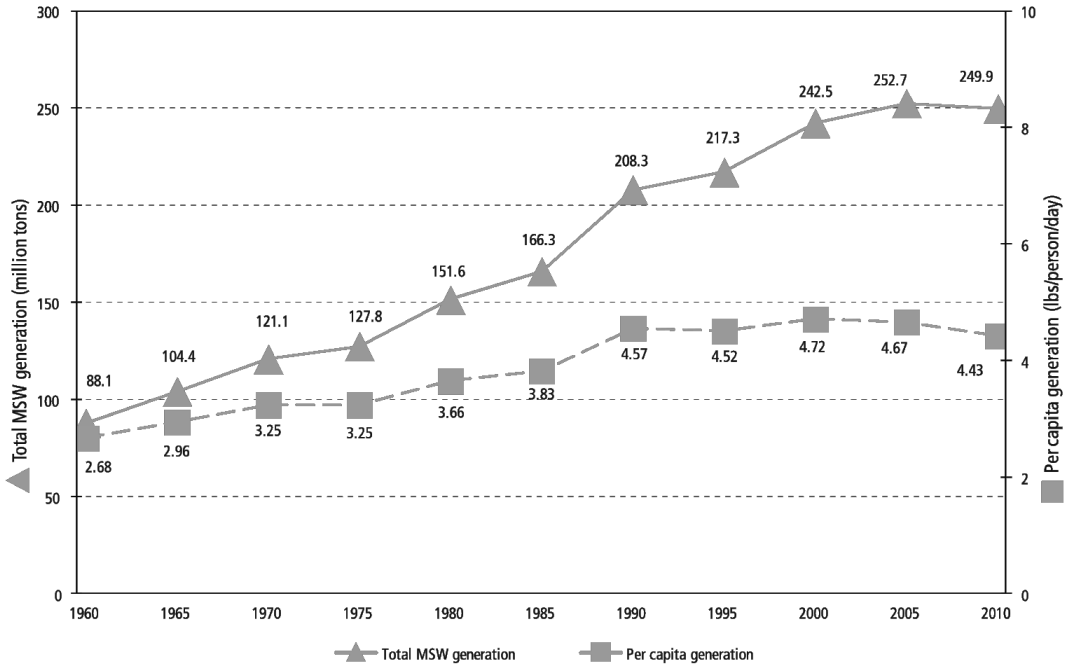

Figure 1-1 Municipal Solid Waste Generation Rates in the US from 1960 to 2010 (EPA, 2011)

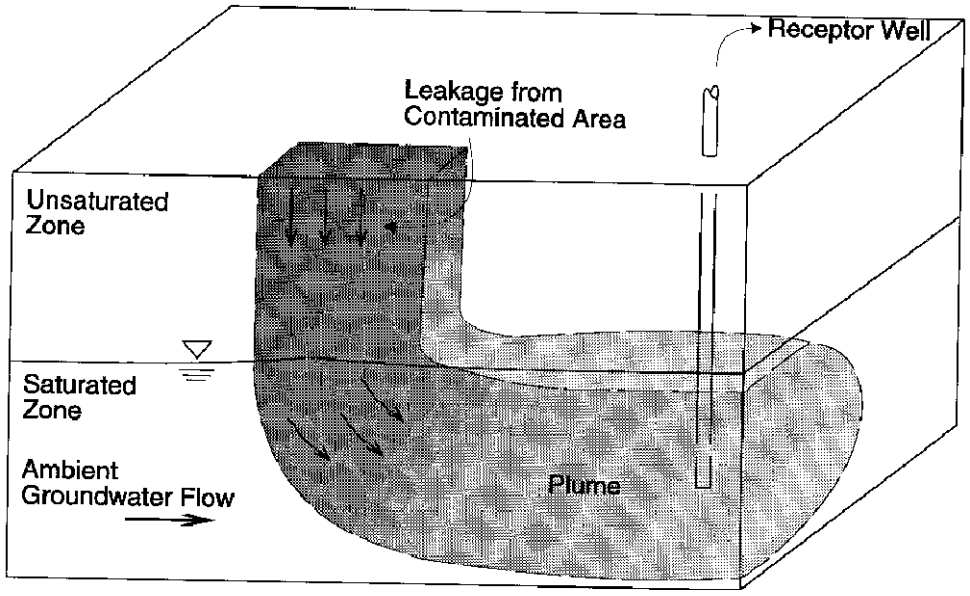

Figure 1-2 Cross-Section of Leachate Migration from Landfill to Groundwater Table (EPA, 1997)

1.2 Research Justification

Biochemical oxygen demand (BOD) and chemical oxygen demand (COD) are the most widely used indicators of leachate organic pollution. These two parameters are monitored regularly during the process of leachate treatment. They can also be used to recognize the solid waste stabilization stage in landfills (discussed in Chapter 2). Understanding the behavior of these two indicators versus the age of landfill via mathematical models would help in predicting the future extent of leachate organic pollution and, hence, the most efficient way of operating the leachate treatment facility. This is where good formulas for predicting the leachate's BOD and COD content would be useful. However, previous studies have been based on data from a single landfill or from regionally specific landfills. The few attempts to model leachate quality/characteristics using statistical techniques or software have also focused on a single landfill or few regional landfills. This study uses a comprehensive lab-scale reactor design (27 reactors) that covers wide ranges of temperatures, rainfall rates, and waste components, the major factors affecting leachate quality.

1.3 Objectives

The objectives of this study are:

1- To develop a relationship to predict the value of the first-order reaction rate constant (k_{BOD}) of leachate Biochemical Oxygen Demand (BOD) as a function of waste fractions (yard, food, paper, and textile), rainfall rate, and temperature. A 27-set of lab scale landfill bioreactors and statistical methods for data analysis will be used to achieve this objective.

2- To develop a second relationship for calculating the first-order reaction rate constant (k_{COD}) of leachate's Chemical Oxygen Demand (COD) using a method similar to that for objective 1.

1.4 Report Organization

This dissertation is divided into five chapters.

Chapter One (Introduction) of this thesis gives general background information about the importance of the topic and research justification. It also lists the objectives of the study. Chapter Two (Background and Literature Review) reviews the literature and published reports related to the main subject of the study. That includes studies related to landfill leachate monitoring and mathematical modeling of leachate characteristics. Chapter Three (Methodology) is a detailed description of the methods used to achieve the study's objectives. This chapter includes experimental design, reactor setup, and data analysis and model building procedure. Chapter Four (Discussion of Results and Regression Modeling) discusses the results of BOD and COD laboratory analysis including plots of BOD:COD ratio versus time. It also walks the reader through the multiple linear regression (MLR) model building process. Chapter Five (Conclusions and Recommendations) lists the main conclusions of this study and gives recommendations to the potential future researchers on the best ways to improve the models in terms of data collection and laboratory procedures.

Chapter 2

Background and Literature Review

2.1 Introduction

Historically, landfilling has been the most common practice of managing solid waste (Christensen, 2011). Landfills have developed throughout the years from simple dump yards to highly engineered systems in some countries. Nevertheless, much work remains to be done because of the many potential impacts landfills can cause to the surrounding environment if not properly designed and/or managed. Also, even if an advanced landfill is operating well with up-to-date technologies, the waste in this landfill will remain a constant potential source of contamination, even after the landfill closure. This is why engineers and experts in the waste management field are continuously working to develop new technologies that will turn landfills into more sustainable systems.

Some of the known environmental impacts of landfills include contamination of groundwater and surface water resources by landfill leachate, and contribution to climate change caused by methane gas (CH_4, one of the landfills' primary gas emissions). Landfills have been found to release a large number of chemicals into the atmosphere (Ludwig *et al.*, 2002).

2.2 Landfilling

The practice of landfilling has been the most common management method for solid waste (Christensen, 2011). Throughout the years, landfills have developed from mere dump yards to technologically advanced waste management facilities. Because the landfill is still considered an accumulation of waste in the environment, there has been a strong need for a process-based landfill operation technology to replace the traditional waste storage concept (Warith, 2002; Christensen, 2011). An advanced knowledge of the process by which solid waste

decomposes in landfills is essential to achieve the intended level of waste stabilization. The biodegradation of organic matter is the dominant process occurring in the landfill and it controls the chemical environment inside it; hence, it should be well understood and properly controlled (Reinhart & Townsend, 1998; Christensen, 2011). Adding moisture to the waste keeps it wet and enhances the anaerobic microbial reactions and hence leads to faster waste degradation and increased methane gas generation. The forms of moisture that are typically added to the waste are water, leachate (recirculated), or other liquids. Landfills operated with moisture addition are termed bioreactor landfills, or enhanced leachate recirculation landfills.

Organic solid waste in landfills undergoes many phases of decomposition before it is completely stabilized. Figure 2-1 shows these phases in terms of landfill leachate strength and gas composition. The phases are similar to the ones in anaerobic digesters or any anaerobic microbiological reaction in general. They can be summarized as follows (Rowe, 1995; Reinhart & Townsend, 1998; Christensen, 2011):

1- Aerobic or Adjustment Phase: Immediately after placing the top soil cover on the waste, aerobic microbial reactions (oxidation) take place for a few days due to the presence of oxygen gas in the waste voids.

2- Acidic phase: After all oxygen has been used up, anaerobic bacteria start the hydrolysis and fermentation of organic compounds (carbohydrates, proteins, and fats) and convert them into volatile fatty acids (VFA), carbon dioxide (CO_2), and hydrogen (H_2). Then, acetogenic bacteria convert VFAs into acetic acid and other simpler acids. During this stage of decomposition, leachate becomes acidic (pH < 6, i.e. contains high concentrations of VFA), has high BOD and COD concentrations, high BOD:COD ratio, and has high metal and soluble inorganic content. This phase can last from a few days to a few months depending on the landfill operating conditions (moisture content, pH control, temperature, fractions of organic waste, etc.).

3- Methane production: Methanogens/methanogenic bacteria (strictly anaerobic bacteria) start, in this phase, converting acetic acid into CH_4 and CO_2. To a lesser extent, methane is also formed from CO_2 and H_2. Subsequently, this reaction reduces the oxygen demand, represented by BOD and COD, of the remaining landfill waste (see Figure 2-1). Metals are precipitated (due to high pH) and accumulated in the solid phase.

4- Maturation Phase: The organic waste or available substrate becomes limited and gas production drops. Concentrations of leachate parameters (such as BOD and COD) decrease. Void size increases in the landfill waste, which will eventually permit oxygen and other atmospheric gases to infiltrate and disrupt the anaerobic reactions.

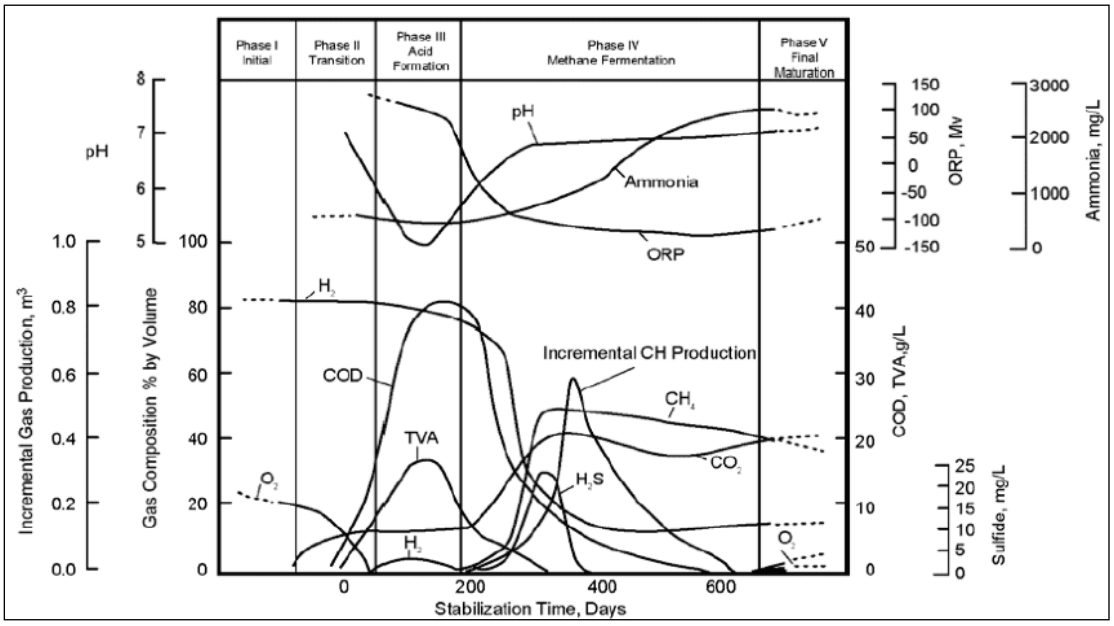

Figure 2-1 Stages of Waste Decomposition in Landfills (Zanetti, 2008).

2.3 Importance of Leachate Characterization and Management

Many field studies have indicated that landfill leachate represents a great threat to the environment, especially groundwater and surface water resources, even if the leachate is generated from small municipal landfills (Qasim & Chiang, 1994). Leachate consists of material

removed from waste mass via leaching of soluble substances and soluble products of chemical and biological transformation within landfill waste (Reinhart & Townsend, 1998). Waste material could also be washed out to travel/migrate with leachate flow in a landfill. Today, many federal and state regulations require treatment of landfill leachate to reduce its strength before discharging it into surface waters (Qasim & Chiang, 1994; Senior, 1995). Treatment of leachate can cost up to 67% of the total landfilling cost, due to the complexity of leachate constituents (Johannessen, 1999). For this reason, it is very crucial to realize that a proper design, operation and management plan for the leachate can highly reduce its quantity and strength and, therefore, reduce threats to the environment as well as the treatment cost.

Many research studies, at both field-scale and lab-scale, have been carried out on landfill leachate quantity and quality characterization (Farquhar, 1989; Grellier *et al.*, 2006; Aziz *et al.*, 2010; Fellner & Brunner, 2010). A common objective of these studies was to investigate the influence of landfill conditions (temperature, moisture content, type of waste, age of landfill) on leachate quality/strength. However, most studies have been based on data from a single landfill or from regionally specific landfills. The few attempts to model leachate quality/characteristics using statistical techniques or software have also focused on a single landfill or few regional landfills.

There is a long list of organic compounds in particular that can be found in leachate. The list includes organic acids, aromatic compounds (fuel oils), chlorinated aromatic compounds, ketones, alcohols, pesticides, and others (Reinhart & Townsend, 1998). Volatile organic acids (VOAs) are generally the dominant (highest concentration) class of organic compounds found in leachates. These VOAs are byproducts of the decomposition of carbohydrates, lipids, and proteins.

The wide variety of organics in leachate can be quantified by the lumped parameters: chemical oxygen demand (COD) and biochemical oxygen demand (BOD). Leachate COD measures all oxidizable matter in leachate (including organics and other compounds), while

BOD measures the biodegradable organic mass (El-Fadel *et al.*, 2002). BOD is the most widely used indicator of organic pollution in wastewater and surface water (Metcalf & Eddy, 2004). This study focused on the organic content of leachate that is governed by BOD and COD.

Today, many leachate treatment plants are designed to treat both biodegradable and non-biodegradable matter in leachate (Christensen, 2011). Therefore, it would help these plants' engineers and operators to have a general idea about the expected behavior of leachate in terms of BOD and COD with time in order to meet the effluent concentration standards. This is where good formulas for predicting the leachate's BOD and COD content would be useful.

The BOD and COD values of leachate vary greatly from one region to another due to climate conditions, type of MSW, and landfill age (Chain, 1977; Chen, 1996; Al-Yaqout & Hamoda, 2003; Fan *et al.*, 2006). Table 1 shows some of those variations in several countries.

Table 2-1 Leachate BOD and COD Values from Landfills in Different Regions

Study	BOD (mg/L)	COD (mg/L)	Country
Fan *et al.* (2006)	12 - 492	320 – 4,340	Taiwan
Al-Yaqout and Hamoda (2003)	30 - 600	158 – 9,400	Kuwait
Reinhart and Grosh (1998)	13,400	400 – 40,000	USA
Pohland *et al.* (1985)	4 – 57,700	31 – 71,700	Germany

The values in this table were obtained from long-term leachate monitoring programs, which are essential for these parameters not to be over/underestimated. The long-term monitoring programs are also important in determining the appropriate leachate treatment processes (Fan *et al.*, 2006). For example, if the organic content (BOD and COD) of leachate were low, treatment via biological processes would not be efficient.

The BOD/COD ratio represents the proportion of biodegradable organics in leachate. This ratio is normally higher in young landfills (fresh waste) than it is in older or stable ones. Fan *et al.* (2006) calculated this ratio for leachate from three landfills in Taiwan, of age ranging from 10 to 17 years. The BOD/COD ratios for these landfills ranged from 0.05 to 0.08 (very low). The study concluded that those landfills had reached a stable status and were not suitable for biological treatment processes. In this study, BOD/COD ratio was calculated for all reactors to determine whether the biodegradable portion of waste was still available, hence, whether BOD and COD analysis for leachate should continue. Overall, knowing this ratio helped in determining the waste stabilization stage in the reactors.

There is significant evidence from many studies to suggest that the strength of leachate declines with time (Pohland *et al.*, 1985; Qasim & Chiang, 1994; Chen, 1996; Reinhart & Townsend, 1998). The cause of this decrease could be biological decomposition of waste and/or dilution effects.

2.4 Factors Affecting Leachate Quality

Leachate strength and composition vary according to the landfill waste stabilization phase. For example, leachate in the acid phase will have low pH and high BOD and COD values, and the opposite is true for the methanogenic phase (Christensen, 2011). There are many factors than can affect the leachate quality, including waste moisture content/seasonal variation of rainfall rates, landfill age, composition of waste, temperature, pH, available O_2 in the landfill, and other operational factors (Lu *et al.*, 1985; Qasim & Chiang, 1994; Reinhart & Al-Yousfi, 1996; Christensen, 2011).

2.4.1 Waste Moisture Content

Moisture content of landfill waste plays a very significant role in controlling the quantity and strength of landfill leachate as well as waste stabilization (Qasim & Chiang, 1994). Chen (1996) studied the effect of rainfall rates on leachate strength in 9 different landfills in Taiwan

over a 4.5 years period of time. The researcher reported an overall decrease in leachate constituents/strength as rainfall rates increased.

The rate which water infiltrates into waste depends on many factors like type of landfill cover, rainfall rate, evapotranspiration rate, and field capacity of the landfill (Palmisano & Barlaz, 1996). Addition of water to landfills has been reported by many studies to have a stimulating effect on the process of methane production in landfills (Barlaz *et al.*, 1990). Water within a landfill has several functions such as (James & Arnold, 1991):

a- transporting nutrients;

b- acting as a reactant in hydrolysis reactions;

c- working as a pH buffer;

d- dissolving substances for easier metabolism;

e- diluting reaction inhibiting compounds; and

f- preparing waste surfaces area for microbes' attack.

The functions of water listed above would tend to facilitate microbial decomposition of waste. However, rates of fluid addition that are too high can limit microbial activity by flushing microbes and nutrients out of the landfill (Armstrong & Rowe, 1999). In Addition, application of water in high rates, especially in the early life of a landfill, has been reported to remove most of the waste contaminants (Qasim & Chiang, 1994). Accordingly, some researchers have attributed low rates of waste stabilization and methane production to low moisture content within the landfill, and other researchers have reported low rates of waste stabilization and methane production to high moisture content (Sulfita *et al.*, 1992; Miller *et al.*, 1994). Some researcher like Barlaz *et al.* (1990) and Chen (1974) recommended minimum moisture content of 25% and 40-70% as an optimum range.

2.4.2 Landfill Age

Many studies described the quality of leachate as a function of time because organic waste continues to decompose/stabilize as a landfill ages (Qasim & Chiang, 1994; McBean *et al.*, 1995). Also, most leachate organic indicators (e.g., BOD, COD, and bacterial populations) have shown peak concentrations in the initial stages (2-3 years) of a landfill and start to decrease gradually in the following years until they level off after 10 years of landfilling (Chen, 1996; Reinhart & Grosh, 1998). Kulikowska and Klimiuk (2008) observed a similar trend in leachate from a landfill in Poland (Figure 2-2).

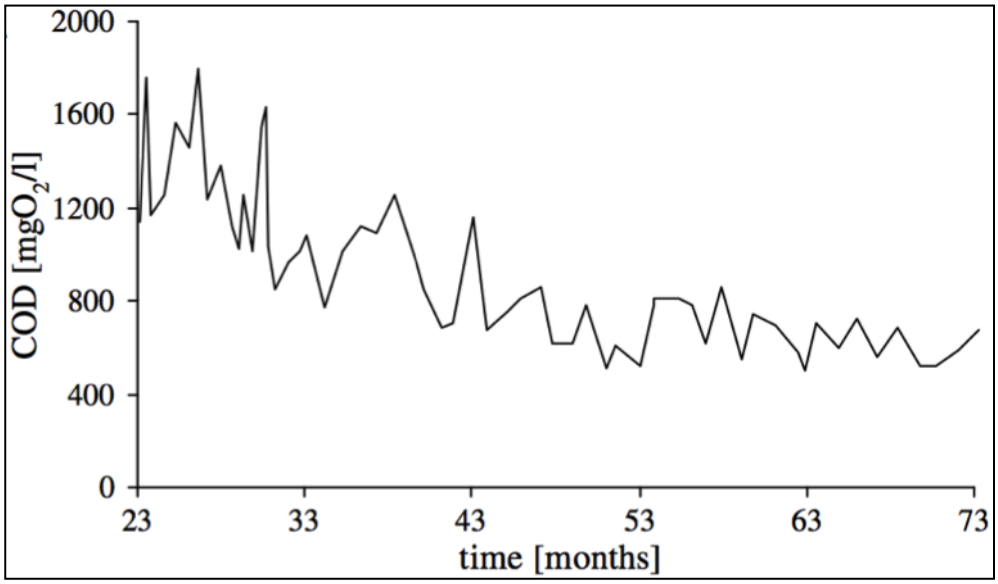

Figure 2-2 COD vs. Time in Landfill Leachate in Poland (Kulikowska & Klimiuk, 2008).

Warith (2002) compared COD and BOD trends versus time between leachate collected from laboratory cells operated as landfills and another from actual landfill in Ontario, Canada. Those two organic pollution indicators from the lab-scale landfills peaked in the first 2-5 weeks and then showed a declining trend until 17th week of experiments (see Figure 2-3). In contrast, BOD and COD of the actual landfill showed a decreasing trend over 8 years.

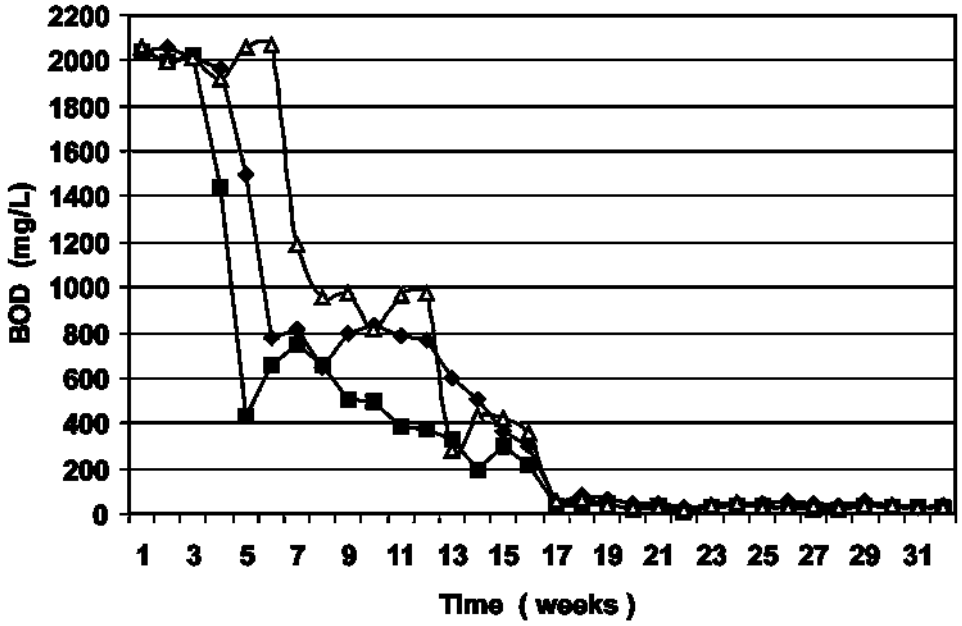

(a)

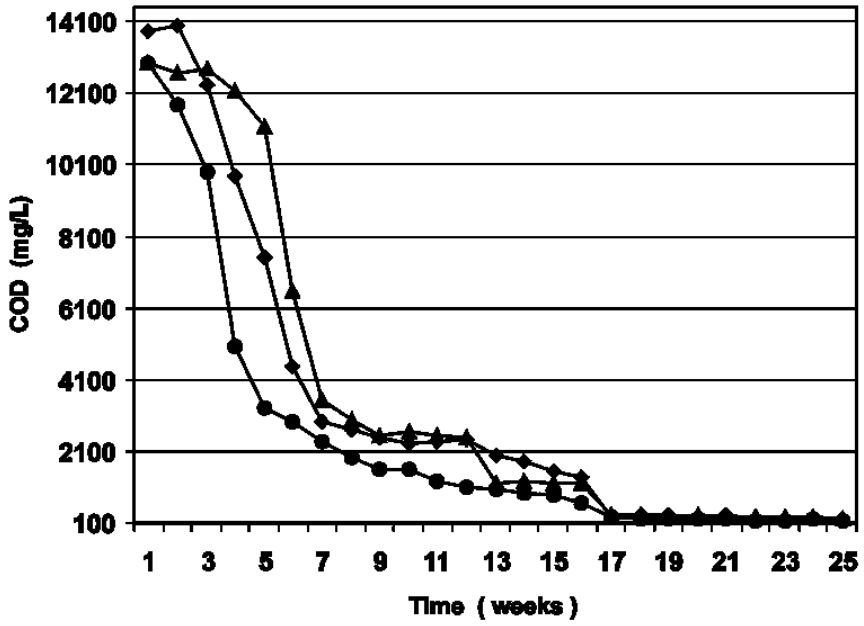

(b)

Figure 2-3 (a) BOD and (b) COD vs. Time Curves of Leachate from Lab-Scale Landfill (Warith, 2002)

Gau *et al.* (1991) reported that microbiological degradation of organic waste starts when wastes are disposed of in the landfill, which results in generating leachate with high concentration of volatile fatty acids (easily broken compounds). The study also showed that the level of these compounds in leachate declined as the landfill ages and that high molecular weight compounds were found instead. Chen (1996) investigated the relationship between leachate characteristics from 9 landfills in Taiwan and landfill age. Figure 2-4 shows BOD/COD ratios of leachate from those landfills against landfill age.

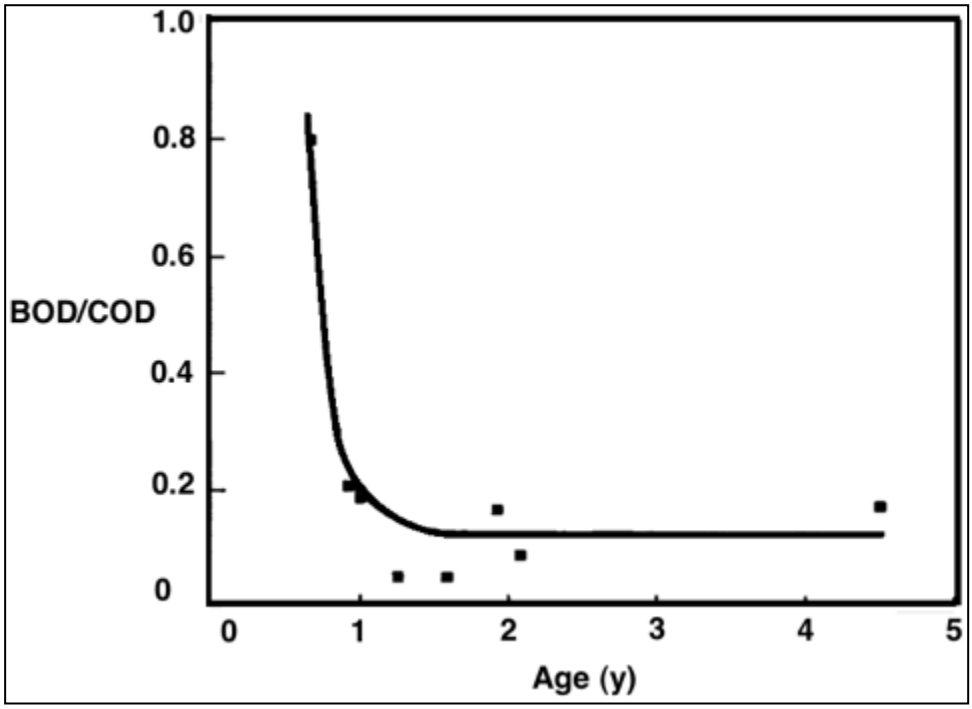

Figure 2-4 Relationship between BOD/COD Ratio and Landfill Age (Chen, 1996)

The study suggests that this ratio peaks within the first 1.5 years of the landfill age because of the rapid biodegradability of fresh waste. After this period, BOD/COD ratio declines sharply as the availability of biodegradable organic compounds becomes limited. This conclusion is helpful for selecting the type of leachate treatment processes. In this case, biological processes would be very effective only in the first one and a half years of the landfill

age. Leachate inorganic constituents decrease steadily in their concentrations because of the washout effect caused by infiltrating water (Lu *et al.*, 1981; Qasim & Chiang, 1994).

2.4.3 Composition of Waste

Factors that affect the generation and composition of municipal solid waste are population, socioeconomic status of people, season, location, and methods of collecting and disposing waste (Reinhart & Townsend, 1998; El-Fadel *et al.*, 2002). In a report by the U.S. EPA on municipal solid waste generation and composition in the Unites States in 2007, it was reported that paper and paperboard wastes made up about 32.7% (by weight) of the total MSW generated in the U.S. (EPA, 2008); Figure 2-5).

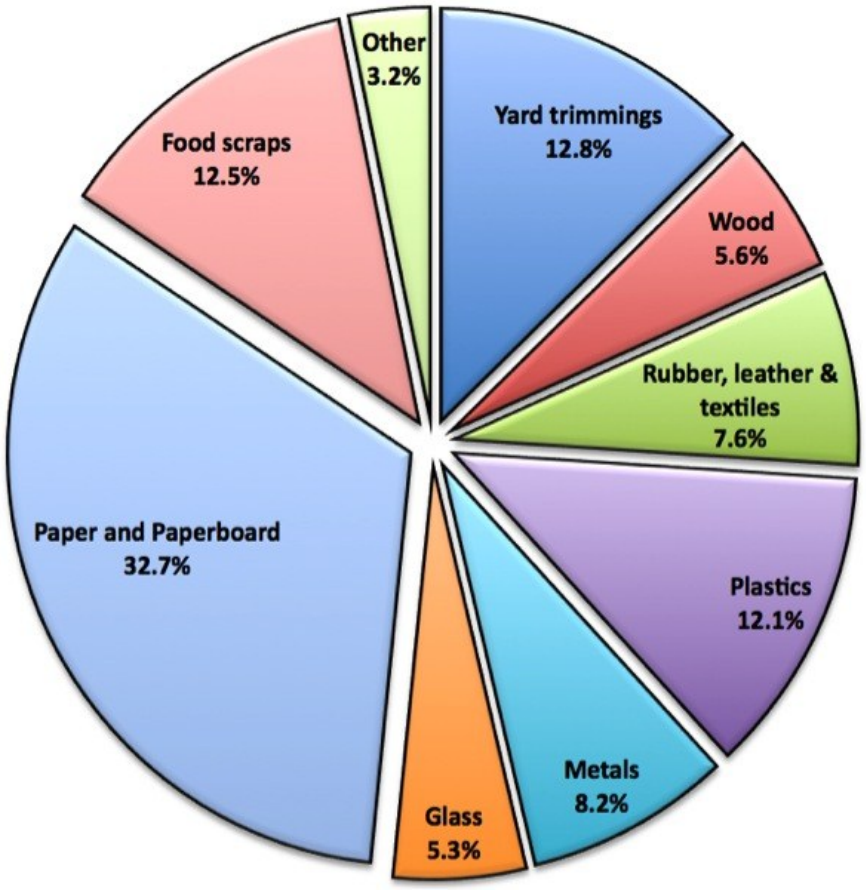

Figure 2-5 Materials Generated in MSW, 2007 (254 Million Tons before Recycling) (EPA, 2008)

In Lebanon, 62% of MSW generated in the whole country is food waste (El-Fadel *et al.*). Despite these classifications of MSW by the different studies, there is still a great variability in the characteristics and constituents of municipal solid waste from one landfill to another. Composition of MSW has a large impact on the level of biological activity in landfills (Qasim & Chiang, 1994; Gau & Chow, 1998). The biological activity is enhanced with more biodegradable organic fraction of the waste such as food, plant, and animal wastes (Rowe, 1995). In addition to the organic compounds in leachate, there are also inorganic constituents, which mainly come from ash and construction wastes as well as landfill soil (Pohland *et al.*, 1985). Therefore, the dominant waste type in a certain region affects leachate quantity and/or quality. For example, paper is primarily made of lignin, which resists anaerobic biological reactions, the main mechanism of waste degradation within a landfill (Reinhart & Grosh, 1998). Hence, paper waste may slow down the waste stabilization process. Very few researchers have tried to study the rate and extent of decomposition of individual waste components in landfills (Eleazer *et al.*, 1997; Barlaz, 2006).

To the best of the author's knowledge, no research study in the literature has investigated the effect of each type of major municipal solid wastes on leachate quality. In this study, the behavior of leachate organic constituents (represented by BOD and COD) was studied in terms of paper, food, yard, textile, and inorganic wastes as well as rainfall rate and temperature (see Chapter 3 for more details).

2.4.4 Temperature and Available Oxygen

Ambient temperature largely affects leachate quality and its variations from one season to another are uncontrollable (Lu *et al.*, 1985). Temperature is a major factor in microbial growth and chemical reactions in landfills. Waste degradation rate increases with temperature (Reinhart & Townsend, 1998). Two processes control temperature in landfills: heat lost to soil and atmosphere and heat produced during biodegradation reactions (McBean *et al.*, 1995; Reinhart & Grosh, 1998). Each microbe functions in an optimum temperature, and its growth is

disrupted with that going higher or lower (Senior, 1995). That is because enzymes deactivate and cell walls are damaged when a microbe experiences a deviation from its optimum temperature (Senior, 1995).

The amount of O_2 available to microorganisms within a landfill determines whether aerobic or anaerobic waste decomposition will dominate. Chemical compounds produced from aerobic reactions differ largely from the ones produced as a result of anaerobic reactions. Hence, leachate quality is affected by the type of reaction taking place (McBean *et al.*, 1995). While aerobic microbes decompose organic matter into water, carbon dioxide, secondary organics, and heat; anaerobic microbes produce organic acids, hydrogen, ammonia, methane gas, carbon dioxide, and water (McBean *et al.*, 1995). As mentioned in the previous section, aerobic reactions in landfills occur typically in the initial stage of landfilling until trapped O_2 within waste is depleted and an anaerobic environment develops. Aerobic decomposition can still take place after this stage in the top landfill layer as a result of interaction with the atmosphere (McBean *et al.*, 1995).

2.4.5 pH

As mentioned earlier, the anaerobic decomposition of MSW in landfills goes through a process of four consecutive phases; hydrolysis, acidogenesis (VFA formation), acetogenesis (conversion of VFAs into acetic acid), and finally methane formation. There are several bacterial groups involved in this process and each group favors certain environmental conditions such as pH, temperature, and moisture content. In a balanced situation, VFAs are produced the acidogenesis phase and converted into acetic acid in the acetogenesis phase at the same rate (Jung *et al.*, 2000; Ponsá *et al.*, 2008). When acidogenesis is much faster than acetogenesis, VFAs would build-up in the reactor and pH would drop sharply. This process imbalance could cause a reactor to fail because highly acidic environment has been reported to limit or even stop bacterial growth (Pohland *et al.*, 1985; Ponsá *et al.*, 2008).

2.4.6 Operational Factors

In a typical landfill, waste is usually placed in different cells of different age. The waste is compacted in those cells in multiple layers. The age of each cell, degree of compaction, and whether the waste is shredded before being landfilled; all play an important role in the quality of leachate that is collected from the landfill (Armstrong & Rowe, 1999). For example, when fresh waste is placed in an old cell and on top of well-decomposed waste, the concentration of leachate contaminants would jump after being stable at minimum levels. Also, the degree of compaction determines the porosity of waste inside the landfill. In a porous landfill, water moves faster through the waste and has less contact time with waste constituents, and vice versa. Contact time between water and waste is important in dissolving waste contaminants and preparing them for microbial attack. Depth of landfill cells is also significant in leachate quality. Deeper cells allow longer contact time between water and waste and, therefore, stronger or more concentrated leachate (Qasim & Chiang, 1994). Shredding waste means increasing its surface area for more water contact and microbial decomposition. Higher waste decomposition rates (higher leachate concentration) have been reported with shredded waste against non-shredded waste (Fuller *et al.*, 1979; Kemper & Smith, 1981).

2.5 Modeling of Leachate Constituents

Mathematical modeling of leachate concentration profiles has been widely attempted in the past (Wigh, 1979; Demetracopoulos *et al.*, 1986; Gönüllü, 1994; Rowe, 1995; Daskalopoulos *et al.*, 1998; Gau & Chow, 1998; Kouzeli-Katsiri *et al.*, 1999; Ozkaya *et al.*, 2006). Two main modeling methods were used in the previous studies. The first one simply involves fitting empirical formulas to the different leachate concentration curves (Wigh, 1979; Lu *et al.*, 1984; Ozkaya *et al.*, 2006). The concentration curves were fit against either time or cumulative leachate. The second modeling method is more complicated because it includes biological processes that take place in the leaching of contaminants within a landfill (Gönüllü, 1994; Kouzeli-Katsiri *et al.*, 1999). In general, almost each researcher developed their own modeling

equation and included the parameters they believed were most important or relative to their experimental setup. The following studies were selected from the literature to illustrate various modeling approaches using laboratory data, field data, or both.

(1) Wigh (1979) – Field-Scale Cells

In this study, three cylindrical field-scale test cells were constructed and filled with refuse of known compositions. The researcher simulated measured COD data using the dissolved oxygen (DO) deficit equation used for determining DO concentration in a stream subjected to organic pollution. The equation is in terms of generated volume of leachate:

$$C = C_{max} \frac{e^{-k_1 v} - e^{-k_2 v}}{e^{-k_1 v_{max}} - e^{-k_2 v_{max}}}$$

The equation has two first-order reactions representing aerobic decomposition and natural aeration. C is COD concentration; C_{max} is the peak COD concentration; k_1 and k_2 are rate constants; v is leachate volume and v_{max} is cumulative leachate volume where C_{max} value occurred. Using trial and error, k_1 and k_2 were determined to be 0.00098 mm^{-1} and 0.0145 mm^{-1}, respectively. COD vs. leachate volume curves of both measured data and model predicted data for test cell 2A are shown in Figure 2-6.

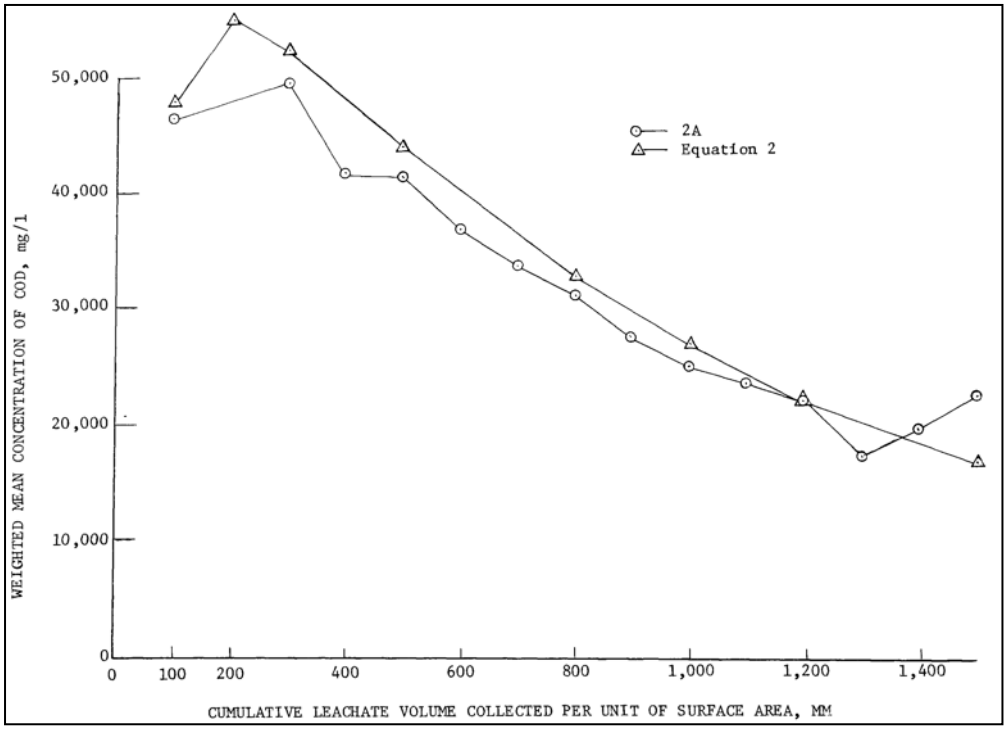

Figure 2-6 Curves of Measured (2A) and Simulated COD Concentration vs. Leachate Volume

(2) Lu *et al.* (1984)

This is one of the early studies that attempted developing relationships between leachate constituents and landfill age. Data from field cell tests of over 50 years was used in this study to develop the relationships based on the first-order rate equation:

$$C = C_0\ 10^{-kt}$$

where: C is the pollutant concentration, C_o is the initial pollutant concentration, k is the first-order reaction rate constant, and t is time. BOD and COD upper boundary curves were plotted versus time as shown in Figure 2-7. Values of the reaction rate constant, k, for BOD and COD were found to be 0.043 and 0.045 yr^{-1}, respectively.

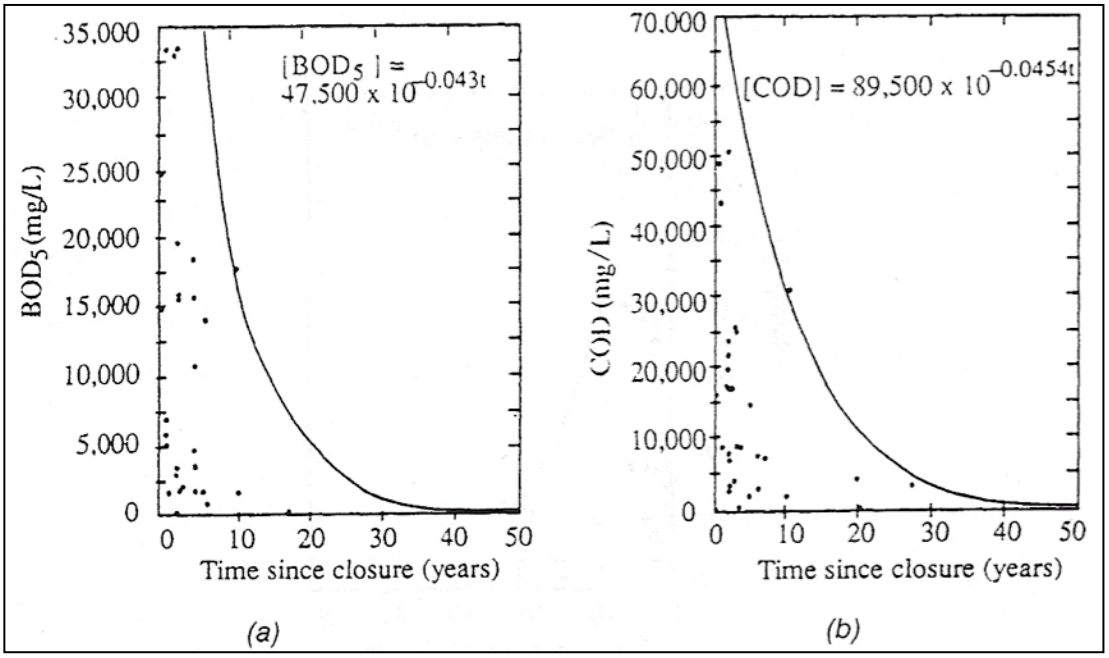

Figure 2-7 (a) BOD and (b) COD Upper Boundary Curves (Lu *et al.*, 1984)

(3) Gönüllü (1994) – Lab Data

Leachate COD data from two lab-scale reactors was simulated using a model for estimating COD that the author recommended. The proposed model,

$$C(t) = e^{-G(t)}\{C_0 + \oint (R + R_1 + R_2)\, e^{-G(t)} dt\},$$

takes into account processes like dilution (*G*), mass transfer (*R*), substrate utilization (R_1), and microbial mass production (R_2). One of the model weaknesses is that it requires input of assumed values for some parameters such as: maximum COD value (C_0), mass transfer rate constant, yield coefficient, leachate velocity constant, and others. Although the author provided graphs of good COD simulation curves, no statistical values for the goodness of fits were reported.

(4) Rowe (1995) compared two equations used to model leachate concentrations with time. The first equation was used by Lu *et al.* (1981):

$$C(t) = C_0 e^{-kt} \rightarrow [1]$$

where: C is the pollutant concentration, C_0 is the maximum/initial pollutant concentration, k is the first-order reaction rate constant, and t is time. The second equation takes into account the dilution effect. It was developed by Rowe (1991):

$$C(t) = C_0 exp\left[-\left(\frac{q_0}{H_r} + \lambda\right)t\right] \rightarrow [2]$$

and

$$H_{\mathrm{r}} = \frac{p\ m_0}{A_0\ C_0}$$

where: q_0 is volume of generated leachate, H_r is reference height of leachate, λ is first-order decay constant, m_0 is total mass of waste, p is proportion of mass contributed by the chemical of interest, and A_0 is landfill area. The author suggested that the empirically derived equation [1] has the same form as the theoretically derived equation [2]. This makes k, the empirical first-order constant in equation [1], dependent on volume of generated leachate per unit time ($q_0 A$), mass of contaminant ($p\ m_0$), peak concentration (C_0), and first-order degradation constant (λ) as follows:

$$k = \frac{q_0\ A\ C_0}{p\ m_0} + \lambda$$

(5) Kouzeli-Katsiri *et al.* (1999) – Laboratory Data

Two models, with and without leachate recirculation, were developed in this study using data from six lab-scale lysimeters and verified using actual landfill data from literature. The models involve two main processes: the exchange of organic matter between solid and liquid phases and the depletion of dissolved organics as a result of biodegradation and flushing. COD represented the concentration of organic matter in leachate.

Model 1 (without recycle):

$$C(t) = K_1 M_{s0} \left(\frac{1}{Q + K_2 V - K_1 V}\right)\left(e^{-K_1 t} - exp\left[-\left(\frac{Q}{V} + K_2\right) t\right]\right)$$

Model 2 (with recycle):

$$M(t) = \frac{M_{s0}}{K_2 - K_1}[K_1 e^{-K_1 t} + e^{-K_2 t}]$$

where: C (g/L) is COD concentration in leachate, K_1 (yr^{-1}) is the rate constant of the decrease of organic matter in solid phase due to solubilization, K_2 (yr^{-1}) is the rate constant of biological decomposition of biodegradable COD in liquid phase, M is mass of COD in liquid phase, M_{so} (g) is initial mass of leachable COD in solid phase, Q (L^3/yr) is leachate flow rate, t (yr) is time, and V (L^3) is reactor volume. Simulations of lab data and data from literature gave very good fits with correlation coefficients greater than 0.90 in all cases (Figure 2-8). The authors suggested using K_1 and K_2 value ranges of 0.0027 to 0.0055 day^{-1} and 0.0016 to 0.0027 day^{-1}, respectively, for new landfills.

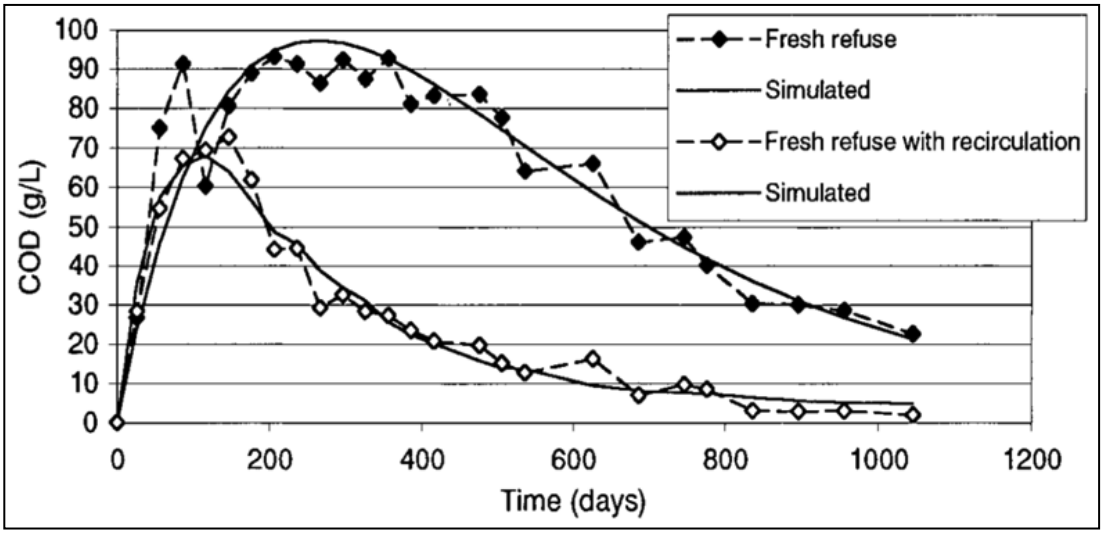

(a)

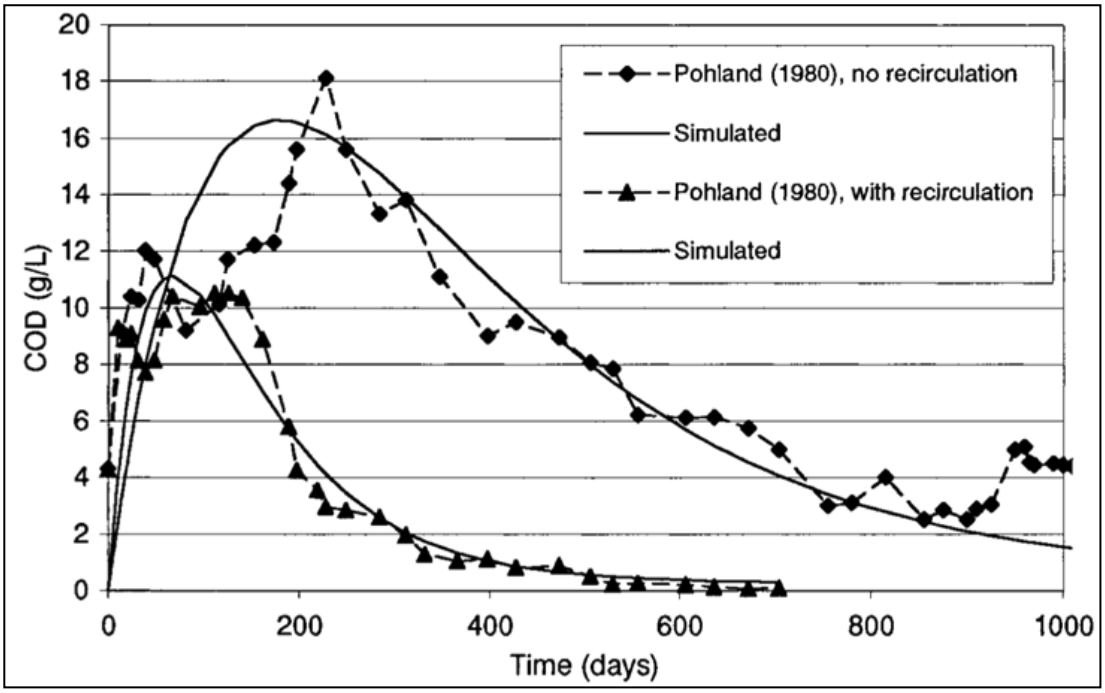

(b)

Figure 2-8 Simulation of (a) Lab Data and (b) Data from Literature (Kouzeli-Katsiri *et al.*, 1999)

(6) Ozkaya *et al.* (2006) – Field Data

The following equation was used in this study to simulate measured data of leachate BOD and COD concentrations:

$$y = a_0 + a_1\, e^{-t} + a_2\, t\, e^{-t}$$

where: y is concentration of BOD/COD in g/L; a_0, a_1, and a_2 are unknown constants which were evaluated using the least square method; and *t* is time in months. Leachate was produced in two large-scale cells (25 m wide, 50 m long, and 5 m deep) at a landfill in Istanbul, Turkey. One cell was operated without leachate circulation (C1) and the other with circulation (C2). Good curve fits (R^2=0.87-0.92) were obtained between measured data and model simulations (Figure 2-8). It is clear from BOD and COD curves in Figure 2-9 that leachate recirculation did not have a significant impact on the refuse decomposition rate.

There are several drawbacks in the experimental setup of the previous studies that focused on developing models for calculating leachate BOD and COD. Three important factors were not considered while designing the lab-scale landfills that were intended to simulate the behavior of leachate strength and composition in actual landfills:

1- temperature variations among different landfill locations and climates;

2- different precipitation rates from one season to another;

3- different types of waste; and

4- combinations of factors 1-3.

In this study, a different method was developed to estimate the degradability of landfill waste using landfill leachate as an indicator. The method involved 27 lab-scale anaerobic reactor landfills designed with several combinations of temperatures, rainfall rates, and different fractions of five waste components (paper, food, yard, textile, and inorganic waste). The reactor setup and data analysis approach are explained in details in the next chapter.

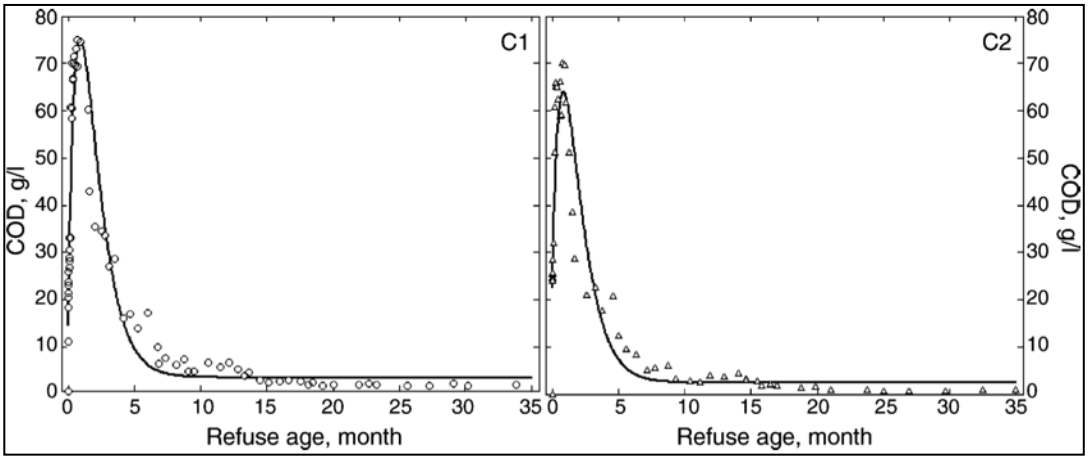

(a)

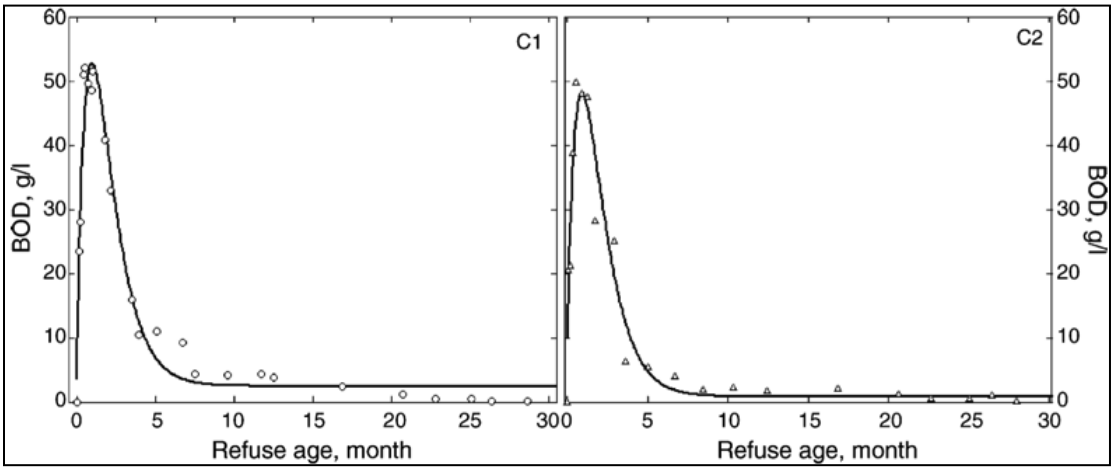

(b)

Figure 2-9 Model Simulations over Field Data (C1 & C2) of (a) COD and (b) BOD (Ozkaya *et al.*, 2006).

Chapter 3

Methodology

3.1 Reactor Setup

Twenty-seven 16-L high-density polyethylene (HDPE) wide-mouth plastic reactors were built as lab-scale landfills. The reactors were filled with various waste components and operated at the rainfall rate/temperature combinations discussed below.

Before filling the reactors, leak-checks were performed with a U-tube manometer. Head difference was recorded to confirm that it was within 0.5 inch H_2O after 12 hours and within 3 inch H_2O after 24 hours. Once reactors were leak-tested, their empty weight was measured. Reactors were then filled with refuse components, as described in the Experimental Design section below. Anaerobic digested sewage sludge was used as seed, obtained from Fort Worth Village Creek Wastewater Treatment Plant and added to each reactor to achieve 10-12 % by volume. Each reactor was then weighed and placed in its position in one of the constant temperature locations, and connected to a leachate collection bag (2-L Kendall-KenGuard Drainage Bag) and gas collection bag (22-L Cali 5-Bond Bag, Calibrated Instruments, Inc.), as shown in Figure 3-1.

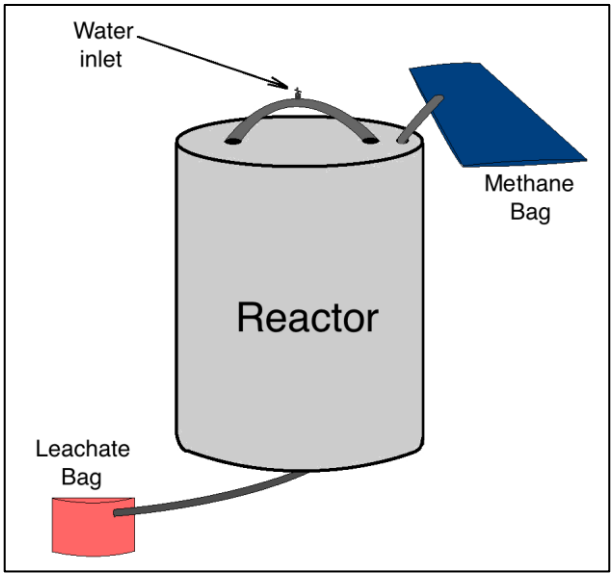

(a)

(b)

Figure 3-1 (a) Schematic of Reactor Setup, (b) Picture of Reactors in Constant Room Temperature

3.2 Waste Components

Refuse components were the major biodegradable wastes: food, paper, yard/wood, and textile, as well as inert inorganics (Weitz *et al.*, 2002). Food waste was obtained from local restaurants. A mixture of grass, leaves, and tree/brush trimmings was obtained from UTA's grounds department to represent wood/ yard waste. A mixture of textiles was obtained from local tailors. Paper waste was obtained from UTA recycling bins (office paper), researcher personal recycling bins (newspapers, mail, magazines, tissues and towels, diapers), and a local grocery store (corrugated boxes and cartons). Inerts, including sand, dust, stones, glass, metals, plastic, were obtained from UT Arlington grounds and recycling bins and concrete pieces were collected from the Civil Engineering Lab Building.

3.3 Rainfall Rates

Rainfall rates of 2, 6, and 12 mm/day (30, 240, and 450 mm/month) encompass precipitation rates for most locations around the globe except deserts (Pidwirny, 2010). The number of rainfall rates was kept small to limit the number of reactors due to time required for measurements and limited space in the constant temperature rooms. Leachate accumulating at the bottom of the reactors was removed daily and characterized, as discussed below.

3.4 Temperatures

To determine how k_{BOD} and k_{COD} vary with temperature, tests were conducted at 70°F, 85°F, and 100°F. Reactors left in the open in the lab room were maintained at approximately 70°F. Two constant temperature rooms maintained reactors at 85°F and 100°F. Testing reactors in a temperature below 70°F would mean that the data would cover a broader range of potential ambient temperatures; however, degradation rates would be slower for temperatures less than 70°F, which means that the lab experiments would take much longer. Also, the number of temperatures was kept small to limit the number of reactors due to time required for measurements and limited space in the constant temperature rooms.

3.5 Experimental Design

BOD and COD were measured over time for 27 16-L lab scale landfills with varying waste compositions (food, wood/straw, textile, paper, and inorganics ranging from 0 to 100 %, as shown in Table 3-1); average rainfall rates of 2, 6, and 12 mm/day; and temperatures of 70, 85, and 100 °F. Tables 3-1 and 3-2 show the combinations used in each reactor. For example, Reactor-1, according to Table 3-2, was operated with 2 mm/day rainfall at a temperature of 70°F, and contained waste component combination b, which according to Table 3-1 is 100% paper waste. The specific combined waste cases were determined by a mixture design. These combined waste cases served as blocking variable levels for an incomplete block design to study the primary factors, temperature and rainfall. This design was useful in keeping the number of reactors to a minimum, as discussed above.

Table 3-1 Component Percent by Weight for Each Waste Combination

Waste Component	Component % by Weight for each Waste Combination								
	a	b	c	d	e	f	g	h	i
Food	100	0	0	0	0	60	30	10	20
Paper	0	100	0	0	60	0	10	30	20
Textile	0	0	100	0	0	30	0	60	20
Yard	0	0	0	100	0	10	60	0	20
Inorganics	0	0	0	0	40	0	0	0	20

Table 3-2 Rainfall, Temperature, and Waste Component Combinations for Testing

Rainfall (mm/day)	Temp. (ºF)	Waste Component Combination								
		a	b	c	d	e	f	g	h	i
2	70		*1*					*2*		*3*
	85	*4*		*5*					*6*	
	100		*7*		*8*					*9*
6	70	*10*		*11*		*12*				
	85		*13*		*14*		*15*			
	100			*16*		*17*		*18*		
12	70				*19*		*20*		*21*	
	85					*22*		*23*		*24*
	100	*25*					*26*		*27*	

Note: Each *italic* number indicates the number of the reactor.

3.6 Analytical Methods

The leachate parameters (pH, BOD, and COD) were measured using Standard Methods for Examination of Water & Wastewater (Clesceri, 1999). BOD and COD were measured on a biweekly basis and leachate pH was measured daily. Some of the 2 mm/day reactors did not produce enough (200 mL) leachate for the laboratory analysis on the scheduled days. For those reactors, leachate was accumulated in the bag over a week period and then collected and analyzed. The standard procedure is to measure BOD after 5 days of incubation period. This is called the 5-day BOD or BOD_5. In this study, it was discovered that the lab analyst responsible for measuring BOD in each leachate sample had been unintentionally incubating the samples for 4 days instead of 5. It was too late to change the incubation period to 5 days. Therefore, leachate samples were analyzed for BOD_4 until the reactors were dismantled.

Two samples from Reactor-4 and Reactor-20 were collected and both BOD_4 and BOD_5 were measured to check the difference between the two. The results are shown below in Table 3-3. The percent difference between BOD_4 and BOD_5 ranged from 3.6 to 7.2% for the two reactors.

Table 3-3 Difference between BOD_4 and BOD_5

Reactor #			mg/L	Difference
4	Sample-1	BOD_4	441	7.2 %
		BOD_5	475	
	Sample-2	BOD_4	417	5.0 %
		BOD_5	439	
20	Sample-1	BOD_4	484	4.2 %
		BOD_5	505	
	Sample-2	BOD_4	434	3.6 %
		BOD_5	450	

3.7 Data Analysis

The effects of temperature, rainfall rate, and types of refuse on the concentrations of BOD and COD were analyzed for any possible trends. In addition, BOD:COD ratio of every reactor was plotted against time to investigate the biodegradability of the studied types of waste.

Like other leachate quality parameters, BOD and COD concentrations versus time resemble hydrograph-type curves, with a rising part, a peak concentration, and a declining part (Kouzeli-Katsiri *et al.*, 1999). During the acidic phase of waste stabilization in landfills, anaerobic microbes decompose organic compounds and convert them into volatile fatty acids and, subsequently, into acetic acid. When leachate passes through waste during this stage, its BOD and COD content increases dramatically and its pH falls below 6. Maximum BOD and COD concentrations in landfill leachate are reached during this stage (Kjeldsen et al., 2002). The generation rate of dissolved organic compounds during this stage is much higher than both the rate of their decomposition by bacteria and the rate of their removal out of the landfill via leachate. This is the reason for the rising part of the BOD and COD concentration curves at the beginning of a landfill's life. The declining part of these curves starts when the dissolved organic compounds in the landfill environment are consumed/decomposed by anaerobes and removed from the landfill by leachate much faster than they are generated. In other words, as waste decomposition in a landfill progresses, BOD and COD concentration curves continue to decline.

Modeling the whole curve requires making assumptions about many constants in the modeling equations, depending on the approach used to develop the curve. In this study, our interest was only in the declining part of the BOD and COD curves, which were modeled using the first-order decay equation:

$$C = C_i \, e^{-kt}$$

where: C is pollutant concentration in mg/L, C_i is the initial (at time=0) concentration in mg/L, k is the exponential decay rate constant in day^{-1}, and t is time in days. The idea was to try a

simple first-order model first, but future work will investigate whether an alternate model fits the data better. McGinley and Kmet (1984), Lu *et al.* (1985), and El-Fadel *et al.* (2002) used the first-order decay equation to fit curves to leachate BOD and/or COD data. The k value here is a net rate constant that can include both formation and decomposition rates of BOD and/or COD. However, the rate of decomposition dominates right after the peak BOD/COD value was reached, which gives k a minus sign.

For each reactor, the highest BOD/COD data point was considered the peak BOD/COD value. For example, the peak COD value from Figure 3-2 is 16,000 mg/L. However, since each reactor's BOD and COD were only measured every 2-4 weeks, the actual peak value of BOD/COD may not have been measured, if it occurred during a week when a sample was not taken.

Figure 3-2 illustrates the curve fitting process. The red dots represent COD lab data and the dashed black line is the fitted exponential curve of the declining part of the data.

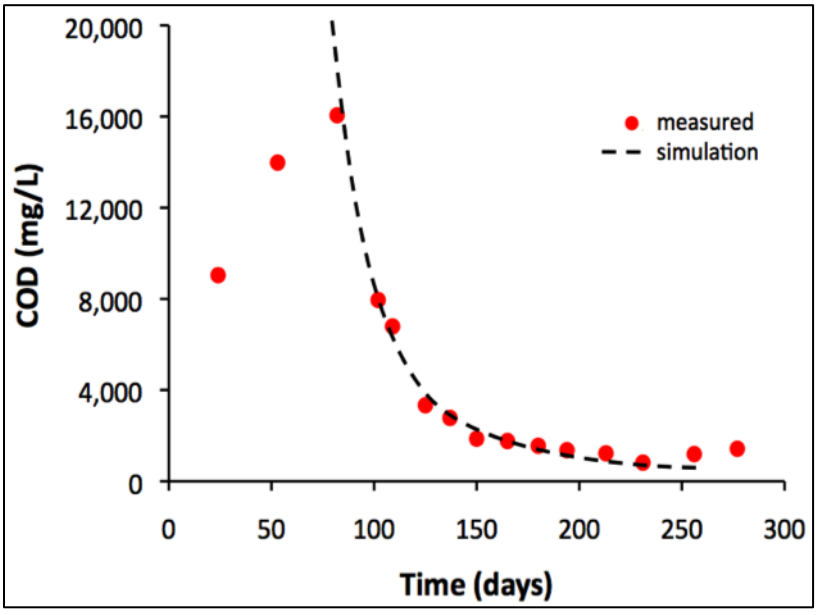

Figure 3-2 Typical COD Data with a Fitting Curve

The initial concentration value (C_i) is the fitted curve's y-intercept where time equals zero. C_i values were estimated using trial and error but they were eventually ignored in this study because they have no physical meaning since the fitted curve does not start from the beginning of the landfill operation (t = 0), instead, it starts somewhere around the peak value. Theoretically, the k value in this situation gives information about the speed of waste leaching and biodegradation within the landfill. The larger the k value, the faster the waste decomposition. Figure 3-3 illustrates this idea. Three COD vs. time curves with three different k values are shown in this figure. It is obvious that the 0.1 (day^{-1}) curve reaches minimum COD value much faster than the 0.04 and 0.01 (day^{-1}) curves.

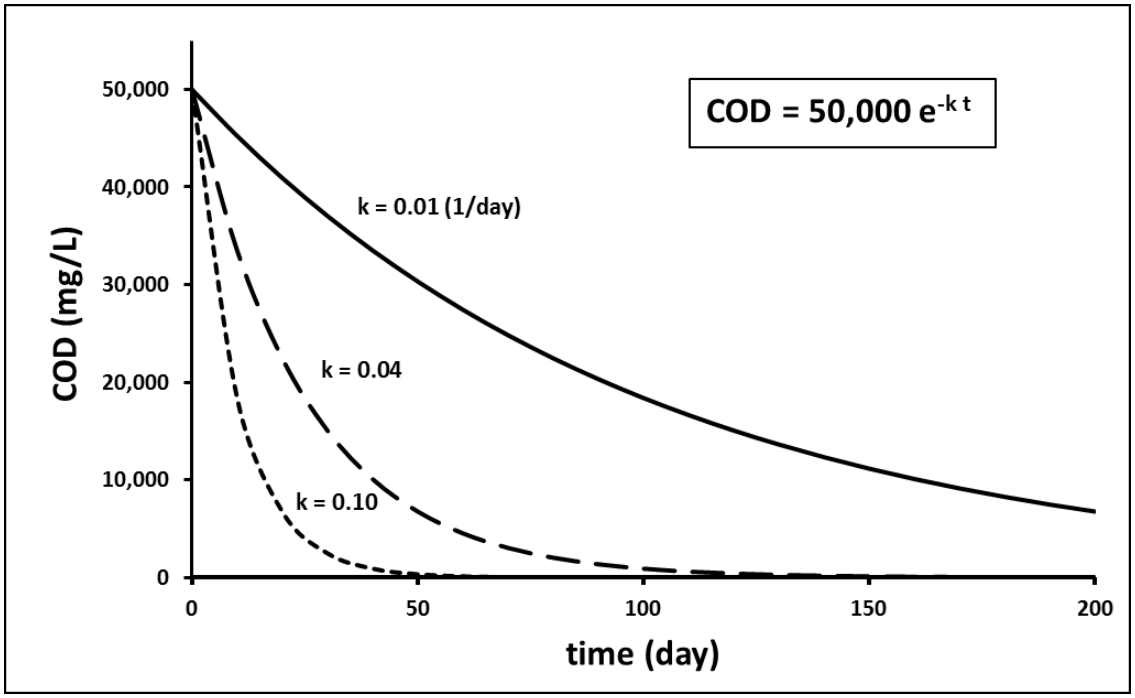

Figure 3-3 Illustration of the Significance of the k Value

The goal here was to obtain two k values for each of the 27 reactors: one for BOD (k_{BOD}) and the other is for COD (k_{COD}). Because reactor #10 failed, 26 k_{BOD} values and 26 k_{COD} values were obtained using an Excel add-in package called XLSTAT. This software program

uses Levenberg-Marquardt Algorithm to fit the exponential curve on the lab data and gives the user values of k, C_i, and R^2 (correlation coefficient).

Using MINITAB and SAS software programs and the collected data, two multiple linear regression models were developed to predict k_{BOD} and k_{COD}. Each k was modeled as a function of rainfall rate (mm/day), temperature (^{0}F), and waste composition as shown in the following equation:

$$k = \beta_0 + \beta_1 R + \beta_2 T + \beta_3 F + \beta_4 P + \beta_5 Y + \beta_6 X + \beta_7 I + \varepsilon$$

where: k = first-order decay constant (day^{-1}); βs = parameters to be determined through multiple linear regression, using the lab data; R = annual rainfall; T = average temperature at the landfill location; F = food fraction of landfilled waste; P = paper fraction of landfilled waste; Y = wood/yard fraction of landfilled waste; X = textile fraction of landfilled waste; I = inorganic fraction of landfilled waste; ε = error uncertainty, modeled as a random variable.

The detailed steps of the multiple linear regression model-building process are explained in Chapter 4. Once the two best models (k_{BOD} and k_{COD}) were finalized, each model parameter was interpreted and its parameters were compared with the other model. The two models will be validated in future work.

Chapter 4

Results and Discussion: Experiments and Regression Modeling

This chapter presents and discusses the experimental results and the development of two mathematical models using multiple linear regression analysis. The two models will be used to predict leachate's k_{BOD} and k_{COD} values for a landfill in terms of rainfall rate, temperature and waste components. The chapter concludes with validation of the two models to evaluate their usefulness in a real situation.

4.1 Leachate BOD and COD Results

Maximum BOD concentrations (BOD_{max}) in all reactors ranged between 856 and 46,134 mg/L. These peak values were recorded within the first 100 days of the reactor's life. It should be noted that since each reactor's BOD was only measured every 2-4 weeks, the time to the peak value is approximate. Also, the actual peak value of BOD may not have been measured, if it occurred during a week when a sample was not taken. The time it took the BOD concentration to reach a stable low value ranged from 54 to 291 days since the first day of operation. COD peak values in this study were between 2,458 and 64,032 mg/L. It took some reactors only 7 days to reach the peak value of COD before the declining trend started. Reactor # 2 took 102 days to reach COD_{max}. The 26 reactors reached stable low COD concentrations at much different times that ranged between 66 and 321 days (see Table 4-1). This wide range emphasizes the significance of temperature, rainfall rate, and waste composition (the experimental factors) in the MSW waste stabilization process in landfills.

Table 4-1 Peak BOD and COD Values of All Reactors

R #	$Time_{BODmax}$ (days)	BOD_{max} (mg/L)	Time Until Stable BOD Value (days)	$Time_{CODmax}$ (days)	COD_{max} (mg/L)	Time Until Stable COD Value (days)
1	41	5,082	223	105	6,094	223
2	102	24,509	256	102	42,606	284
3	53	10,043	179	53	22,674	293
4	48	46,134	225	13	60,760	271
5	53	8,960	180	82	16,054	231
6	20	19,889	132	20	18,129	208
7	50	2,816	127	50	6,212	127
8	33	976	145	33	13,498	242
9	42	18,823	141	42	38,777	239
11	24	856	178	7	2,458	178
12	41	3,183	152	15	9,095	204
13	7	10,277	75	7	20,525	75
14	14	12,361	88	14	30,256	144
15	6	21,928	122	6	47,453	122
16	27	6,008	111	27	6,879	132
17	8	5,460	56	8	12,356	80
18	9	18,401	106	9	50,756	114
19	24	2,507	70	7	10,464	126
20	10	13,805	291	10	28,848	321
21	25	2,592	203	11	13,770	193
22	25	2,318	54	14	9,163	66
23	13	16,958	76	13	34,332	83
24	8	9,081	76	8	16,487	83
25	7	29,891	131	7	64,032	115
26	11	15,755	115	11	39,024	95
27	15	6,250	68	15	14,729	68
Min	6	856	54	6	2,458	66
Max	102	46,134	291	105	64,032	321

The behavior of BOD and COD contents in leachate was expected to change from one reactor to another depending on the levels of the controlled experimental factors (rainfall, temperature, and waste composition). The questions to be answered after the experiment was over were many:

1- Which factor has the largest influence on the magnitudes of landfill leachate's BOD and COD?

2- Which waste components contribute the most/least in rising BOD and COD levels of the landfill leachate? And what information does that tell about the degradability of each type of waste?

3- Which factor contributes the most in speeding up or slowing down the waste decomposition of organics in landfills?

4- What are the optimum rainfall rate and temperature for a faster waste stabilization in landfills?

BOD and COD results (in mg/L) for every reactor were plotted versus time. As mentioned in the methodology chapter, the experimental design of reactors included 9 different waste combinations. Each group of 3 reactors, out of 26 reactors, contained one waste combination. Plots of the reactors that contained the same waste composition (ex: 100% Yard waste) were grouped together in one figure to make observing any potential patterns much easier. All figures are presented in this section (Figure 4-1 to Figure 4-9). Each figure includes six plots (three BOD plots and three COD concentration plots) and each column shows the BOD and COD plots for one reactor. Waste composition (F=Food, P=Paper, Y=Yard, X=Textile, and Inorg.= Inorganic waste), rainfall rate and temperature for each reactor appear on top of each column of plots. Figure 4-1 shows only 4 plots because reactor # 10 failed after a few weeks of operation due to excessive acid accumulation. Microorganisms cannot survive in acidic environments. For this reason, alkaline water (pH=12.0) was added to some reactors

(especially those with food waste) in the acidic phase for 20-40 days in an attempt to neutralize the acidic environment inside those reactors. This method did not work with reactor # 10 and, therefore, it failed and was excluded from the experiment and the dataset. Unit of the vertical axes is mg/L. The title of each plot contains 'BOD' or 'COD' word followed by number of the reactor. For example, BOD-4 means BOD vs. time plot of reactor # 4.

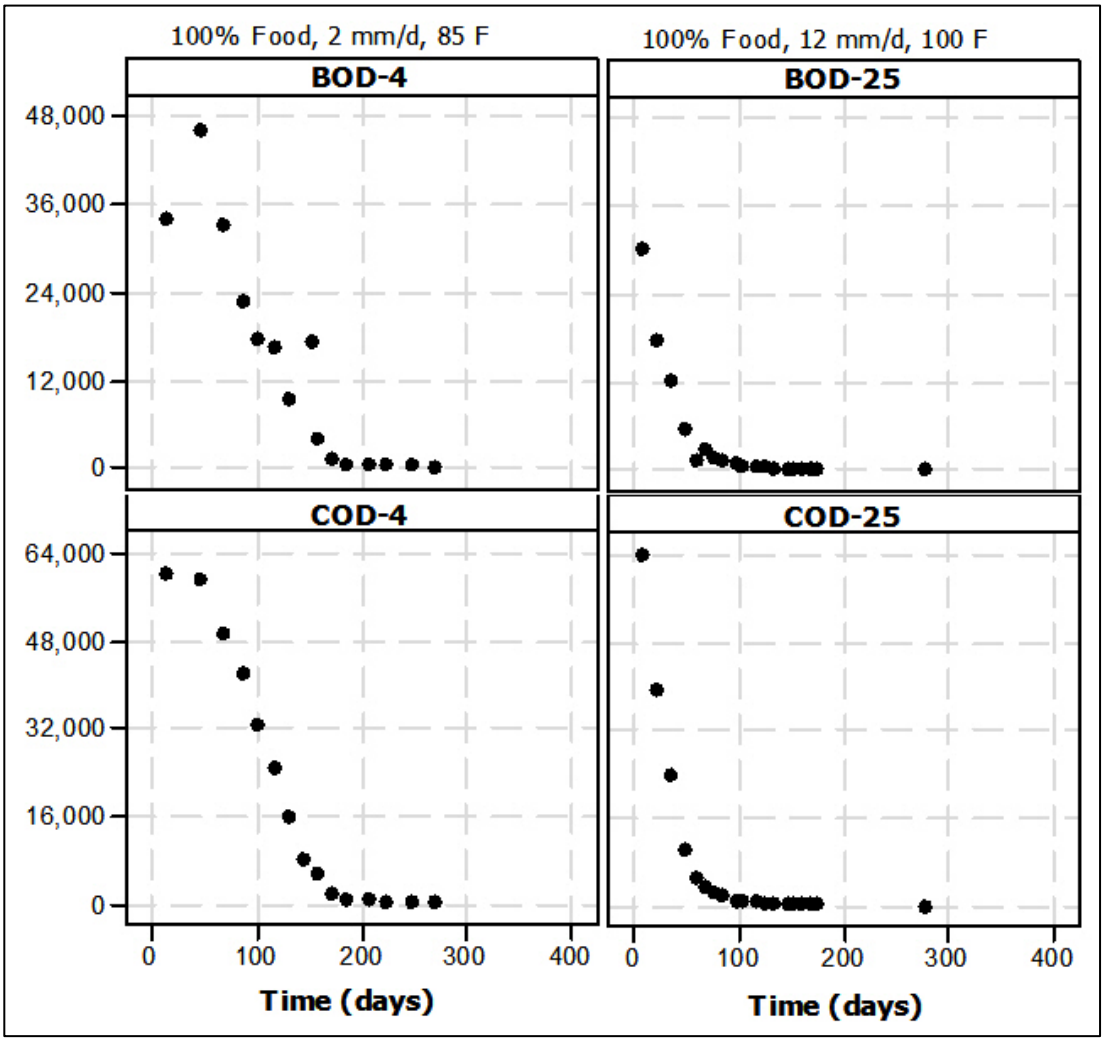

Figure 4-1 BOD and COD Plots of the Waste Composition *a* Reactors

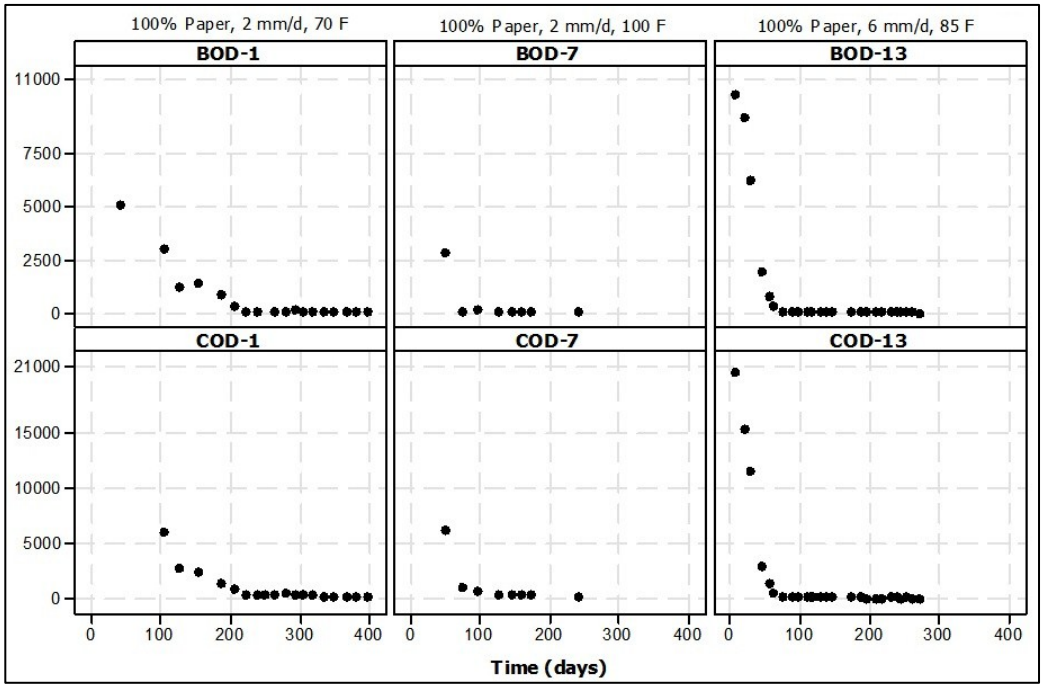

Figure 4-2 BOD and COD Plots of the Waste Composition *b* Reactors

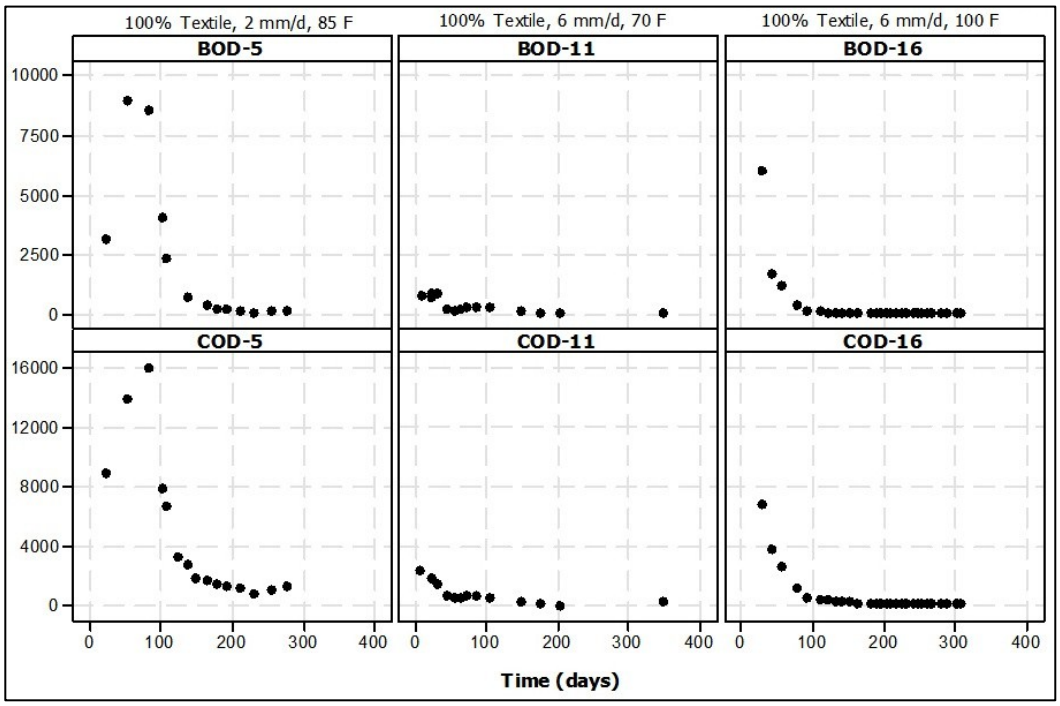

Figure 4-3 BOD and COD Plots of the Waste Composition *c* Reactors

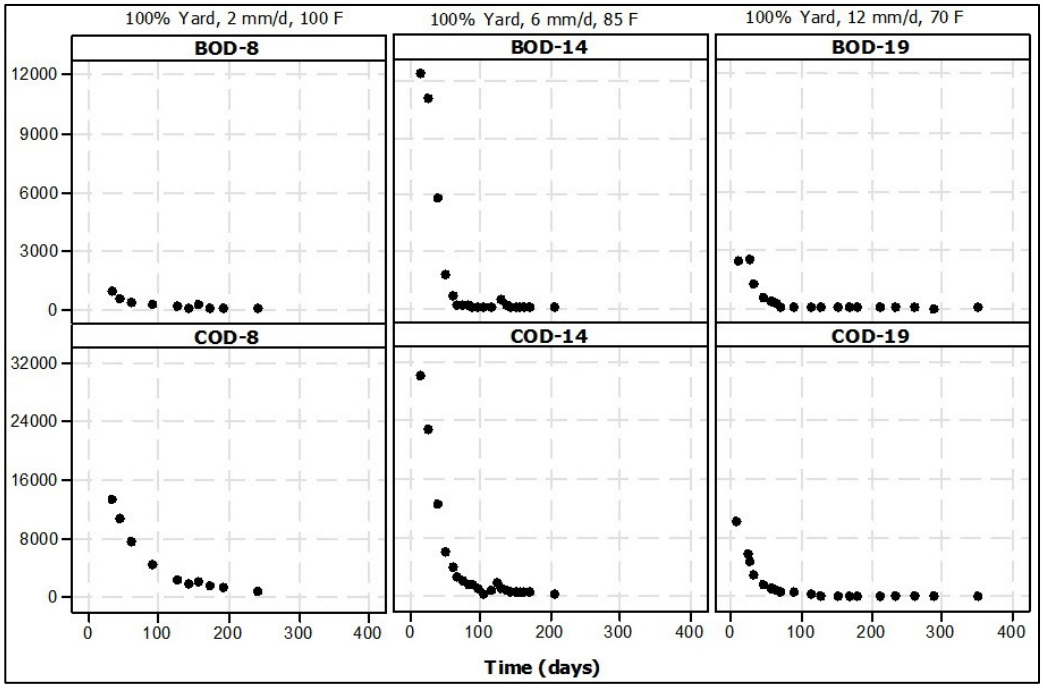

Figure 4-4 BOD and COD Plots of the Waste Composition *d* Reactors

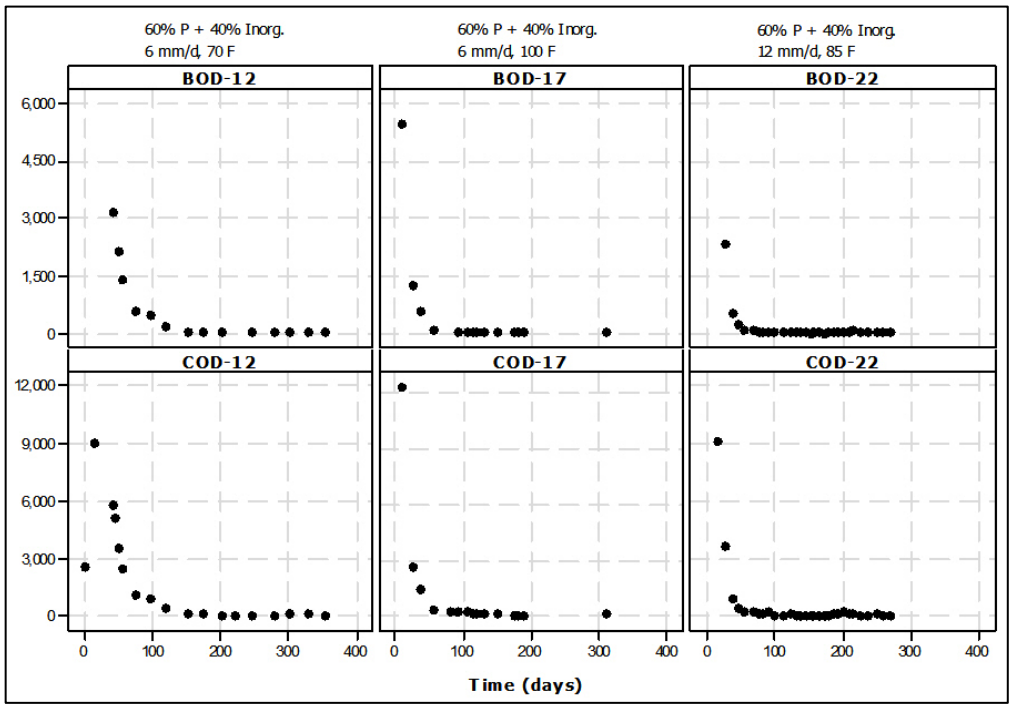

Figure 4-5 BOD and COD Plots of the Waste Composition *e* Reactors

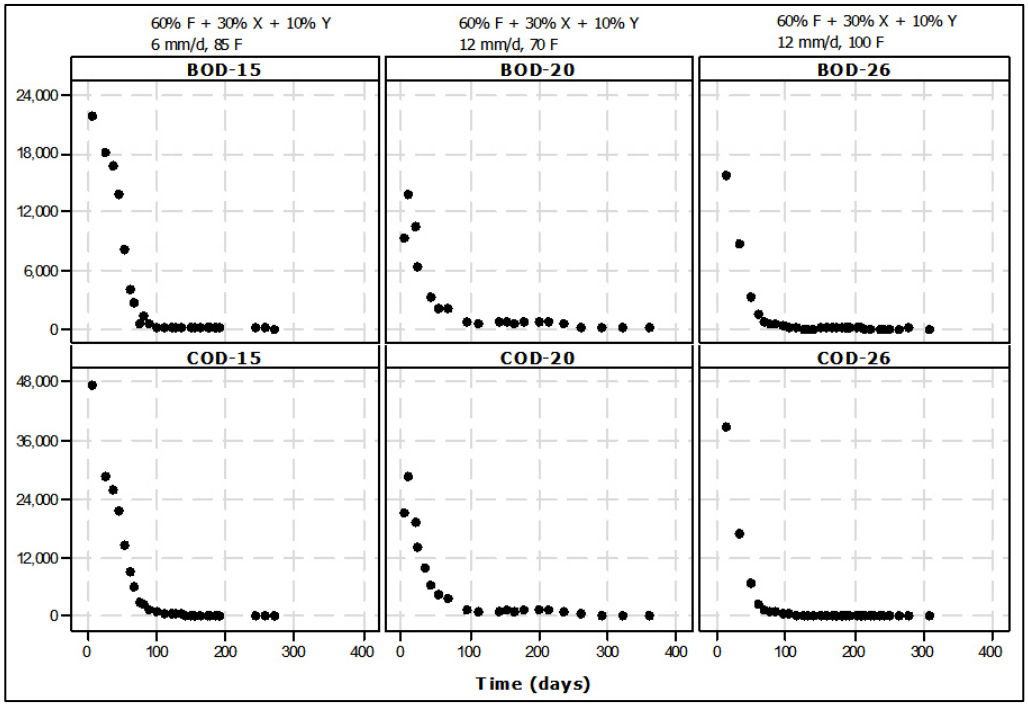

Figure 4-6 BOD and COD Plots of the Waste Composition *f* Reactors

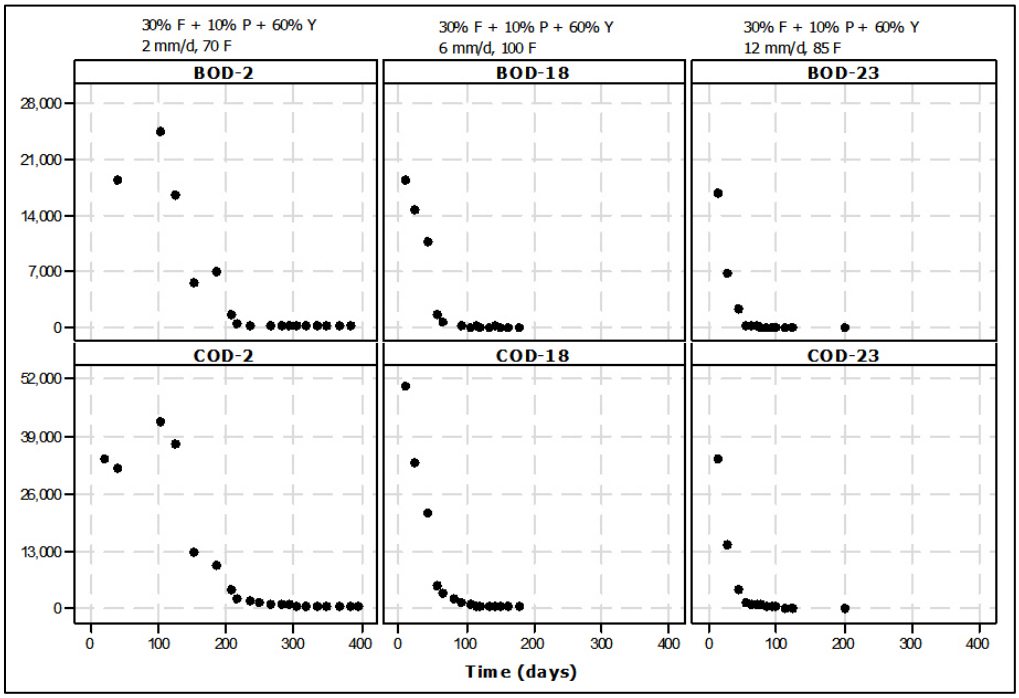

Figure 4-7 BOD and COD Plots of the Waste Composition *g* Reactors

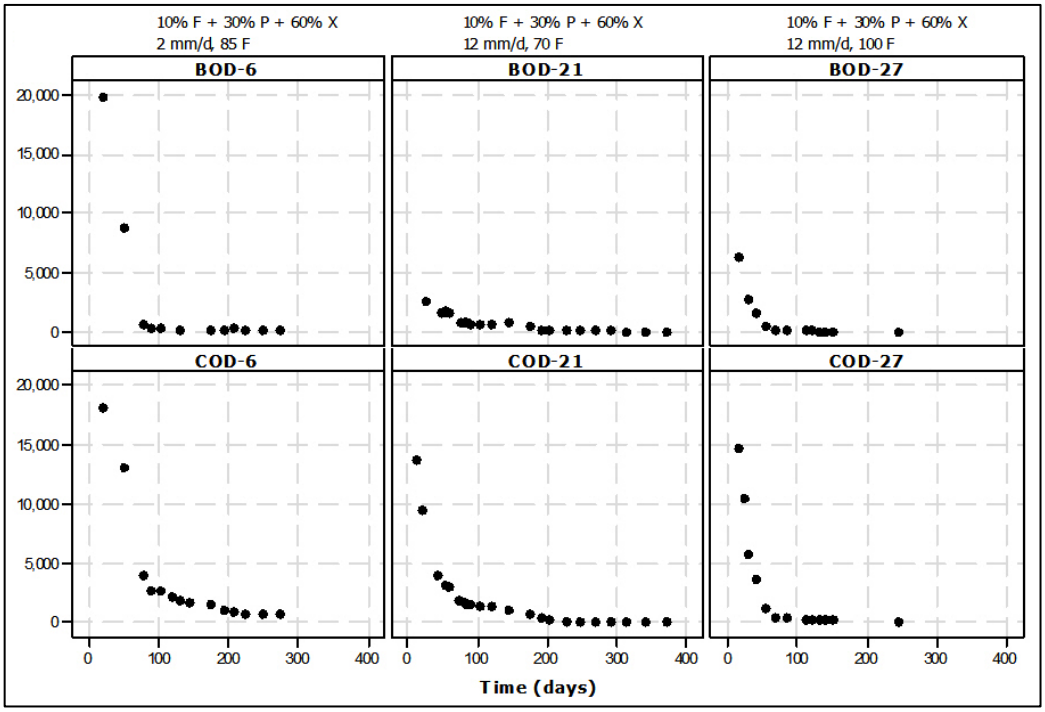

Figure 4-8 BOD and COD Plots of the Waste Composition *h* Reactors

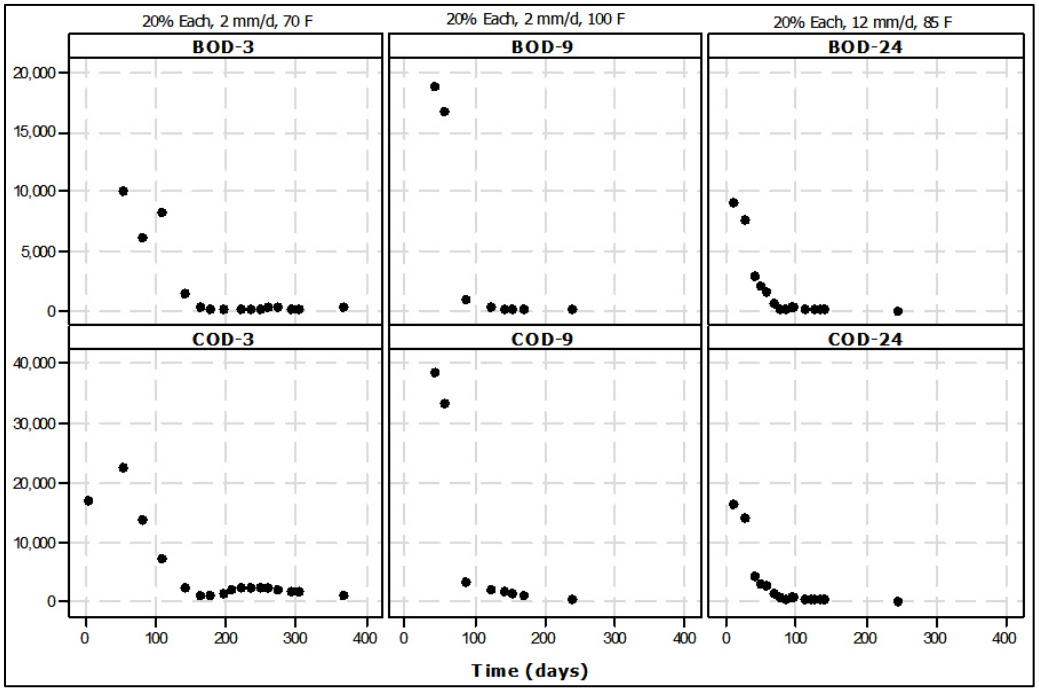

Figure 4-9 BOD and COD Plots of the Waste Composition *i* Reactors

4.1.1 Effects of Temperature and Rainfall Rate on BOD and COD

When waste composition is the same for three reactors, the factors affecting the behavior of BOD and COD become temperature and rainfall rate. All reactors were operated under one of three temperatures, 70 °F (21.1 °C), 85 °F (29.4 °C), or 100 °F (37.8 °C). They were also operated under three rainfall rates, 2 mm/day (100 mL/day), 6 mm/day (300 mL/day), or 12 mm/day (600 mL/day). The data shown in Figures 4-1 to 4-9 clearly indicate that rainfall rate and temperature have a mutual effect on the leaching of organic matter from waste. This will become clearer in the following discussion.

Any reactor that was operated in 85 °F and under either 2 mm/day or 6 mm/day rainfall rates always shows higher levels of BOD and COD than the other two reactors with same waste composition but different temperatures (see Figures 4-1, to 4-4, 4-6, and 4-8). When a 85 °F reactor was operated under 12 mm/day rainfall rate, the 100 °F reactor in same waste composition group showed higher organic content (BOD and COD) in its leachate (see Figures 4-5 and 4-9). This observation suggests that among the three temperatures adopted in this study, 85 °F is probably the closest to being the optimum temperature for microbial growth. Higher microbial growth translates into higher waste decomposition rates. However, when an 85−°F reactor was exposed to 600 mL (12 mm/day rate) of rainfall per day, the story was different. The high rainfall rate caused enough number of microorganisms to be flushed out of the reactor and decreased the waste biodegradation rate.

Reactors 1 through 6 show longer time (180-200 days) to reach minimum or stable BOD and COD concentrations and BOD:COD ratio (will be discussed in the next section) than all other reactors. Those six reactors were all operated under 2-mm/day rainfall rate and either 70 °F or 85 °F temperatures (see Figures 4-1, 4-2, 4-3, 4-7, and 4-9). On the other hand, the 12-mm/day reactors reached BOD and COD stability faster within a given waste composition group. Some researchers attributed low rates of waste stabilization and methane production to low moisture content within the landfill, and others found that higher precipitation rates lead to faster

waste decomposition (Sulfita *et al.*, 1992; Miller *et al.*, 1994). Qasim and Chiang (1994) mentioned an advantage and a disadvantage of applying water to the landfill waste in high rates. The advantage is that water removes most of the waste contaminants especially in the early life of a landfill. The disadvantage is that it also flushes microbes out of the system. Therefore, microbial activity in the landfill would have a much lesser effect on leachate quality.

4.1.2 Waste Composition Effects on BOD and COD

Unlike paper, yard, and textile wastes, the organic constituents of food waste are highly soluble especially in the early stages of the reactor life. Initial moisture content is also much higher in food waste than other waste components. These two properties of food waste make it the favorable for easier biological decomposition. The highest BOD and COD concentrations were recorded in leachates collected from the reactors that contained 100% food waste (R-4 and R-25). Food waste in reactors 4 and 25 underwent nearly complete decomposition. These two reactors were nearly empty when they were dismantled at the end of the experiment. The nine waste compositions used in this study are listed in Table 4-2 and ranked from 1 to 9 according to the peak BOD and COD concentrations recorded for each one.

Based on the reactors that contained one refuse type, Table 4-2 indicates that the order of waste components based on their biodegradability (BOD peak values) is food (46,134 mg/L), yard (12,361 mg/L), paper (10,277 mg/L), and textile (8,960 mg/L). The order appears to be the same for the COD content of the waste. Textile waste was the least favorable to degrade by microbes. Manufacturing textile involves adding large amounts of artificial materials, which probably suppressed microbial activity and the overall leaching process in the 100% textile reactors. The same thing can be said about paper waste to a lesser extent. Also, textile waste could have a filtration effect on leachate and, therefore, decrease its strength.

Table 4-2 BOD and COD Peak Values from Each Waste Composition

BOD Peak Concentrations			
Rank	Waste Composition	Reactor #	BOD (mg/L)
1	100% F	4	46,134
2	30% F + 10% P + 60% Y	2	24,509
3	60% F + 30% X + 10% Y	15	21,928
4	10% F + 30% P + 60% X	6	19,889
5	20% F + 20% P + 20% X + 20% Y + 20% Inorg.	9	18,823
6	100% Y	14	12,361
7	100% P	13	10,277
8	100% X	5	8,960
9	60% P + 40% Inorg.	17	5,460
COD Peak Concentrations			
Rank	Waste Composition	Reactor #	COD (mg/L)
1	100% F	25	64,032
2	30% F + 10% P + 60% Y	18	60,760
3	60% F + 30% X + 10% Y	15	50,756
4	20% F + 20% P + 20% X + 20% Y + 20% Inorg.	9	38,777
5	100% Y	14	30,256
6	100% P	13	20,525
7	10% F + 30% P + 60% X	6	18,129
8	100% X	5	16,054
9	60% P + 40% Inorg.	17	12,356

The BOD:COD ratio is an indicator of the proportion of biologically degradable organic matter to total organic matter (Reinhart & Grosh, 1998). It decreases as the landfill ages. At the final stage of a reactor's life, BOD:COD ratio becomes relatively low (<0.1) because dissolved organic matter that is degradable is consumed as rapidly as it is produced (Barlaz, 2006). BOD:COD ratios for all the reactors were plotted against time (Figure 4-10).

Among all the reactors that contained 100% of one waste component, yard waste (Figure 4-10d) shows the lowest overall BOD:COD ratio. Leachate from yard waste alone was shown above to have higher amounts of BOD and COD than paper waste and textile waste. The ratio ranged from 0.4 to 0.8 in the acidic phase of waste decomposition. The 100% yard

reactors (Figure 4-10d) show a sharp decrease in this ratio from 0.5 to 0.1 within the first 60 days of the reactor's life. Five reactors (1, 2, 4, 20, 21) showed persistent (>0.4) BOD:COD ratio from the beginning of operation until day 200 or later (Figure 4-10a, b, f, g, h). Four of these reactors (2, 4, 20, 21) contained food waste and one reactor (R-1) contained 100% paper waste. It is also important to note that four of those five reactors were operated in the 70 °F room and one reactor was in the 85 °F room. The cause of the persistent BOD:COD ratio in those five reactors could be the presence of food waste, the low temperature (70 °F), or both. In addition, those five reactors show two maxima in their BOD:COD ratio curves. According to Eleazer *et al.* (1997), the occurrence of more than one maxima can be explained by two possible scenarios. The first one is the presence of multiple substrates within a waste component. The second is that as the solid matrix of a waste component changes because of biodegradation, additional organics become bioavailable, which causes the BOD:COD ratio to go up again.

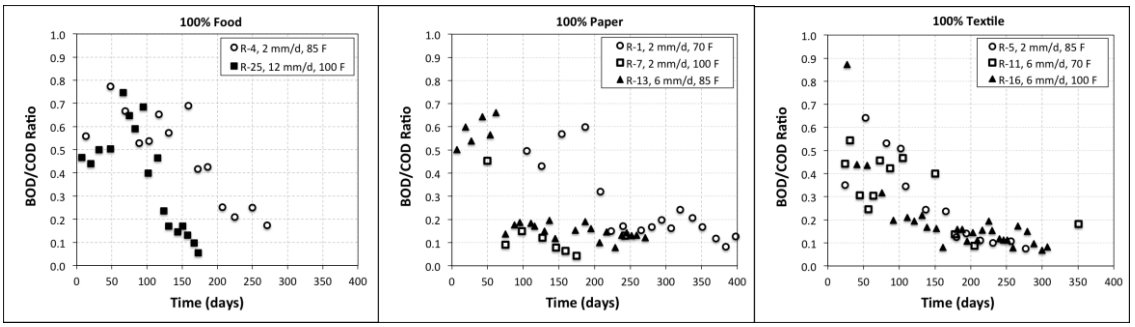

(a) (b) (c)

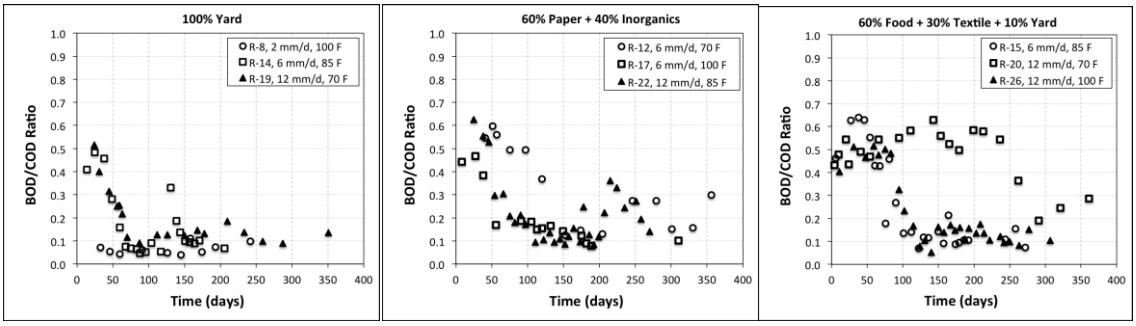

(d) (e) (f)

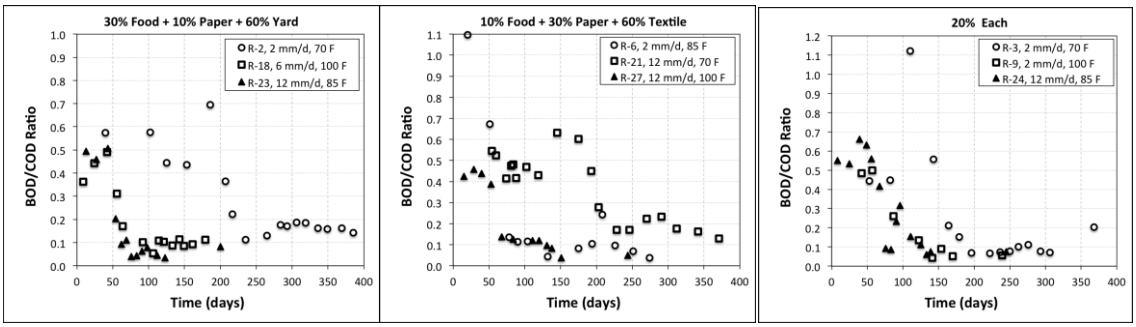

(g) (h) (i)

Figure 4-10 Plots of BOD/COD Ratio vs. Time

4.2 Multiple Linear Regression Analysis

In this chapter, two mathematical relationships were developed using Multiple Linear Regression (MLR) analysis approach. The first one is between the first-order reaction rate constant of leachate COD (k_{COD}) and six parameters that are believed to have an influence on this constant. The second relationship/model is between the first-order reaction rate constant of leachate BOD (k_{BOD}) and the same six parameters. These parameters are rainfall rate, temperature, and fractions of four constituents of municipal solid waste: food, paper, yard, and textile. The initial plan was to include inorganic waste as well, but the five waste components add up to 1.0 in all reactors, which makes them perfectly collinear with each other. Therefore, it was decided to exclude inorganic waste since it has no contribution to the BOD or COD values. Kutner *et al.* (2005) explains in the following quotation why using MLR is the appropriate modeling method in this study.

> Multiple regression analysis is also highly useful in experimental situations where the experimenter can control the predictor variables. An experimenter typically will wish to investigate a number of predictor variables simultaneously because almost always more than one key predictor variable influences the response.

The six predictor variables mentioned above were all well controlled in the lab. The word 'linear' here means linear in the model parameters. This can be clearly seen the general first-order linear relationship between response/dependent variable (Y) and the predictor/independent variables that was used in MLR analysis in this study:

$$Y = \beta_0 + \beta_1 X_1 + \beta_2 X_2 + \beta_3 X_3 + \beta_4 X_4 + \beta_5 X_5 + \beta_6 X_6 + \varepsilon$$

where β_0 to β_6 are the unknown model parameters, X_1 to X_6 are the predictor variables, and ε is the random error term. β_0 is the Y intercept of the regression plane. If all predictor variables equal zero, the response variable Y equals β_0; otherwise β_0 does not mean anything by itself. β_1 represents the change in the response Y per unit increase in X_1 when all other predictor

variables are held constant. The same thing can be said about the other parameters (β_2 to β_6), which are sometimes referred to as *partial regression coefficients*.

The MLR model building process consists of four phases:

1- Data collection and preparation
    a. Choose model response and predictor variables,
    b. Collect data
    c. Fit a preliminary model
        i. Check scatterplots and correlations
        ii. Check model assumptions (no curvature, constant error variance, uncorrelated errors, and normally distributed errors)
        iii. Perform any necessary transformations
        iv. Check model diagnostics (outliers, influence, and multicollinearity).
        v. Explore possibility of interactions
2- Model search

    Find potential best models using three methods: Best Subsets Selection, Stepwise Regression, and Backward Deletion.
3- Model selection
    a. Check model assumptions for potentially best models
    b. Check model diagnostics for potentially best models
4- Model validation

4.3 Obtaining k Values from Experimental Data

The k_{BOD} and k_{COD} values were obtained using the Levenberg-Marquardt algorithm, which is an iterative technique that is used to solve non-linear least squares problems. In other words, this algorithm was applied on BOD and COD data to get their best exponential curve fits. For some reactors, like Reactor # 4 (Figure 4-11), the data shows a rising part and a declining part. In this study, the data used to fit the exponential curve started from the peak BOD or COD value until the end of the reactor's life. Therefore, the fitted curve simulates only the declining part of the data, as shown in Figure 4-11 for Reactor # 4 (R-4). The exponential equation in this figure shows -0.018 day^{-1} as the k_{BOD} value for this reactor. The correlation coefficient (R^2) of the fit is 0.94, which makes it a good curve fit.

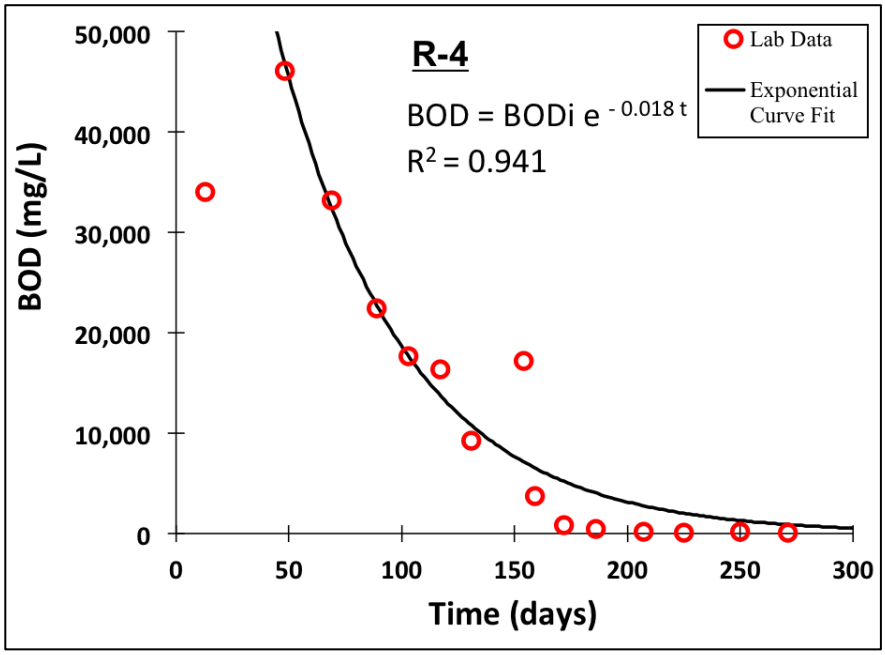

Figure 4-11 BOD Concentration Plot for Reactor 4 Showing Exponential Curve Fit

The R^2 values of all twenty-six COD curve fits are above 0.90. The R^2 values of the twenty-six BOD curve fits are all above 0.85 except for Reactor # 11 (R^2=0.78). Due to the low overall COD and BOD concentration in leachate, It was suspected that reactor #11, among

other reactors, experienced microbial washout due to excessive water addition during the first few days of the experiment. Nevertheless, these reactors' data was included in the modeling dataset. Figure 4-12 shows the BOD fitted exponential curves for six reactors. The rest of the plots can be found in Appendix A. Table 4-3 includes all k_{BOD} and k_{COD} values with reactor number, rainfall rate, temperature, and waste component fractions. All k values have a minus sign since BOD and COD decrease with time, but they are shown as positive for a more convenient linear regression process.

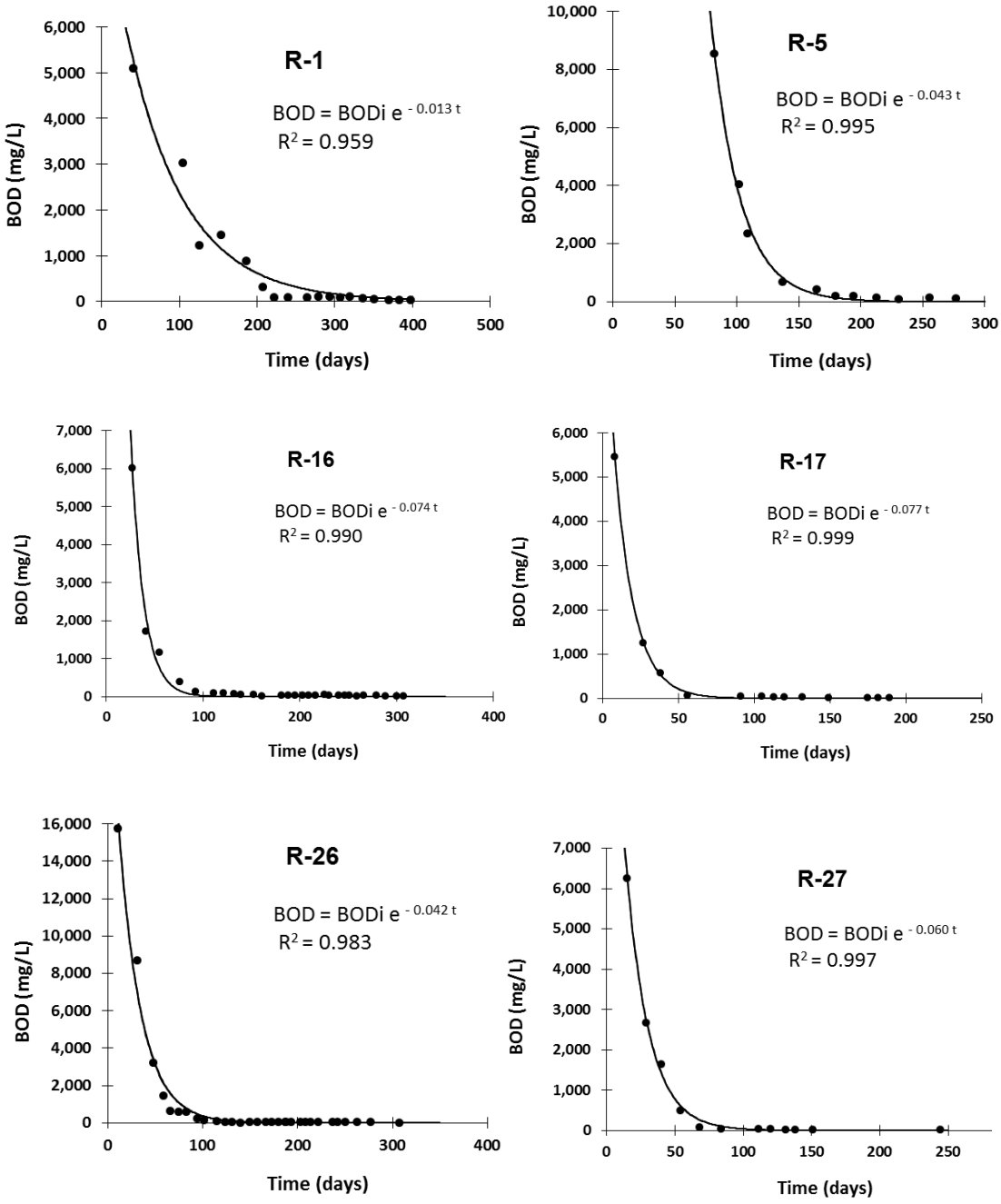

Figure 4-12 BOD Concentration Plots Showing Exponential Curve Fits

Table 4-3 Data Used in the Regression Modeling

R #	k_{BOD} (day^{-1})	k_{COD} (day^{-1})	Rainfall Rate (mm/day)	Temperature (°F)	Waste Fraction By Weight (0-1.0)				
					Food	Paper	Yard	Textile	Inorg.
1	0.013	0.017	2	70	0.0	1.0	0.0	0.0	0.0
2	0.023	0.020	2	70	0.3	0.1	0.6	0.0	0.0
3	0.017	0.019	2	70	0.2	0.2	0.2	0.2	0.2
4	0.018	0.017	2	85	1.0	0.0	0.0	0.0	0.0
5	0.043	0.031	2	85	0.0	0.0	0.0	1.0	0.0
6	0.037	0.021	2	85	0.1	0.3	0.0	0.6	0.0
7	0.129	0.059	2	100	0.0	1.0	0.0	0.0	0.0
8	0.021	0.017	2	100	0.0	0.0	1.0	0.0	0.0
9	0.035	0.032	2	100	0.2	0.2	0.2	0.2	0.2
11	0.019	0.021	6	70	0.0	0.0	0.0	1.0	0.0
12	0.045	0.026	6	70	0.0	0.6	0.0	0.0	0.4
13	0.040	0.043	6	85	0.0	1.0	0.0	0.0	0.0
14	0.045	0.040	6	85	0.0	0.0	1.0	0.0	0.0
15	0.026	0.028	6	85	0.6	0.0	0.1	0.3	0.0
16	0.074	0.033	6	100	0.0	0.0	0.0	1.0	0.0
17	0.077	0.076	6	100	0.0	0.6	0.0	0.0	0.4
18	0.032	0.036	6	100	0.3	0.1	0.6	0.0	0.0
19	0.073	0.044	12	70	0.0	0.0	1.0	0.0	0.0
20	0.042	0.044	12	70	0.6	0.0	0.1	0.3	0.0
21	0.018	0.031	12	70	0.1	0.3	0.0	0.6	0.0
22	0.112	0.087	12	85	0.0	0.6	0.0	0.0	0.4
23	0.070	0.064	12	85	0.3	0.1	0.6	0.0	0.0
24	0.036	0.036	12	85	0.2	0.2	0.2	0.2	0.2
25	0.043	0.043	12	100	1.0	0.0	0.0	0.0	0.0
26	0.042	0.048	12	100	0.6	0.0	0.1	0.3	0.0
27	0.060	0.059	12	100	0.1	0.3	0.0	0.6	0.0

4.4 Modeling k_{COD}

4.4.1 Scatter Plots Matrix and Correlation Matrix

Before fitting a preliminary regression model, the relationship and correlation between k_{COD} and each predictor variable should be evaluated for any existing trends. Also, the predictor-predictor relationships have to be checked for possible multicollinearity. The matrix of scatter plots in Figure 4-13 and the correlation matrix in Table 4-4 were utilized for this purpose. From the matrix of plots below, an upward linear trend was clear between k_{COD} and Rainfall and Temperature. Also, it was surprising to see a slightly declining trend between k_{COD} and each of the Food, Yard, and Textile waste components. Theoretically, it is expected that the exponential decay rate of leachate COD (k_{COD}) will increase when the amount of organics increases. k_{COD} combines two waste decomposition mechanisms in landfills: leaching and degradation via microorganisms. This is also true for k_{BOD}. This issue is discussed thoroughly at the end of this chapter. The scatter plot of k_{COD} vs. Paper did not show a clear trend. There was a slight downward trend in three predictor-predictor scatter plots: Food vs. Paper, Paper vs. Yard, and Yard vs. Textile. This observation might indicate presence of multicollinearity among predictor variables. For the MLR analysis to work, predictor variables have to be independent from each other. The following steps will determine whether the observed multicollinearity is serious or can be ignored.

The matrix of Pearson correlation coefficients (Table 4-4) is another way of evaluating linear dependence among variables. Each value in this matrix is called Pearson's *r*. The *r*-value ranged between -1 and 1 and the closer this value was to 1 or -1, the stronger the positive or negative linear correlation between the two variables. None of the predictor variables had a strong positive/negative linear correlation with k_{COD} ($-0.222 \leq r \leq 0.564$). k_{COD} was positively correlated with Rainfall ($r = 0.564$) and Temperature ($r = 0.373$) and negatively correlated with Food ($r = -0.122$), Yard ($r = -0.094$) and Textile ($r = -0.222$). There were moderately high intercorrelations among predictor variables: Food vs. Paper ($r = -0.441$), Paper vs. Yard ($r =$ -

0.395), Paper vs. Textile (r = -0.326), and Yard vs. Textile (r = -0.395). As mentioned above, the significance of multicollinearity in the predictor variables will be determined later and the decision will be made whether to keep all of the predictors or remove any of them. These observations were consistent with the scatter plots above.

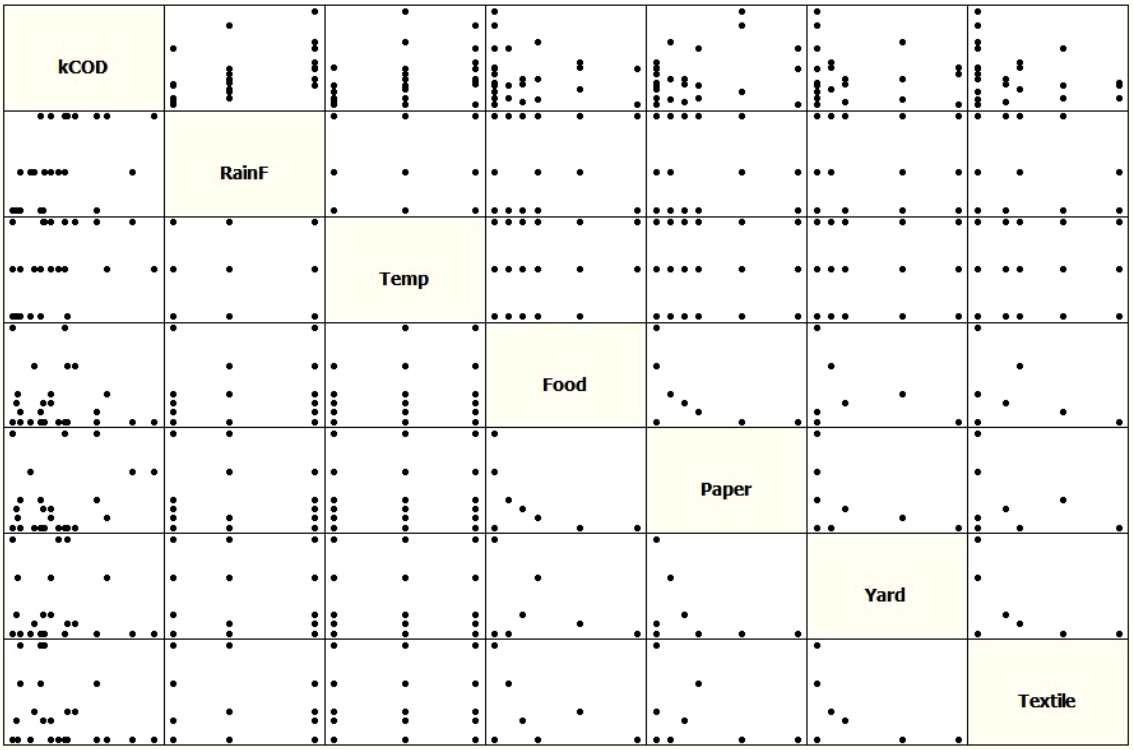

Figure 4-13 Matrix of Scatter Plots

Table 4-4 Correlation Matrix of k_{COD} and the Predictor Variables

	kCOD	RainF	Temp	Food	Paper	Yard	Textile
RainF	0.564	1.000					
Temp	0.373	-0.008	1.000				
Food	-0.122	0.196	0.126	1.000			
Paper	0.277	-0.189	-0.037	-0.441	1.000		
Yard	-0.094	0.001	-0.031	-0.148	-0.395	1.000	
Textile	-0.222	-0.010	-0.034	-0.199	-0.326	-0.395	1.000

Cell Contents: Pearson correlation

4.4.2 Fitting a Preliminary Model

Table 4-5 shows results of regressing k_{COD} on all six predictors: Rainfall, Temperature, Food, Paper, Yard, and Textile. The table contains the preliminary model, coefficient estimates, and the ANOVA (Analysis of Variance) table.

Table 4-5 Preliminary Model, Parameter Estimates and the ANOVA Table

```
kCOD = - 0.0063 + 0.00275 RainF + 0.000614 Temp - 0.0381 Food -
       0.0152 Paper - 0.0285 Yard - 0.0338 Textile

Predictor       Coef    SE Coef      T      P    VIF

Constant    -0.00628    0.02491  -0.25  0.804
RainF        0.00275    0.00057   4.81  0.000  1.077
Temp         0.000614   0.00019   3.20  0.005  1.018
Food        -0.03809    0.01921  -1.98  0.062  6.135
Paper       -0.01522    0.02203  -0.69  0.498  9.937
Yard        -0.02853    0.01901  -1.50  0.150  7.812
Textile     -0.03382    0.01869  -1.81  0.086  7.458

S = 0.0117437   R-Sq = 69.6%   R-Sq(adj) = 60.0%

                    Analysis of Variance

Source          DF         SS         MS     F      P
Regression       6  0.0060050  0.0010008  7.26  0.000
Residual Error  19  0.0026204  0.0001379
Total           25  0.0086254
```

4.4.3 Model Assumptions Check

Before analyzing the preliminary MLR model in details, it should be checked whether the model assumptions are satisfied. These assumptions are:

A- The linear MLR model form is reasonable.

B- The residuals have constant variance.

C- The residuals are normally distributed.

D- The residuals are uncorrelated.

Also, the model must be checked to make sure that:

E- There are no outliers, and that

F- Multicollinearity among predictor variables is not serious.

Residual analysis is very helpful to study the model assumptions and check whether they are satisfied. A residual value (e_i) is the difference between the observed value of the response variable ($\mathrm{k_{CODi}}$) and the fitted value ($\hat{\mathrm{k}}_{\mathrm{CODi}}$).

Assumption A:

The MLR model form can be checked using the matrix of scatter plots that was discussed above. It was observed from that matrix that the response-predictor plots showed some linear trends even though some of them were hard to see. Another way of checking this assumption is to plot residuals vs. predictor variables (Figure 4-14). If these do not show curvature, the linear model form assumption is verified. From Figure 4-14, the Residual vs. Food plot and Residual vs. Yard plot both showed curvature. This means that assumption A was violated and remedial measures should be considered to solve the issue. Model transformations were conducted after all assumptions were checked.

Assumption B:

A plot of residuals versus fitted values can verify whether this assumption is satisfied. If this plot does not show funneling, then it indicates that the residuals have a constant variance. From Figure 4-15, it appeared that a slight funnel shape was present, which meant that the constant variance assumption was violated.

Assumption C:

A Normal Probability Plot is used to check whether the residuals are normally distributed. In this plot, each residual is plotted against its expected value under normality. If this plot shows a linear trend, it suggests that the model's normality assumption is satisfied. Figure

4-16 shows this plot for the preliminary MLR model. It seemed that the points had shorter left and right tails, which indicates that the normality assumption was not satisfied.

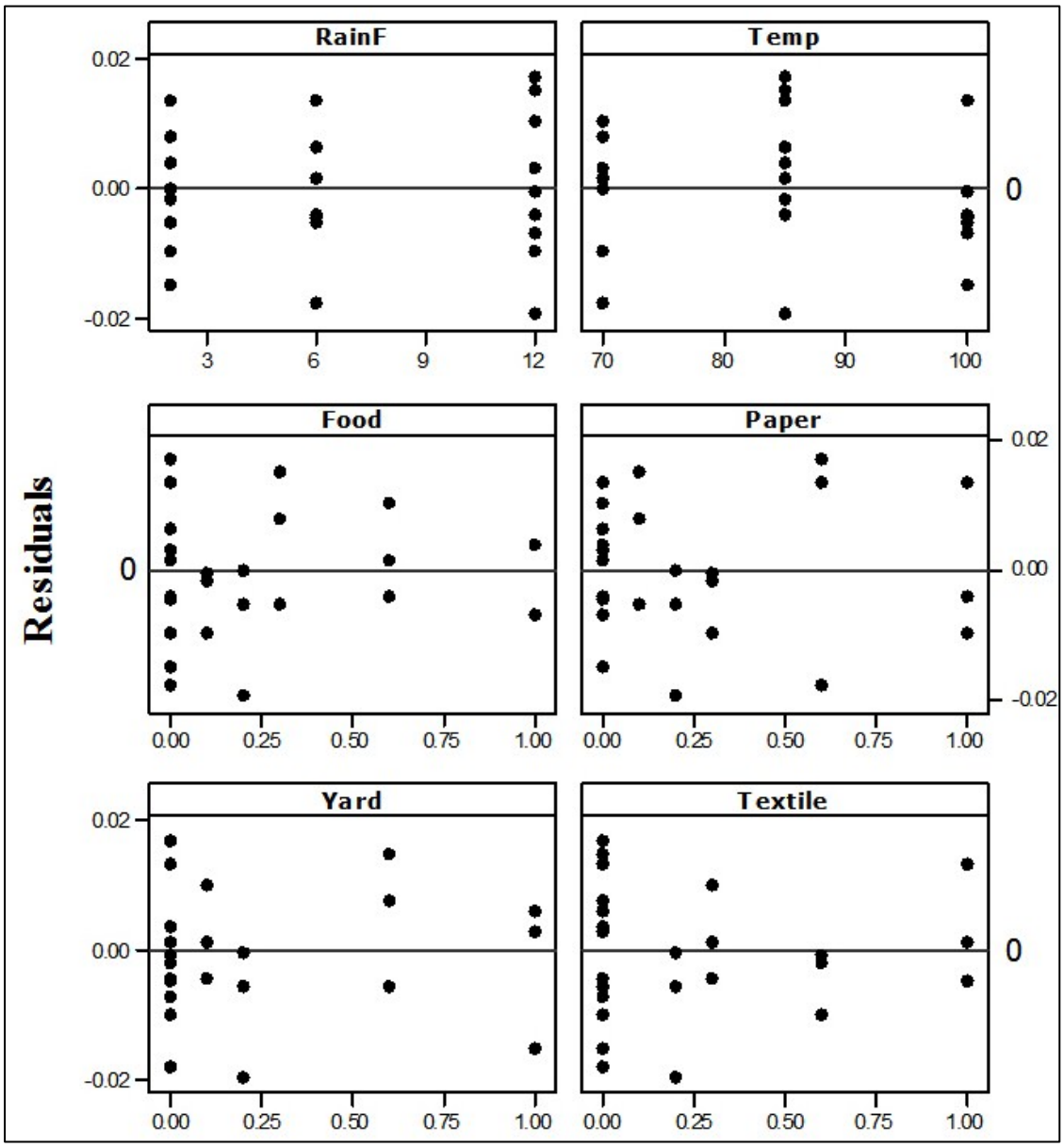

Figure 4-14 Residual vs. Predictor Plots

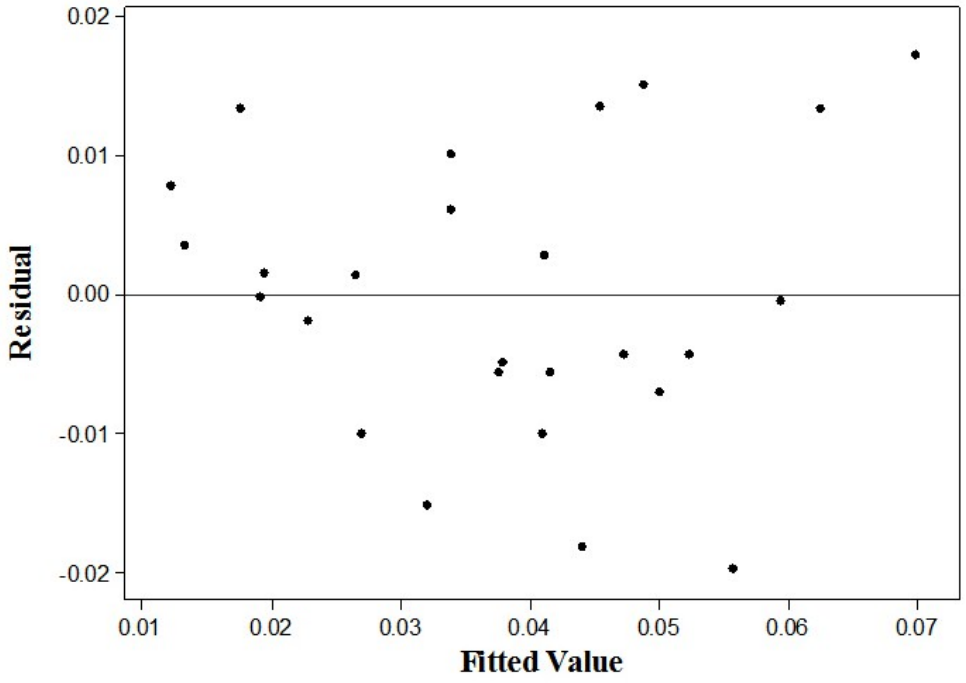

Figure 4-15 Plot of Residuals vs. k_{COD} Fitted Values

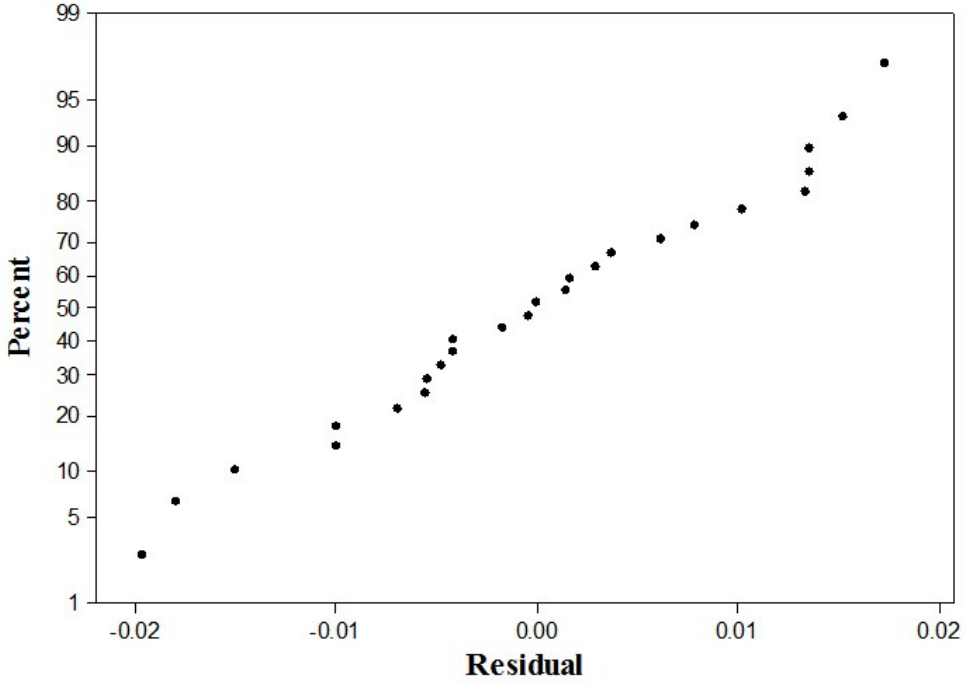

Figure 4-16 Normal Probability Plot

Assumption D:

Since the reactors were operated at the same point of time, they were not expected to be autocorrelated. Hence, this assumption was not checked in this study.

Before moving on to outlier analysis, model transformations will be discussed next.

4.4.4 Transformations

When the linearity assumption and/or the constant variance assumption are violated, transformations can be used to make the linear regression model appropriate for the transformed data. Sometimes a transformation of response variable alone fixes both linearity and constant variance assumptions. If curvature remains present, then additional transformations on the predictor variables can be attempted to address this.

The first step was to transform the response variable k_{COD} into the square root of k_{COD} and check the constant variance and normality assumptions after fitting the regression model with $\sqrt{k_{COD}}$ as the response variable. The residual plots of the new model can be seen in Appendix B. It looked like this first transformation attempt fixed the constant variance assumption, but the normal probability plot still showed left and right short tails. Also, the two plots of Residual vs. Food and Residual vs. Yard showed curvature. Therefore, linear model form and normality assumptions were still in question.

The second transformation attempt was to take the logarithm (base 10) of the response variable, $Log_{10}(k_{COD})$. After fitting the model, both residual vs. fits and normal probability plots improved (see Appendix B). This means that normality and constant variance assumptions were satisfied. However, curvature still appeared in Residual vs. Food and Residual vs. Yard plots (see Appendix B). So, the linearity assumption was not yet satisfied.

Further response variable transformations were not attempted it the response was kept as $Log_{10}(k_{COD})$. However, two predictor variables (Food and Yard) were transformed into

$\sqrt{Food}$ and $\sqrt{Yard}$ in an attempt to mitigate the curvilinear patterns and satisfy the linearity assumption. The regression model was fitted and it turned out that this combination of variable transformations was the best in terms of satisfying the MLR model assumptions as the next few paragraphs and figures will show.

The transformed model was:

$$Log_{10}(k_{COD}) = -2.28 + 0.0350R + 0.00713T - 0.128\sqrt{F} + 0.130P - 0.009\sqrt{Y} - 0.067X$$

where R=Rainfall, T=Temperature, F=Food, P=Paper, Y=Yard, and X=Textile.

The transformed model's parameter estimates are shown in Table 4-6. Overall, there was a low to moderate level of multicollinearity for this model (all VIFs < 5 except one value). Before analyzing the transformed mode, a re-check of the model assumptions had to be made.

Table 4-6 Parameter Estimates of the Transformed Model

Predictor	Coef	SE Coef	T	P	VIF
Constant	-2.2826	0.2403	-9.50	0.000	
R	0.034975	0.006080	5.75	0.000	1.073
T	0.007125	0.002049	3.48	0.003	1.021
sqrt(F)	-0.1278	0.1166	-1.10	0.287	2.580
P	0.1303	0.1725	0.76	0.459	5.355
sqrt(Y)	-0.0094	0.1325	-0.07	0.944	3.883
X	-0.0669	0.1428	-0.47	0.645	3.825

Assumption A: From the six residual-predictor plots shown in Figure 4-17, slight curvature still appeared in the $\sqrt{F}$ plot and the Textile plot, but the curvature was not clear, and the plots could not be further improved with further transformations. Hence, it was concluded that the linear model form was acceptable.

Assumption B: Figure 4-18 does not exhibit a funnel shape, so, the constant variance assumption was satisfied.

Assumption C: The normal probability plot in Figure 4-19 shows a slightly shorter right tail than normality. However, the linearity in the plot is mostly straight, so normality appears mostly reasonable. Modified Levene Test and Normality Test were performed (see Appendix B) to confirm that transformed model satisfied the constant variance and normality assumptions.

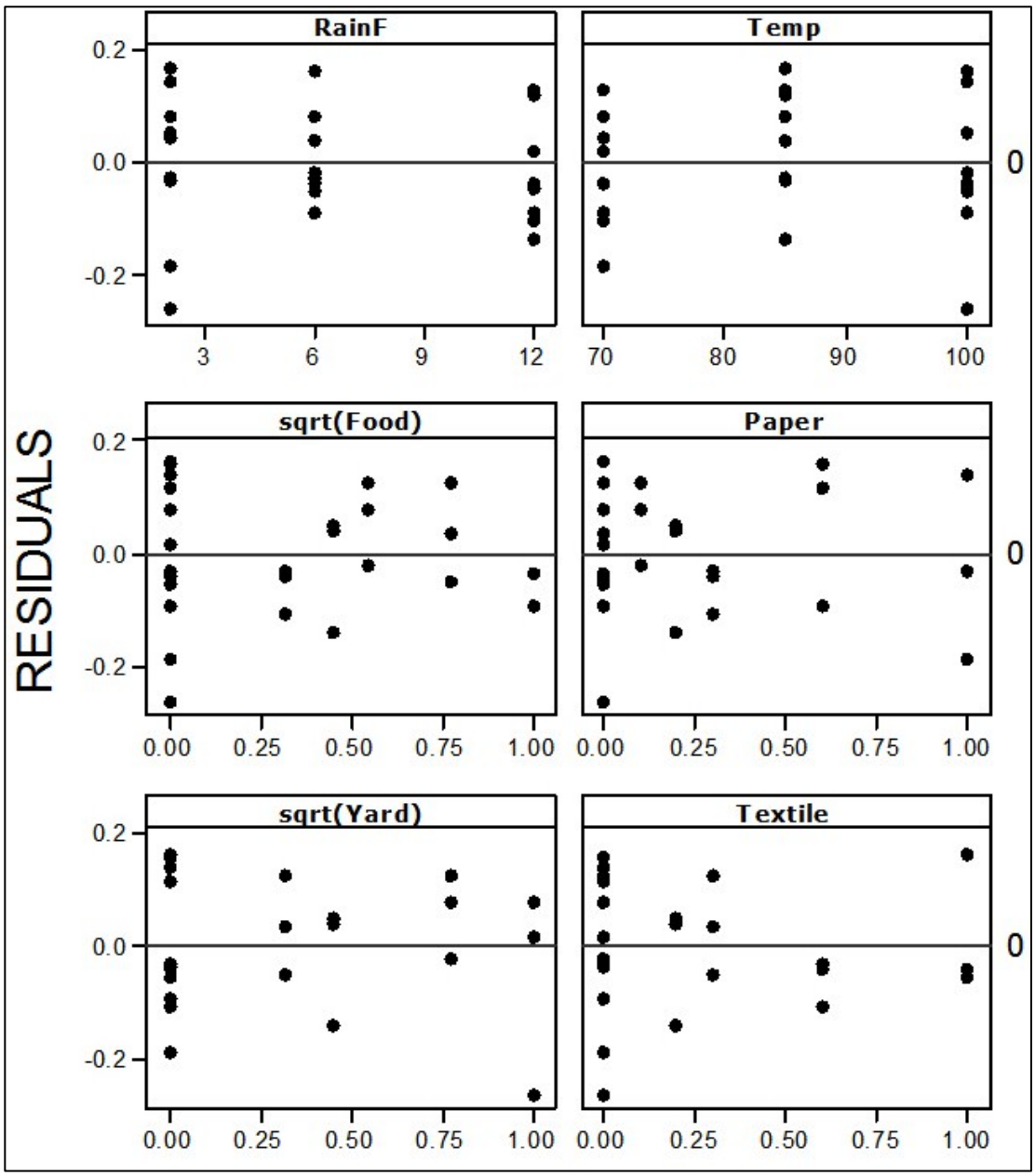

Figure 4-17 Residual-Predictor Plots of the Transformed Model

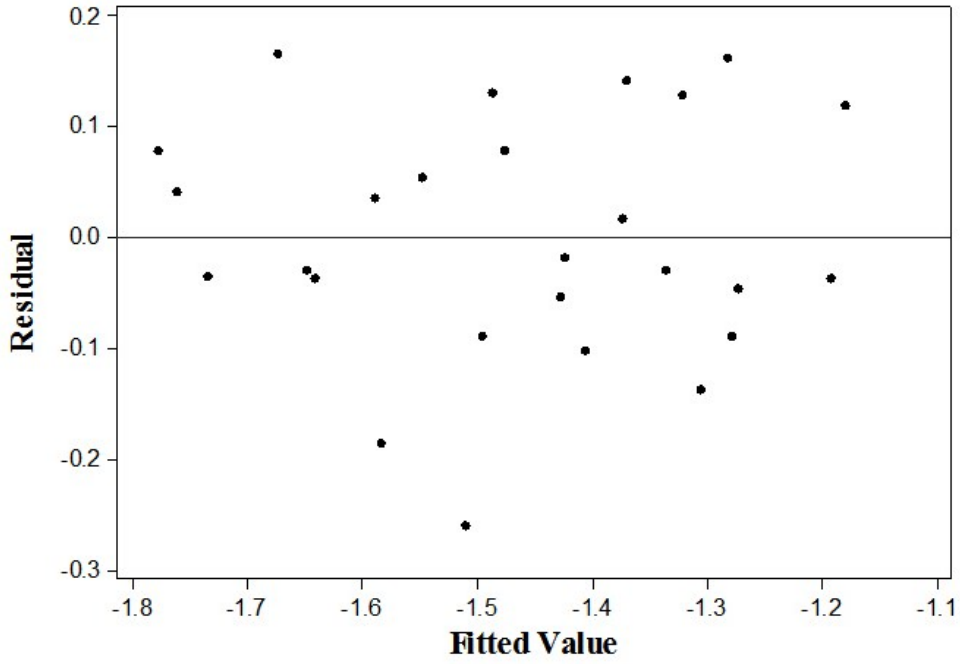

Figure 4-18 Transformed Model's Plot of Residuals vs. Fitted Values

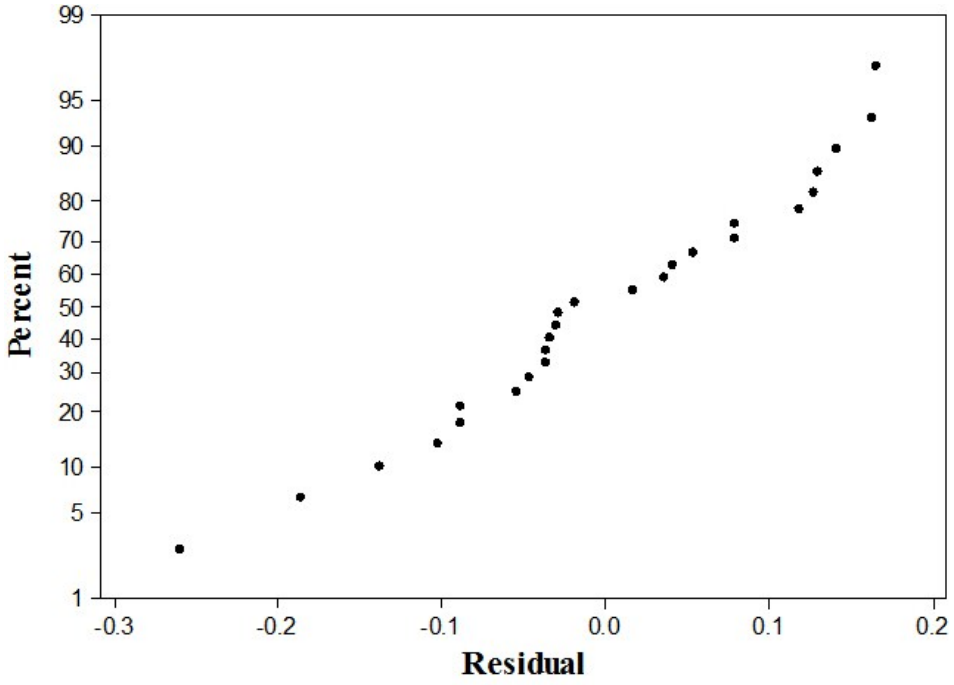

Figure 4-19 Normal Probability Plot of the Transformed Model

Outlier Analysis:

An outlier is an extreme observation that is distant from the rest of the data. There are two types of outliers: x-outliers and y-outliers. Once an outlier has been identified, its influence on the regression is evaluated.

Leverage values (h_{ii}) are used to identify x-Outliers. If $h_{ii} > \frac{2p}{n}$, then observation *i* is an x-outlier, where *p* is the number of parameters and *n* is the number of observations. In the case of this study's data, $\frac{2p}{n} = \frac{2(7)}{26} = 0.538$ and the maximum h_{ii} value from Table 4-7 was 0.501; therefore, there were no x-outliers.

The Bonferroni test is used to identify y-Outliers. If $|t_i| > t\left(1 - \frac{\alpha}{2n}; n - p - 1\right)$, then observation *i* is a y-outlier. The absolute Studentized Deleted Residuals $|t|$ for this study's data are shown in Table 4-7. Choosing the confidence level to be 90%:

$$Bonferroni: t\left(1 - \frac{0.1}{2(26)}; 26 - 7 - 1\right) = t(0.99809; 18) = 3.316$$

All $|t|$ values in Table 4-7 were less than 3.316; therefore, there were no y-outliers.

ANOVA of the Transformed Model (Table 4-8):

- SSTO (Total Sum of Squares) = 1.054.
- SSE (Error Sum of Squares) = 0.298.
- SSR (Regression Sum of Squares) = 0.756.

SSTO is the measure of total variability in the values of $Log_{10}(k_{COD})$; the purpose of the regression model is to seek predictor variables that explain this variability. SSR is the measure of variability of $Log_{10}(k_{COD})$ values that is explained by the current model. Finally, SSE is the measure of variability of the $Log_{10}(k_{COD})$ values that is not explained by the current model.

Table 4-7 Residuals, Leverage Values, and Studentized Deleted Residuals

Observation	e_i	h_{ii}	$\|t_i\|$
1	-0.186	0.325	1.932
2	0.079	0.267	0.729
3	0.041	0.184	0.357
4	-0.035	0.501	0.383
5	0.165	0.308	1.658
6	-0.029	0.155	0.248
7	0.141	0.336	1.414
8	-0.260	0.367	3.167
9	0.054	0.173	0.464
10	-0.037	0.320	0.348
11	-0.089	0.289	0.837
12	-0.030	0.256	0.268
13	0.079	0.260	0.720
14	0.036	0.128	0.303
15	-0.054	0.327	0.518
16	0.163	0.261	1.570
17	-0.019	0.204	0.167
18	0.017	0.384	0.169
19	0.130	0.229	1.191
20	-0.103	0.237	0.938
21	0.119	0.294	1.136
22	0.128	0.201	1.150
23	-0.138	0.127	1.190
24	-0.088	0.410	0.914
25	-0.046	0.210	0.406
26	-0.037	0.249	0.335
Max		0.501	3.167

R^2 is the coefficient of determination. It was calculated as follows:

$$R^2 = \frac{SSR}{SSTO} \times 100 = \frac{0.756}{1.054} \times 100 = 71.7\%,$$

and it can be interpreted as the percentage of total variability of the $Log_{10}(k_{COD})$ values that is explained by the model.

Table 4-8 ANOVA Table of the Transformed Model

Analysis of Variance

Source	DF	SS	MS	F	P
Regression	6	0.75583	0.12597	8.03	0.000
Residual Error	19	0.29820	0.01569		
Total	25	1.05402			

S = 0.125278 R-Sq = 71.7% R-Sq(adj) = 62.8%

4.4.5 Interaction Terms

In some cases, two of the predictor variables may have an interaction effect on the model instead of an additive effect. The following is an example of this case:

$Y = \beta_0 + \beta_1 X_1 + \beta_2 X_2$→ Additive Effect,

$Y = \beta_0 + \beta_1 X_1 + \beta_2 X_2 + \beta_3 X_1 X_2$→ Interaction Effect.

The term $\beta_3 X_1 X_2$ is referred to as interaction term. In this section, only the possibility and the method of adding interaction terms to the model will be discussed. Interpretation of these terms, if any, will be discussed after finalizing the best model.

Because there were already six predictor variables in the model, adding more could further complicate it. For this reason, Partial Regression Plots were used to determine which interaction term(s) might improve the model if added to it. A partial regression plot is created in three steps:

a- Regressing the response variable $Log_{10}(k_{COD})$ on the six original predictors $(R, T, \sqrt{F}, P, \sqrt{Y}, X)$ and calculating the residuals of this regression,

b- Regressing the interaction term (example: RX) on the six original predictors and calculating the residuals of this regression,

c- Plotting residual from step (a) versus residual from step (b).

After that, if any of these plots show a reasonable linear trend, it suggests that the associated interaction term could improve the model if added to it. Figure 4-20 shows the three plots where good linear trends were observed (the rest of the partial regression plots can be seen in Appendix B). Therefore, it was decided to add those three interaction terms (*RX, TP*, and $T\sqrt{Y}$) to the model. Before adding the terms, it was important to check whether they are highly correlated with the original predictor variables. Table 4-9 shows the correlation matrix of the interaction terms to be against all original variables. All three terms were highly correlated (High *r* values in the table were *italicized*) with at least one original predictor variable. Standardizing an interaction term usually mitigates its high multicollinearity with original predictors. Here is an example of standardizing an interaction term:

$$std(RX) = \left(\frac{R_i - \bar{R}}{S_R}\right)\left(\frac{X_i - \bar{X}}{S_X}\right)$$

where $std(RX)$ is the standardized RX term, $\overline{R}$ is the average rainfall, and S_R is the standard deviation of rainfall. The same can be said about X. The lower part of Table 4-9 shows the correlation matrix of the standardized terms against the original model variables. It was clear from the *italicized r* values that the multicollinearity problem was solved by standardizing the interaction terms.

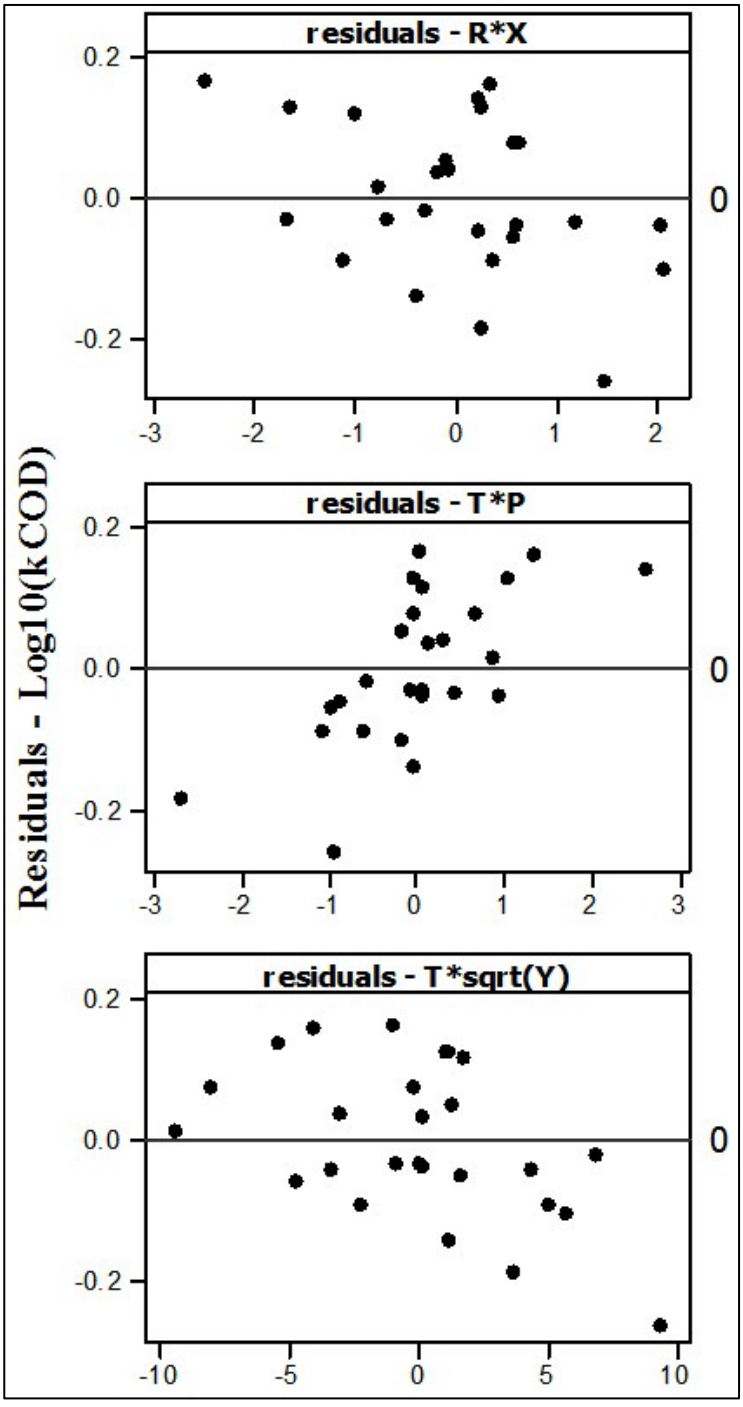

Figure 4-20 Partial Regression Plots

Table 4-9 Correlation Matrix of the Interaction Terms

	LOG10(kCOD)	R	T	rtF	P	rtY	X
RX	0.02998	0.38003	-0.03196	0.00287	-0.25776	-0.35005	*0.79088*
TP	0.30163	-0.18373	0.07429	-0.46777	*0.98386*	-0.45004	-0.32048
TrtY	-0.08513	-0.00098	0.07728	0.05797	-0.44982	*0.98337*	-0.39754
Std(RX)	-0.17426	-0.06878	0.00728	0.11151	0.25863	0.03517	*-0.29223*
Std(TP)	0.38062	0.02874	0.01855	-0.0511	*-0.01929*	0.05096	0.04175
Std(TrtY)	-0.38116	-0.20926	0.01932	-0.07949	0.05100	*-0.01696*	0.04657

4.4.6 Model Search

After considering the three interaction terms to be added to the model, the number of possible predictor variables (*p*) became 9:

$$R, T, \sqrt{F}, P, \sqrt{Y}, X, std(RX), std(TP), std(T\sqrt{Y})$$

The number of possible models that could be formed from 9 predictor variables was 256 ($2^{(p-1)} = 2^{(8)} = 256$ models). It would have taken too long to assess each possible model to determine the best one to explain the variability in the k_{COD} data. Instead, three model search methods with time saving algorithms were used in this study to achieve this goal. The three methods, Best Subsets, Backward Elimination, and Stepwise Selection, were conducted using the SAS software program.

Method 1: Best Subsets

Best subsets algorithms identify the best model based on certain criteria. The user chooses the number of best models to be fitted and the number of variables in each model. Five criteria were used in this method to recognize the best models:

1- R^2 (the coefficient of multiple determination) explains the total variability in the fitted $Log_{10}(k_{COD})$ data that is explained by the model. R^2 always increases as more predictor variables are added to the model. The intent here was to find the point where this value does not increase much by adding more predictors to the model.

2- R^2_{adj} (the adjusted coefficient of multiple determination) does not account for the number of predictors in the regression model, which makes it a better criterion than R^2. R^2_{adj} increases only if the added predictor variable improves the model. Also, an R^2_{adj} close to R^2, indicates the model does not contain unimportant variables.

3- *C(p)* (Mallow's criterion) is a measure of the total mean squared error of the fitted values. A lower the *C(p)* value with *C(p)* close to *p* is preferred.

4- *AIC* (Akaike's information criterion): Models with small *AIC* are preferred.

5- *SBC* (Schwarz' Bayesian criterion): Models with small *SBC* are preferred.

The best subsets algorithm was run using a 0.1 significance level. Two potentially good models (highlighted in Table 4-10) were identified using this method; the first model has five predictor variables and the second has six. These two models were chosen because their *C(p)*, *AIC*, and *SBC* values were the lowest among all other possible models. When the six-variable model was fitted, it showed one statistically insignificant (*p-value* > 0.1) predictor ($\sqrt{Y}$). Therefore, this model was removed from consideration. The 4-predictor model was not considered because it showed higher *C(p)*, *AIC*, and *SBC* values, and lower R^2_{adj} and R^2 values than the 5-predictor model.

Method 2: Backward Elimination

In this method, all predictor variables are included in the model as the first step. In the next step, the predictor variable with the highest *p-value* (denoted Pr > F in Table 4-11) that

exceeds a predetermined level (α = 0.1 in this case) is considered insignificant, and it is removed from the model. The second step is repeated, as many times as needed, until all

Table 4-10 MINITAB Output of Best Subsets Model Search Method

No. of Model Variables	R-Sq(adj)	R-Sqr	C(p)	AIC	SBC	Variables in
4	0.7831	0.8178	10.0120	-117.5902	-111.29968	R T P Std(TP)
5	0.8325	0.8660	5.1312	-123.5784	-116.02978	R T P Std(RX) Std(TP)
6	0.8409	0.8791	5.2638	-124.2488	-115.44210	R T P rtY Std(RX) Std(TP)
7	0.8384	0.8836	6.6149	-123.2449	-113.18009	R T rtF P X Std(RX) Std(TP)
8	0.8349	0.8878	8.0266	-122.1822	-110.85936	R T rtF P X Std(RX)Std(TP) Std(TrtY)

remaining predictor variables in the model are statistically significant (their *p-values* are below 0.1). This final step is shown in Table 4-11 where only one potentially good model was left. The model had five predictor variables:

$$R, T, P, std(RX), std(TP)$$

Method 3: Stepwise Selection

This method starts with no predictor variables in the model. The variables are entered in the model and removed from it according to two predetermined limits (α_{in} = 0.1 and α_{out} = 0.1). The process is done in steps like the previous method and only one potentially good model is left in the final step. The final model determined by this method was the same as that determined by the previous two methods (see Table 4-12). To summarize, the three model-search methods were all pointing to one potentially good model. The next step is to verify whether this model satisfies the model assumptions.

Table 4-11 MINITAB Output of the Backward Elimination Model Search Method

The REG Procedure
Model: MODEL1
Dependent Variable: LOG10kCOD
Backward Elimination: Step 4
Variable X Removed: R-Square = 0.8660 and C(p) = 5.1312

Analysis of Variance

Source	DF	Sum of Squares	Mean Square	F Value	Pr > F
Model	5	0.91371	0.18274	25.86	<.0001
Error	20	0.14136	0.00707		
Corrected Total	25	1.05507			

Variable	Parameter Estimate	Standard Error	Type II SS	F Value	Pr > F
Intercept	-2.34153	0.12298	2.56233	362.53	<.0001
R	0.03328	0.00401	0.48606	68.77	<.0001
T	0.00690	0.00136	0.18131	25.65	<.0001
P	0.25563	0.05267	0.16652	23.56	<.0001
Std(RX)	-0.05644	0.02104	0.05084	7.19	0.0143
Std(TP)	0.07393	0.01709	0.13224	18.71	0.0003

All variables left in the model are significant at the 0.100 level.

Table 4-12 MINITAB Output of the Stepwise Selection Model Search Method

The REG Procedure
Model: MODEL1
Dependent Variable: LOG10kCOD
Stepwise Selection: Step 5
Variable Std(RX) Entered: R-Square = 0.8660 and C(p) = 5.1312

Analysis of Variance

Source	DF	Sum of Squares	Mean Square	F Value	Pr > F
Model	5	0.91371	0.18274	25.86	<.0001
Error	20	0.14136	0.00707		
Corrected Total	25	1.05507			

Variable	Parameter Estimate	Standard Error	Type II SS	F Value	Pr > F
Intercept	-2.34153	0.12298	2.56233	362.53	<.0001
R	0.03328	0.00401	0.48606	68.77	<.0001
T	0.00690	0.00136	0.18131	25.65	<.0001
P	0.25563	0.05267	0.16652	23.56	<.0001
Std(RX)	-0.05644	0.02104	0.05084	7.19	0.0143
Std(TP)	0.07393	0.01709	0.13224	18.71	0.0003

4.4.7 Checking the Selected Model's Assumptions

Figures 4-21, 4-22, and 4-23 are the selected model's residual plots. The residual-predictor plots in Figure 4-21 did not show serious curvature or funneling and neither did the plot of residuals vs. fitted values (Figure 4-22). So, the linearity and constant variance assumptions were satisfied. The normal probability plot in Figure 4-23 showed a strong linear trend; therefore, normality was reasonable. Two hypothesis tests were performed to confirm whether the selected model satisfied the constant variance and normality assumptions.

Modified Levene Test is a tool that is to test whether the residuals have a constant variance. It divides the 26 residuals, at their median value, into two groups of 13 observations each; d_1 and d_2. Variances $(\sigma_{d_1}, \sigma_{d_2})$ of the two groups are then tested to check whether they are equal.

1- F-test

- Hypothesis:

$$H_0 : \sigma_{d_1} = \sigma_{d_2}$$

$$H_1 : \sigma_{d_1} \neq \sigma_{d_2}$$

- Decision Rule:

If the p-value from the F-test is < 0.1, then reject H_0.

Table 4-13 is SAS output of the Modified Levene Test (also called Brown and Forsythe test). The F-test p-value (denoted Pr > F) was 0.4842 > 0.1, so failed to reject H_0.

- Conclusion:

Variances of d_1 and d_2 were equal.

2- T-test was performed to check whether the means of d_1 and d_2 populations were equal.

- Hypothesis:

H_0 : $error\ variance\ is\ constant$

H_1 : $error\ variance\ is\ not\ constant$

- Decision Rule:

If the p-value from the t-test is < 0.1, then reject H_0.

The p-value from Table 4-13 (pooled- Pr > | t |) was 0.8459 > 0.1, so failed to reject H_0.

- Conclusion:

The model's error variance was constant.

Table 4-13 SAS Output of Modified Levene Test

The TTEST Procedure
Variable: d

group	N	Mean	Std Dev	Std Err	Minimum	Maximum
1	13	0.0550	0.0547	0.0152	0	0.1460
2	13	0.0589	0.0445	0.0123	0	0.1561
Diff (1-2)		-0.00384	0.0498	0.0195		

Method	Variances	DF	t Value	Pr > |t|
Pooled	Equal	24	-0.20	0.8459
Satterthwaite	Unequal	23.041	-0.20	0.8460

Equality of Variances

Method	Num DF	Den DF	F Value	Pr > F
Folded F	12	12	1.51	0.4842

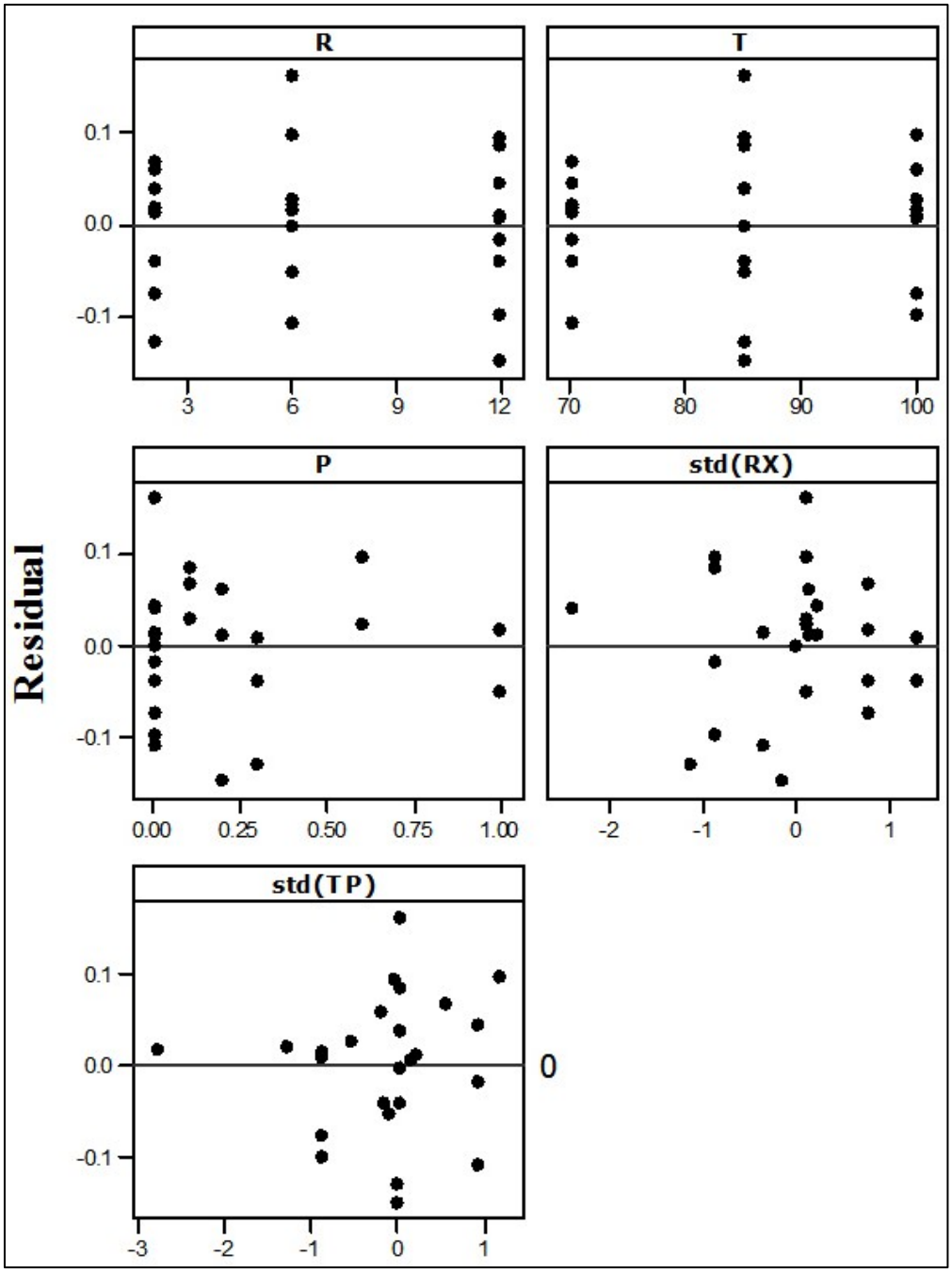

Figure 4-21 Residuals vs. Predictor Plots of the Selected Model

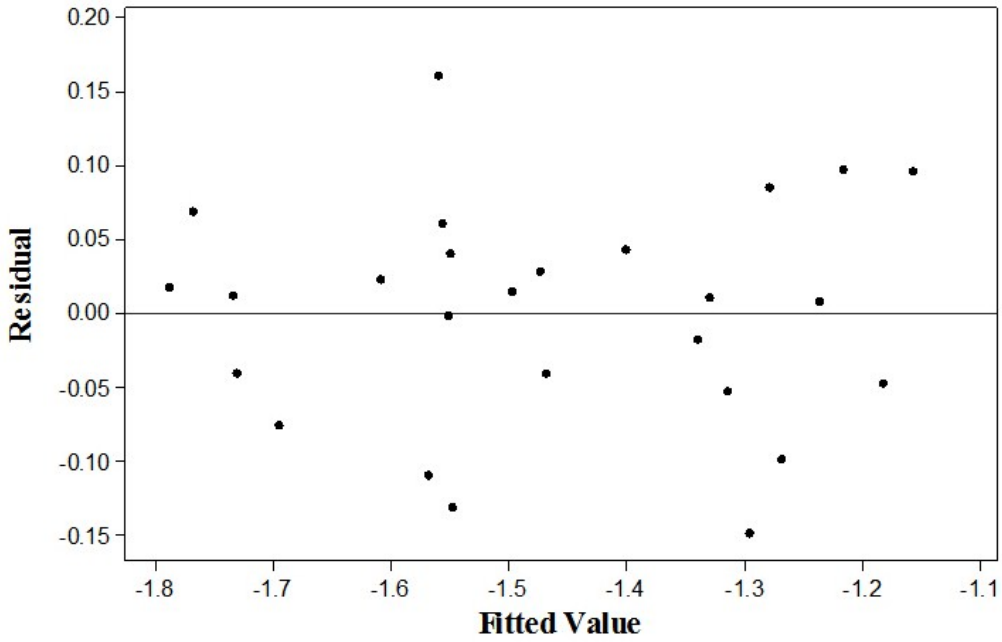

Figure 4-22 Residuals vs. Fits Plot of the Selected Model

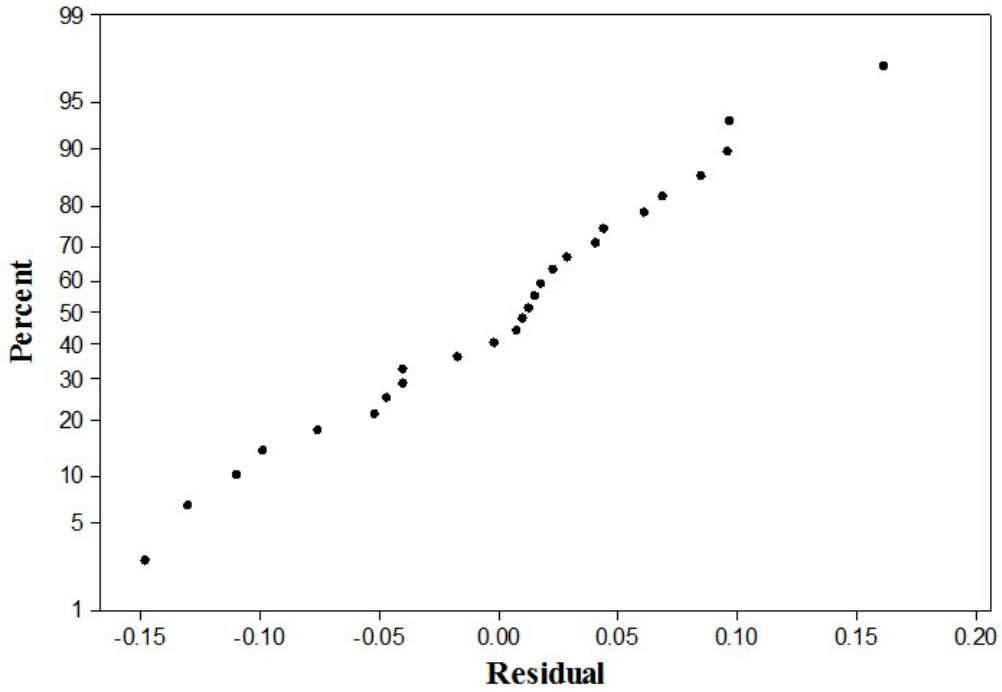

Figure 4-23 Normal Probability Plot of the Selected Model

The Normality Test is performed to confirm whether the residuals are normally distributed. It is conducted by calculating the correlation coefficient between the residuals (e) and their expected values under normality (enrm).

- Hypothesis:

H_0 : $Normality\ is\ okay$

H_1 : $Normality\ is\ violated$

- Decision Rule:

If the correlation coefficient *p* is < $C(\alpha, n)$, then reject H_0. C is the critical value, α was 0.1 and n was 26. $C(\alpha, n) = (0.1{,}26) = 0.967$

Table 4-14 shows SAS output of the normality test.

p = 0.9918 > 0.967, so failed to reject H_0.

- Conclusion:

Normality assumption was satisfied.

Table 4-14 SAS Output of the Normality Test

	e	enrm
e e(Log10kCOD | R T P stdRX stdTP)	1.00000	0.99180
enrm Normal scores	0.99180	1.00000

X-Outliers:

Leverage values (h_{ii}) of two observations (see Table 4-15) exceeded the cutoff value $\left(\frac{2p}{n} = \frac{2(6)}{26} = 0.462\right)$. Therefore, observations 1 and 7 were x-outliers.

Y-Outliers:

The Bonferroni test was performed and no $|t_i|$ values were found to exceed $t\left(1-\frac{\alpha}{2n};n-p-1\right)=t\left(1-\frac{0.1}{2\times 26};26-6-1\right)=t(0.99808;19)=3.29.$

Therefore, there were no y-outliers.

Table 4-15 Measures for Outlier Analysis

Obs.	e_i	h_{ii}	|DFFITS|	D_i	$\|t_i\|$
1	0.017	0.613	0.405	0.0286	0.322
7	-0.047	0.616	1.151	0.2228	0.908

Three measures were used to check whether the two x-outliers highly influenced the model:

1- Influence on Single Fitted Value – DFFITS:

If $|\text{DFFITS}|>2\sqrt{\frac{p}{n}}=2\sqrt{\frac{6}{26}}=0.961$, then the outlier is influential. |DFFITS| value of observation 7 (1.151) was larger than 0.961; however, this is not much larger than the cutoff.

2- Influence on All Fitted Values – Cook's Distance (D_i):

If $D_i>F(0.5;p,n-p)=F(0.5;6,20)=0.922$, then the outlier highly influences the fitted values. From Table 4-15, the two D_i values were less than 0.922, so they did not influence the fitted values.

It could be concluded from the two measures that the two x-outliers were not highly influential and, therefore, they were kept in the dataset.

The selected regression model was fitted. The parameter estimates and ANOVA table are shown in Table 4-16. The p values of the parameters were used to check whether the predictor variables were statistically significant. If the p-value is larger than the critical level (0.1), it means that the predictor variable is not significant. From Table 4-16, all p values were less than 0.1; therefore, all predictor variables were statistically significant. The variable inflation factors (VIF), shown in this table, were used to determine if serious multicollinearity is an issue in this model. If the VIF is not larger than 1.0 by much, it can be safely said that multicollinearity is not a problem in the model. All VIF's in the table were very close to 1.0; therefore, multicollinearity was not a problem. R^2_{adj} (83.3%) and R^2 (86.6%) were close to each other and relatively high, which means that the selected model explains the lab data sufficiently.

Table 4-16 Model Parameter Estimates and ANOVA Table

Predictor	Coef	SE Coef	T	P	VIF
Constant	-2.3409	0.1228	-19.07	0.000	
R	0.033285	0.004007	8.31	0.000	1.038
T	0.006895	0.001360	5.07	0.000	1.002
P	0.25546	0.05258	4.86	0.000	1.108
std(RX)	-0.05643	0.02101	-2.69	0.014	1.073
std(TP)	0.07387	0.01706	4.33	0.000	1.002

S = 0.0839373 R-Sq = 86.6% R-Sq(adj) = 83.3%

Analysis of Variance

Source	DF	SS	MS	F	P
Regression	5	0.91311	0.18262	25.92	0.000
Residual Error	20	0.14091	0.00705		
Total	25	1.05402			

The selected model was:

$$\mathrm{Log_{10}(k_{COD})} = -2.34 + 0.0333\,\mathrm{R} + 0.00690\,\mathrm{T} + 0.255\,\mathrm{P} - 0.0564\,\mathrm{std(RX)} + 0.0739\mathrm{std\,(TP)}$$

To simplify the standardized interaction terms:

$$\mathrm{std(RX)} = \left(\frac{\mathrm{R_i} - \bar{\mathrm{R}}}{\mathrm{S_R}}\right)\left(\frac{\mathrm{X_i} - \bar{\mathrm{X}}}{\mathrm{S_X}}\right) = \left(\frac{\mathrm{R} - 6.692}{4.269}\right)\left(\frac{\mathrm{X} - 0.242}{0.343}\right)$$

$$= 0.683\,RX - 0.165\,R - 1.57\,X + 1.106 \text{ -------- > (1)}$$

and

$$\text{std}(TP) = \left(\frac{T_i - \overline{T}}{S_T}\right)\left(\frac{P_i - \overline{P}}{S_P}\right) = \left(\frac{T - 85.577}{12.355}\right)\left(\frac{P - 0.254}{0.336}\right)$$

$$= 0.241\,TP - 0.0612\,T - 20.615\,P + 5.236 \text{ -------- > (2)}$$

After substituting (1) and (2) back into the model, it became:

$$\text{Log}_{10}(k_{COD}) = -2.015 + 0.0426\,R + 0.0024\,T - 1.268\,P + 0.0178\,TP + 0.258\,X - 0.0385\,RX$$

The final form of the model was thus:

$$k_{COD} = 10^{(-2.015 + 0.0426\,R + 0.0024\,T - 1.268\,P + 0.0178\,TP + 0.258\,X - 0.0385\,RX)}$$

4.5 Modeling k_{BOD}

The same steps were followed while modeling k_{BOD}. Also, six predictor variables were considered in the MLR analysis: Rainfall (R), Temperature (T), and four solid waste fractions; Food (F), Paper (P), Yard (Y), and Textile (X).

4.5.1 Scatter Plots and Correlation Matrices

The plot matrix in Figure 4-24 shows upward linear trends between k_{BOD} and each of Rainfall, Temperature, and Paper. The k_{BOD} vs. Food scatter plot shows a downward trend with some curvature.

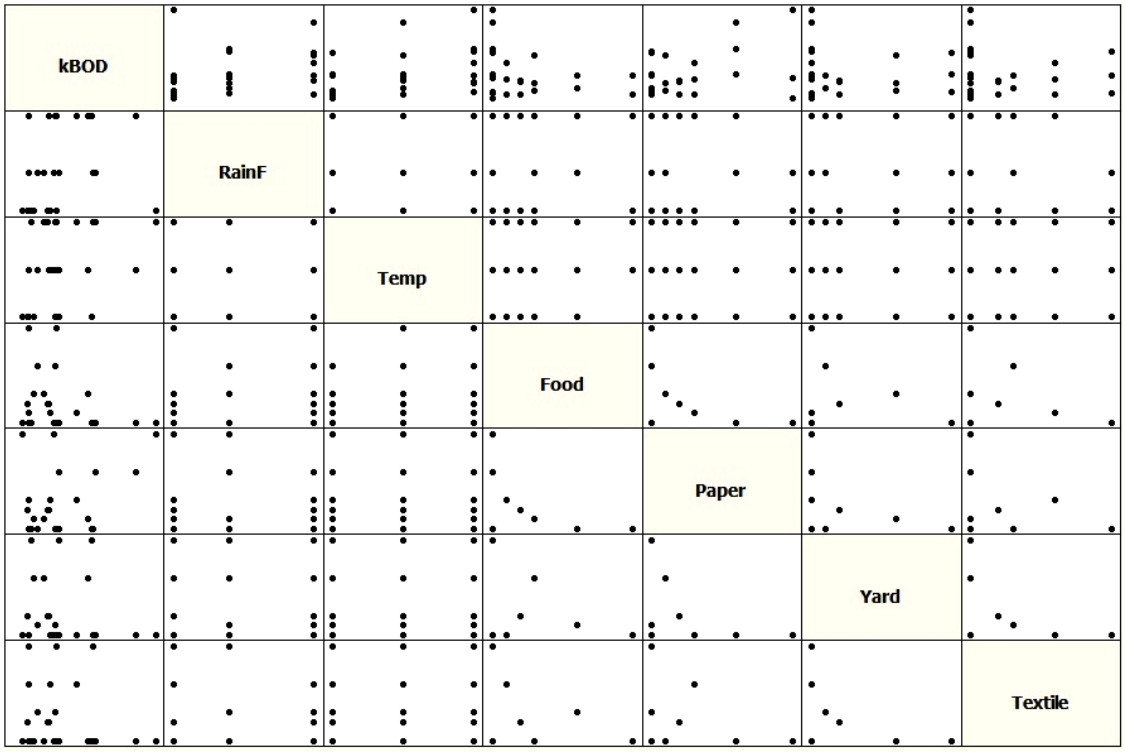

Figure 4-24 Plot Matrix between k_{BOD} and the Predictor Variables

The correlation matrix in Table 4-17 shows low *r*-values between k_{BOD} and the predictor variables. Multicollinearity could be a problem between *F* and *P*, *P* and *Y*, and *Y* and *X*.

Table 4-17 Correlation Matrix between k_{BOD} and the Predictor Variables

	kBOD	R	T	F	P	Y
R	0.262					
T	0.365	-0.008				
F	-0.287	0.196	0.126			
P	0.350	-0.189	-0.037	-0.441		
Y	-0.073	0.001	-0.031	-0.148	-0.395	
X	-0.132	-0.010	-0.034	-0.199	-0.326	-0.395

4.5.2 Fitting a Preliminary Model and Checking Model Assumptions

SAS output in Table 4-18 shows the preliminary MLR model that was fitted against the six predictor variables (*R, T, F, P, Y, X*). The model's R^2 value was very low (45.5%). The Model assumptions were checked before discussing the significance of the regression parameters.

Table 4-18 Parameter Estimates and ANOVA Table of the k_{BOD} Preliminary Model

```
kBOD = - 0.0307 + 0.00245 R + 0.000966 T - 0.0497 F - 0.0010 P - 0.0229 Y
             - 0.0278 X

      Predictor       Coef    SE Coef      T      P    VIF

      Constant    -0.03066    0.05189  -0.59  0.562
      R            0.00245    0.001189  2.06  0.053  1.077
      T            0.00097    0.000399  2.42  0.026  1.018
      F           -0.04966    0.04000  -1.24  0.230  6.135
      P           -0.00099    0.04588  -0.02  0.983  9.937
      Y           -0.02287    0.03960  -0.58  0.570  7.812
      X           -0.02777    0.03894  -0.71  0.484  7.458

      S = 0.0244617   R-Sq = 45.5%   R-Sq(adj) = 28.3%

      Analysis of Variance

      Source          DF         SS         MS     F      P
      Regression       6  0.0094875  0.0015812  2.64  0.049
      Residual Error  19  0.0113691  0.0005984
      Total           25  0.0208566
```

Preliminary Model Assumptions Check:

A- The linear model from assumption seemed to be violated. Residuals vs. *X* plot (Figure 4-25) showed curvature.

B- The constant variance assumption was also violated. A funnel shape existed in the Residual vs. Fitted Values plot that is shown in Figure 4-26.

C- Normality assumption was violated as well. Figure 4-27 shows the normal probability plot with left and right tails.

4.5.3 Transformations

Several transformations were applied to the preliminary MLR model to mitigate these violations of the model assumptions. The first attempt was $\sqrt{k_{BOD}}$. Residual plots of the model after this transformation can be found in APPENDIX B. The residual vs. fits plot still showed a slight funneling and the normal probability plot showed a right-skewed distribution; therefore, constant variance and normality assumption were not satisfied yet. A stronger transformation, $\mathrm{Log}_{10}(k_{BOD})$, was attempted in the next step. The residual plots can also be seen in APPENDIX B. Both residual vs. fits plot and normal probability plot looked slightly better with this transformation. The residual vs. F plot showed a funnel shape and residual vs. X plot showed curvature. By transforming F and X into $\sqrt{F}$ and $\sqrt{X}$, in addition to $\mathrm{Log}_{10}(k_{BOD})$, the model assumptions were satisfied, as the next section will show.

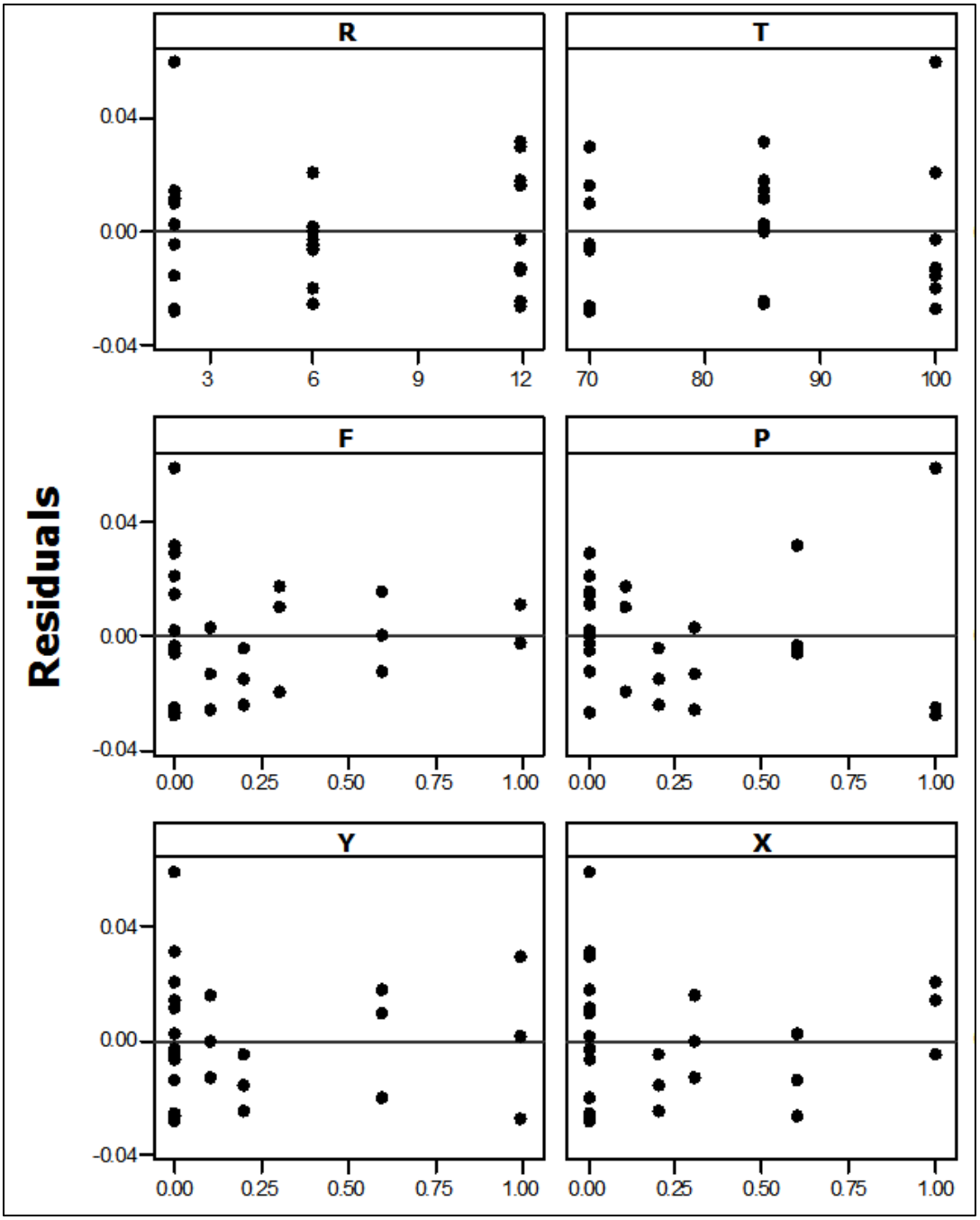

Figure 4-25 Residuals vs. Predictor Plots of k_{BOD} Preliminary Model

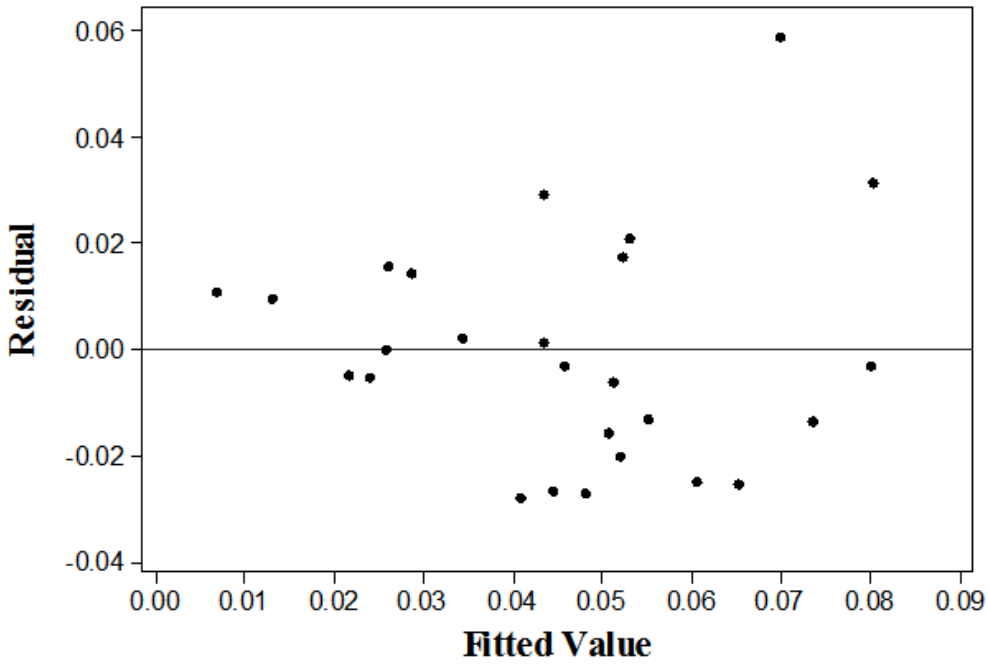

Figure 4-26 Plot of Residuals vs. Fitted Values of k_{BOD} Preliminary Model

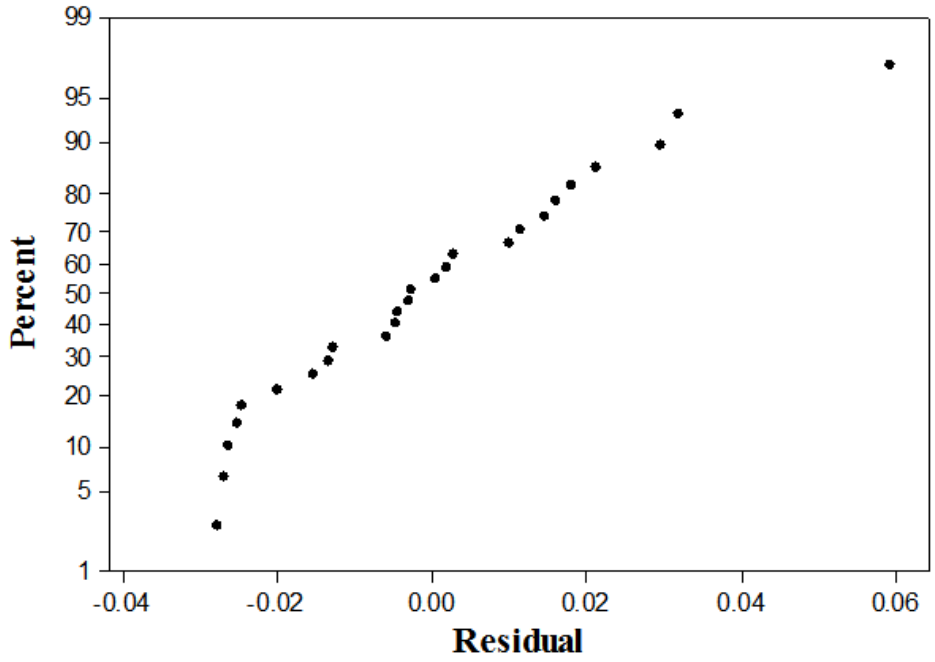

Figure 4-27 Normal Probability Plot of k_{BOD} Preliminary Model

Transformed Model Assumptions Check:

Three transformation were performed on the model variables

- Logarithm (base 10) of the response variable, $\mathrm{Log}_{10}(\mathrm{k_{BOD}})$
- Square root of the Food variable, $\sqrt{\mathrm{F}}$.
- Square root of the Textile variable, $\sqrt{\mathrm{X}}$.

The transformed response variable, $\mathrm{Log}_{10}(\mathrm{k_{BOD}})$, was regressed on R, T, $\sqrt{\mathrm{F}}$, P, Y, and $\sqrt{\mathrm{X}}$. The new fitted model was:

$$\mathrm{Log}_{10}(\mathrm{k_{BOD}}) = -2.15 + 0.0293\,\mathrm{R} + 0.0966\,\mathrm{T} - 0.414\,\sqrt{\mathrm{F}} - 0.141\,\mathrm{P} - 0.208\,\mathrm{Y} - 0.225\,\sqrt{\mathrm{X}}$$

The model assumptions were checked again.

A- Figure 4-28 shows Residuals vs. Predictor plots. Curvature did not exist in any of the plots. Therefore, the linear model form assumption was satisfied.

B- The funnel shape disappeared from the Residual-Fits plot (Figure 4-29). The constant variance assumption was satisfied.

C- The normal probability plot of the transformed model (Figure 4-30) did not show any tails. Therefore, the normality assumption was reasonable.

Modified Levene Test and Normality Test were performed (see Appendix B) to confirm that the transformed model satisfied the constant variance and normality assumptions.

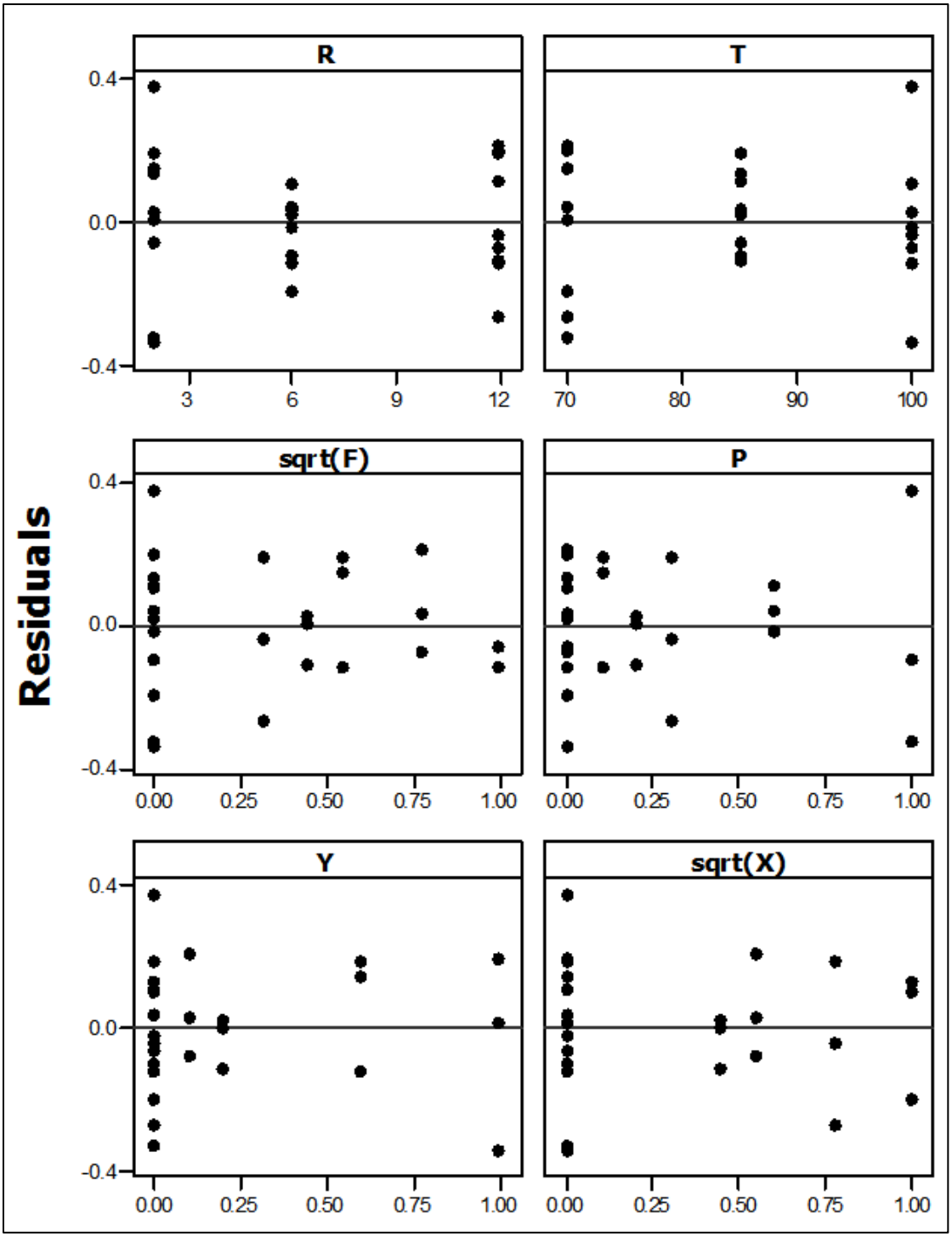

Figure 4-28 Residuals vs. Predictor Plots of the Transformed Model

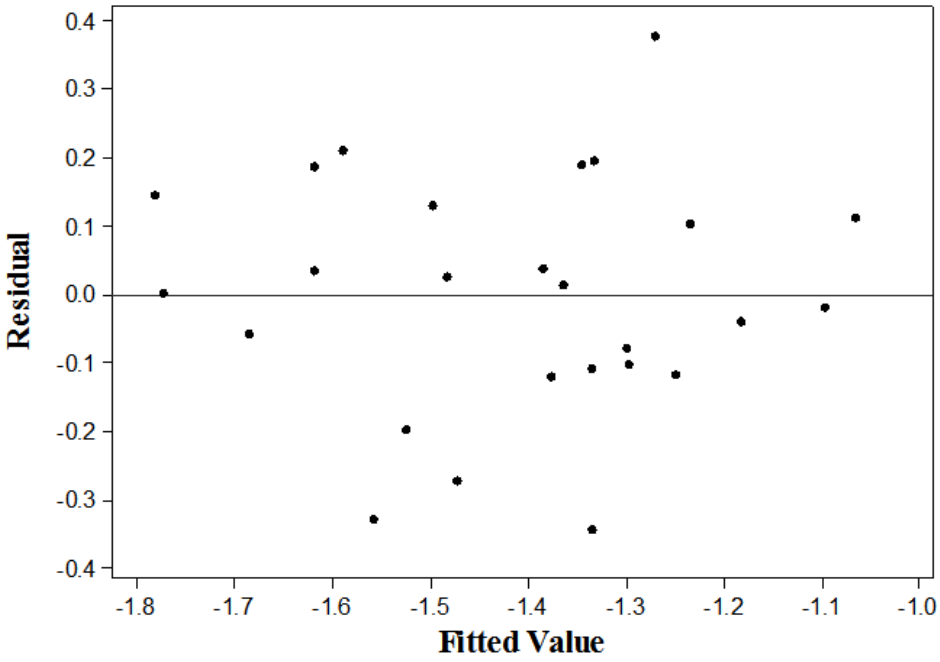

Figure 4-29 Residuals vs. Fits Plot of the Transformed Model

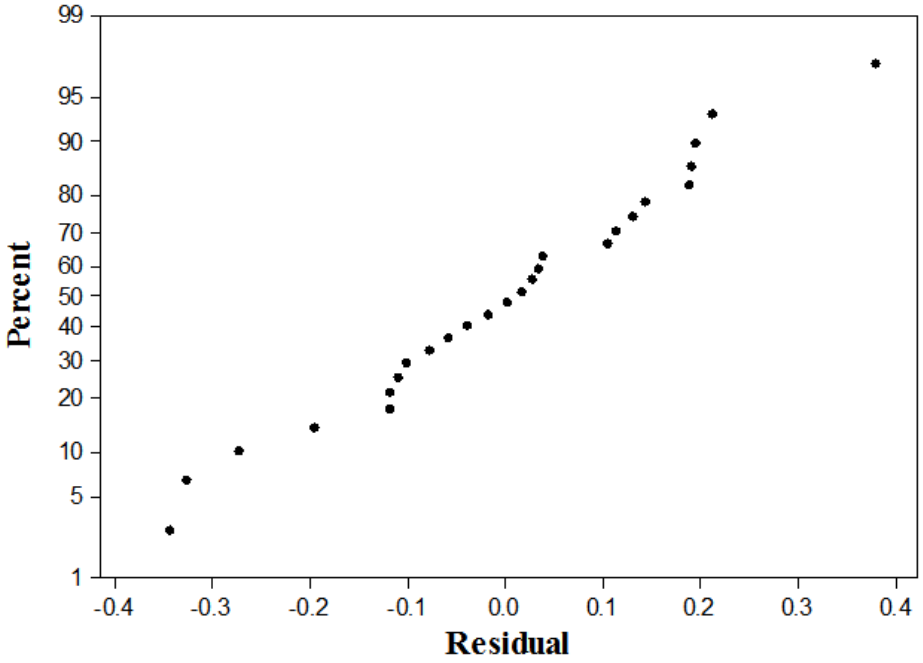

Figure 4-30 Normal Probability Plot of the Transformed Model

X-Outliers:

None of the leverage values (h_{ii}) of the transformed model, that are shown in Table 4-19, exceeded the cutoff value $\left(\frac{2p}{n} = \frac{2(7)}{26} = 0.538\right)$. Therefore, there were no x-outliers.

Y-Outliers:

The Bonferroni test was performed and no $|t_i|$ values (Table 4-19) were found to exceed

$t\left(1-\frac{\alpha}{2n}; n-p-1\right) = t\left(1-\frac{0.1}{2\times 26}; 26-7-1\right) = t(0.99808; 18) = 3.316$; therefore, there were no y-outliers.

4.5.4 Interaction Terms and Model Search

The possibility of adding interaction terms was checked using partial regression plots. Two of these plots showed linear trends, TY and TP as shown in Figure 4-31 (the rest of the partial regression plots can be seen in Appendix B). These two terms were added to the model to improve its performance. Table 4-20 shows that the TP term was highly correlated with P (r=0.984) and the TY term was highly correlated with Y (r=0.986). Standardizing these two interaction terms clearly eliminated the high multicollinearity (see Table 4-20).

The same model search methods that were used for the k_{COD} model were also utilized here. These methods were best subsets, backward elimination, and stepwise regression. SAS outputs of the three methods are shown in Tables 4-21, 4-22, and 4-23, respectively. All three methods were pointing to one potential good model with five predictor variables: R, T, $\sqrt{F}$, std(TP), and std(TY).

Table 4-19 Measures for Outlier Analysis

Observation	e_i	h_{ii}	$\|t_i\|$
1	-0.327	0.325	2.175
2	0.145	0.260	0.831
3	0.003	0.186	0.017
4	-0.058	0.452	0.383
5	0.130	0.305	0.772
6	0.188	0.191	1.045
7	0.380	0.335	2.670
8	-0.343	0.371	2.414
9	0.027	0.174	0.145
10	-0.196	0.316	1.199
11	0.038	0.288	0.221
12	-0.101	0.252	0.573
13	0.016	0.267	0.092
14	0.035	0.138	0.183
15	0.104	0.320	0.621
16	-0.018	0.263	0.103
17	-0.119	0.179	0.644
18	0.195	0.397	1.276
19	0.212	0.234	1.227
20	-0.273	0.256	1.648
21	0.114	0.310	0.674
22	0.190	0.176	1.049
23	-0.109	0.118	0.566
24	-0.117	0.397	0.746
25	-0.077	0.215	0.426
26	-0.040	0.278	0.227
Max.		0.452	2.670

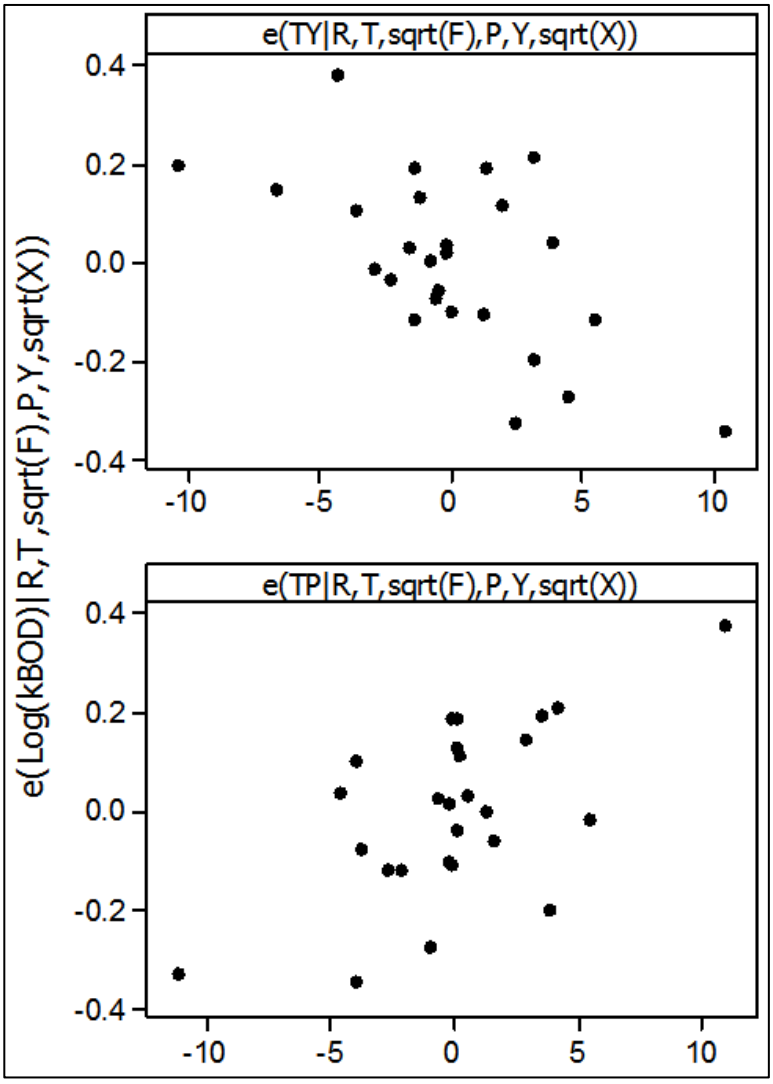

Figure 4-31 Partial Regression Plots with Linear Trends

Table 4-20 Correlation Matrix Between TP, TY, and the Model Variables

	LOG10(kBOD)	R	T	sqrt(F)	P	Y	sqrt(X)
TP	0.304	-0.184	0.074	-0.468	*0.984*	-0.389	-0.351
TY	-0.048	-0.034	0.063	-0.107	-0.390	*0.986*	-0.415
std(TP)	0.435	0.029	0.019	-0.051	*-0.019*	0.042	0.048
std(TY)	-0.493	-0.249	0.016	-0.05	0.042	*-0.027*	0.046

Table 4-21 SAS Output of the Best Subsets Model Search Method

Number In Model	Adjusted R-Square	R-Square	C(p)	AIC	SBC	Variables
3	0.4998	0.5599	16.2493	-84.5766	-79.544	T rt(F) std(TY)
3	0.4357	0.5034	20.6432	-81.4383	-76.405	R T std(TY)
4	0.6169	0.6782	9.0415	-90.7181	-84.427	R T rt(F) std(TY)
4	0.5887	0.6545	10.8818	-88.8743	-82.583	R T rt(F) std(TP)
5	0.6676	0.7341	6.6923	-93.6781	-86.129	R T rt(F) std(TP) std(TY)
5	0.6161	0.6929	9.8982	-89.9331	-82.384	R T rt(F) rt(X) std(TY)
6	0.6761	0.7538	7.1546	-93.6858	-84.879	R T rt(F) rt(X) std(TP) std(TY)
6	0.6706	0.7496	7.4824	-93.2447	-84.437	R T rt(F) P std(TP) std(TY)
7	0.6871	0.7747	7.5331	-93.9855	-83.920	R T rt(F) Y rt(X) std(TP) std(TY)
7	0.6657	0.7593	8.7279	-92.2716	-82.206	R T rt(F) P rt(X) std(TP) std(TY)
8	0.6787	0.7815	9.0000	-92.7884	-81.465	R T rt(F) P Y rt(X) std(TP) std(TY)

Table 4-22 SAS Output of the Backward Elimination Model Search Method

Backward Elimination: Step 3

Variable sqrt(X) Removed: R-Square = 0.7341 and C(p) = 6.6923

Analysis of Variance

Source	DF	Sum of Squares	Mean Square	F Value	Pr > F
Model	5	1.23243	0.24649	11.04	<.0001
Error	20	0.44644	0.02232		
Corrected Total	25	1.67887			

Variable	Parameter Estimate	Standard Error	Type II SS	F Value	Pr > F
Intercept	-2.32328	0.21479	2.61163	117.00	<.0001
R	0.02313	0.00743	0.21648	9.70	0.0055
T	0.00997	0.00243	0.37489	16.79	0.0006
sqrt(F)	-0.31131	0.08954	0.26984	12.09	0.0024
std(TP)	0.06876	0.03354	0.09383	4.20	0.0537
std(TY)	-0.08430	0.03447	0.13354	5.98	0.0238

All variables left in the model are significant at the 0.1000 level.

Table 4-23 SAS Output of the Stepwise Selection Model Search Method

Stepwise Selection: Step 5

Variable std(TP) Entered: R-Square = 0.7341 and C(p) = 6.6923

Analysis of Variance

Source	DF	Sum of Squares	Mean Square	F Value	Pr > F
Model	5	1.23243	0.24649	11.04	<.0001
Error	20	0.44644	0.02232		
Corrected Total	25	1.67887			

Variable	Parameter Estimate	Standard Error	Type II SS	F Value	Pr > F
Intercept	-2.32328	0.21479	2.61163	117.00	<.0001
R	0.02313	0.00743	0.21648	9.70	0.0055
T	0.00997	0.00243	0.37489	16.79	0.0006
sqrt(F)	-0.31131	0.08954	0.26984	12.09	0.0024
std(TP)	0.06876	0.03354	0.09383	4.20	0.0537
std(TY)	-0.08430	0.03447	0.13354	5.98	0.0238

All variables left in the model are significant at the 0.1000 level.

4.5.5 Checking Assumptions of the Selected Model

Figures 4-32, 4-33, and 4-34 are the selected model's residual plots. The residual-predictor plots in Figure 4-32 did not show serious curvature or funneling and neither did the plot of residuals vs. fitted values (Figure 4-33). So, the linearity and constant variance assumptions were satisfied. The normal probability plot in Figure 4-34 showed a linear trend with no tailing; therefore, normality was reasonable. Two hypothesis tests were performed to confirm that the selected model satisfied the constant variance and normality assumptions.

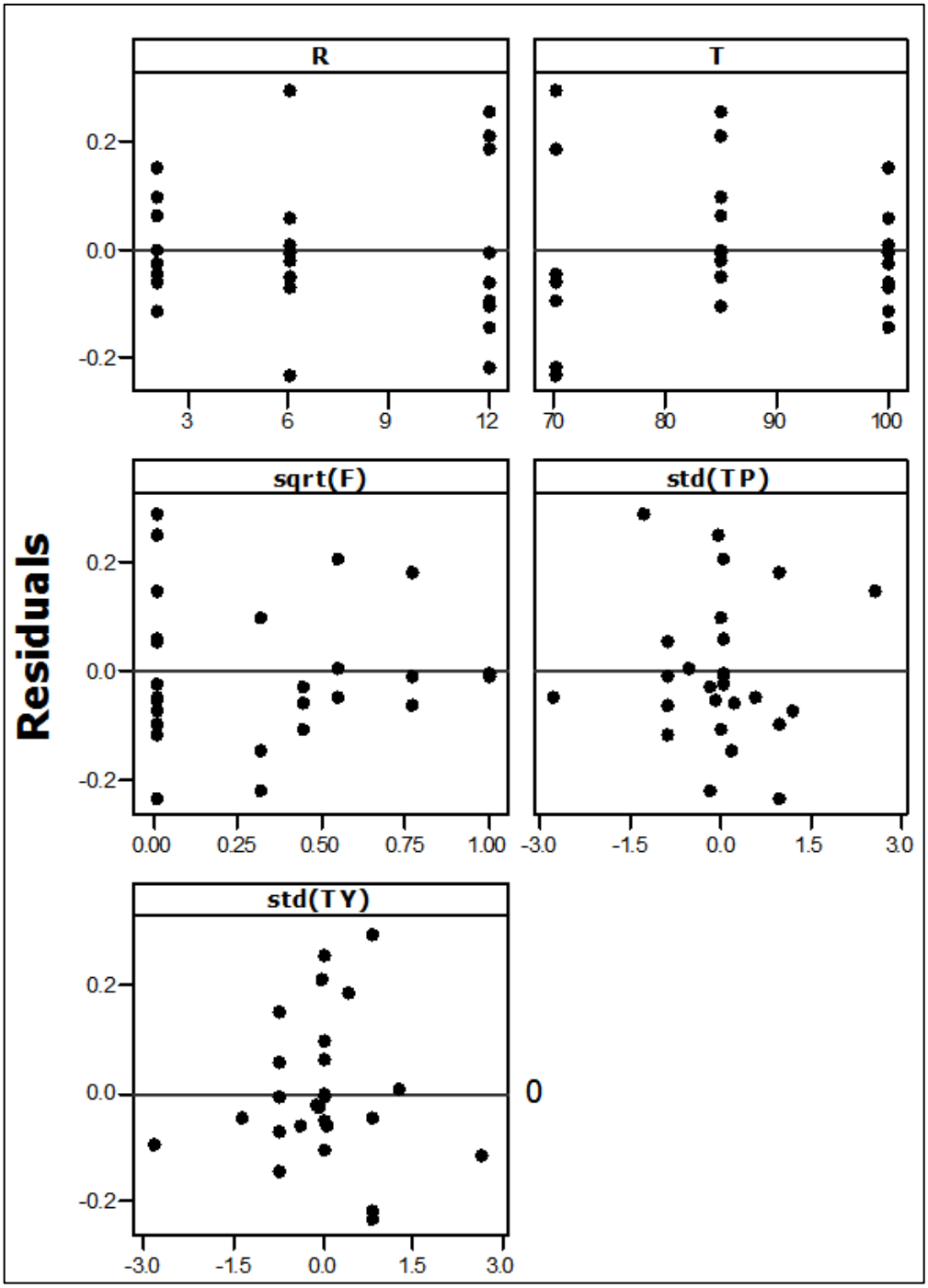

Figure 4-32 Residual-Predictor Plots of the Selected Model

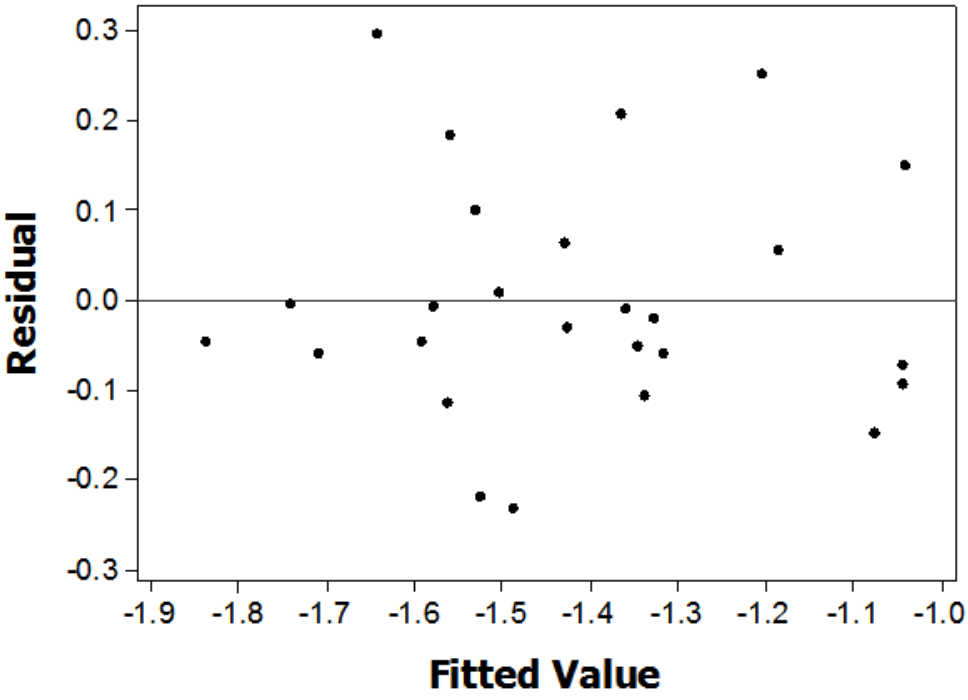

Figure 4-33 Residuals vs. Fits Plot of the Selected Model

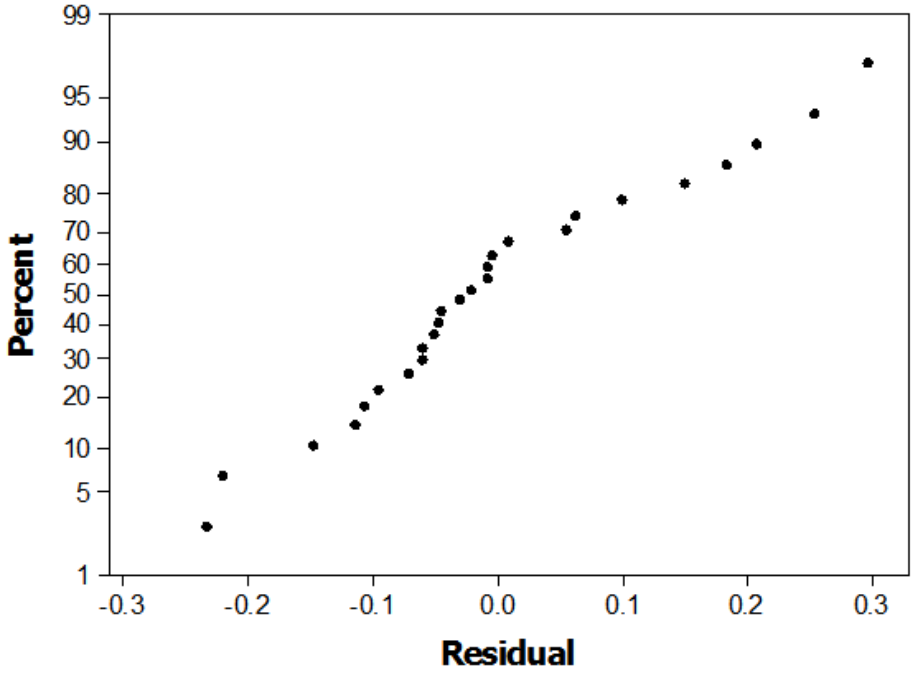

Figure 4-34 Normal Probability Plot of the Selected Model

Modified Levene Test:

1- F-test

- Hypothesis:

$H_0 : \sigma_{d_1} = \sigma_{d_2}$

$H_1 : \sigma_{d_1} \neq \sigma_{d_2}$

- Decision Rule:

If the p-value from the F-test is < 0.1, then reject H_0.

Table 4-24 is SAS output of the Modified Levene Test (also called Brown and Forsythe test). The F-test p-value (denoted Pr > F) was 0.91 > 0.1, so failed to reject H_0.

- Conclusion:

Variances of d_1 and d_2 were equal.

2- T-test was performed to check whether the means of d_1 and d_2 populations were equal.

- Hypothesis:

$H_0 : error\ variance\ is\ constant$

$H_1 : error\ variance\ is\ not\ constant$

- Decision Rule:

If the p-value from the t-test is < 0.1, then reject H_0. The p-value from Table 4-24 (denoted Pr > | t |) was 0.9655 > 0.1, so failed to reject H_0.

- Conclusion:

The model's error variance was constant.

Table 4-24 SAS Output of Modified Levene Test

The TTEST Procedure

Variable: d

group	N	Mean	Std Dev	Std Err	Minimum	Maximum
1	14	0.0990	0.0972	0.0260	0.0107	0.3151
2	12	0.0974	0.0936	0.0270	0.0151	0.2895
Diff (1-2)		0.00164	0.0956	0.0376		

Method	Variances	DF	t Value	Pr > |t|
Pooled	Equal	24	0.04	0.9655
Satterthwaite	Unequal	23.641	0.04	0.9654

Equality of Variances

Method	Num DF	Den DF	F Value	Pr > F
Folded F	13	11	1.08	0.9119

Normality Test:

- Hypothesis:

H_0 : $Normality\ is\ okay$

H_1 : $Normality\ is\ violated$

- Decision Rule:

If the correlation coefficient *p* is < $C(\alpha, n)$, then reject H_0. C is the critical value, α was 0.1 and n was 26. $C(\alpha, n) = (0.1{,}26) = 0.967$

Table 4-25 is SAS output of the normality test.

p = 0.9761 > 0.967, so failed to reject H_0.

- Conclusion:

Normality assumption was satisfied.

Table 4-25 SAS Output of the Normality Test

	e	enrm
e	1.00000	0.97613
e(Log10(kBOD) | R T sqrt(F) std(TP) std(TY))		
enrm	0.97613	1.00000
Normal scores		

X-Outliers:

Leverage values (h_{ii}) of two observations (see Table 4-26) exceeded the cutoff value $\left(\frac{2p}{n} = \frac{2(6)}{26} = 0.462\right)$. Therefore, observations 1 and 18 were x-outliers.

Y-Outliers:

The Bonferroni test was performed and no $|t_i|$ values were found to exceed $t\left(1-\frac{\alpha}{2n}; n-p-1\right) = t\left(1-\frac{0.1}{2\times 26}; 26-6-1\right) = t(0.99808; 19) = 3.29.$

Therefore, there were no y-outliers.

Table 4-26 Measures for Outlier Analysis

Obs.	e_i	h_{ii}	$\|t_i\|$	D_i	|DFFITS|
1	-0.047	0.492	0.432	0.0314	0.425
18	-0.095	0.488	0.879	0.124	0.858

Three measures are used to check whether the two x-outliers were influential.

Influence on Single Fitted Value – DFFITS:

If $|DFFTIS| > 2\sqrt{\frac{p}{n}} = 2\sqrt{\frac{6}{26}} = 0.961$, then the outlier is influential. From Table 4-26, neither |DFFITS| value was > 0.961, therefore, the two x-outliers did not highly influence

the fitted values.

Influence on All Fitted Values – Cook's Distance (D_i):

If $D_i > F(0.5; p, n-p) = F(0.5; 6,20) = 0.922$, then the outlier influences the fitted values. From Table 4-26, the two D_i values were less than 0.922, so they did not highly influence the fitted values.

It could be concluded from the two measures that the two x-outliers did not highly influence the fitted values or the regression model; therefore, they were kept in the dataset.

The selected regression model was fitted. The parameter estimates and ANOVA table are shown in Table 4-27. The p values of the parameters are used to check whether the predictor variables are statistically significant. If the p-value is larger than the critical level (0.1), it means that the predictor variable is not significant. From Table 4-27, all p values were less than 0.1; therefore, the predictor variables were statistically significant. The variable inflation factors (VIF), shown in this table, were used to test whether the predictor variables were correlated with each other (multicollinearity). If the VIF was not larger than 1.0 by much, it could be safely said that multicollinearity effects were not expected in this model. All VIF's in the table were very close to 1.0; therefore, multicollinearity was not serious.

Table 4-27 Model Parameter Estimates and ANOVA Table

Predictor	Coef	SE Coef	T	P	VIF
Constant	-2.3232	0.2148	-10.82	0.000	
R	0.023125	0.007426	3.11	0.005	1.125
T	0.009968	0.002433	4.10	0.001	1.012
sqrt(F)	-0.31131	0.08954	-3.48	0.002	1.069
std(TY)	-0.08430	0.03447	-2.45	0.024	1.296
std(TP)	0.06875	0.03354	2.05	0.054	1.222

S = 0.149416 R-Sq = 73.4% R-Sq(adj) = 66.8%

Analysis of Variance

Source	DF	SS	MS	F	P
Regression	5	1.23235	0.24647	11.04	0.000
Residual Error	20	0.44650	0.02233		
Total	25	1.67885			

The selected model was:

$$\mathrm{Log_{10}(k_{BOD})} = -2.32 + 0.0231\ \mathrm{R} + 0.00997\ \mathrm{T} - 0.311\ \sqrt{F} - 0.0843\ \mathrm{std(TY)}$$

$$+0.0688\ \mathrm{std(TP)}$$

To simplify the standardized interaction terms

$$\mathrm{std(TY)} = \left(\frac{\mathrm{T_i} - \overline{\mathrm{T}}}{\mathrm{S_T}}\right)\left(\frac{\mathrm{Y_i} - \overline{\mathrm{Y}}}{\mathrm{S_Y}}\right) = \left(\frac{\mathrm{T} - 85.577}{12.355}\right)\left(\frac{\mathrm{Y} - 0.219}{0.345}\right)$$

$$= 0.235\ \mathrm{TY} - 0.0514\ \mathrm{T} - 20.0768\ \mathrm{Y} + 4.397 \text{ --------- > (1)}$$

$$\mathrm{std(TP)} = \left(\frac{\mathrm{T_i} - \overline{\mathrm{T}}}{\mathrm{S_T}}\right)\left(\frac{\mathrm{P_i} - \overline{\mathrm{P}}}{\mathrm{S_P}}\right) = \left(\frac{\mathrm{T} - 85.577}{12.355}\right)\left(\frac{\mathrm{P} - 0.254}{0.336}\right)$$

$$= 0.241\ \mathrm{TP} - 0.0612\ \mathrm{T} - 20.615\ \mathrm{P} + 5.236 \text{ --------- > (2)}$$

After substituting (1) and (2) back into the model it becomes:

$$\mathrm{Log_{10}(k_{BOD})} = -2.330 + 0.0231\ \mathrm{R} + 0.0101\ \mathrm{T} - 1.418\ \mathrm{P} + 0.0166\ \mathrm{TP} + 1.693\ \mathrm{Y}$$

$$-0.0198\ \mathrm{TY} - 0.311\ \sqrt{F}$$

The final form of the model was thus:

$$\mathrm{k_{BOD}} = 10^{(-2.330+0.0231\ \mathrm{R}+0.0101\ \mathrm{T}-1.418\ \mathrm{P}+0.0166\ \mathrm{TP}+1.693\ \mathrm{Y}-0.0198\ \mathrm{TY}-0.311\ \sqrt{F})}$$

4.6 Models Interpretation

The selected models are repeated here for convenience.

$$k_{COD} = 10^{(-2.015+0.0426\,R+0.0024\,T-1.268\,P+0.0178\,TP+0.258\,X-0.0385\,RX)}$$

$$k_{BOD} = 10^{(-2.330+0.0231\,R+0.0101\,T-1.418\,P+0.0166\,TP+1.693\,Y-0.0198\,TY-0.311\,\sqrt{F})}$$

The two models look similar in the first five terms. This is expected considering that COD and BOD concentration profiles followed almost the same trend in leachate collected from a given reactor. The rainfall rate (R) and Temperature (T) terms are positive in both models, which would be expected for the reasons mentioned in Chapter 2. The k_{COD} model does not account for food and yard wastes, while the k_{BOD} model misses only textile variable out of the six predictor variables that were included in the MLR analysis. The first explanation for the missing variables is from a statistical point of view. The confidence level that was chosen during model search process was 90%. At this level, Food and Yard were found to be significant to the k_{BOD} model but not to the k_{COD} model. Textile being a mixture of cotton, polyester, and other fabrics could have influenced k_{COD} but not k_{BOD} because it is often not bioavailable. The next discussion is an attempt to explain the physical meaning of the absent variables from either model as well as the meaning of interaction terms in both models.

Food waste is known to have a high content of biodegradable organics: therefore, it is reasonable that it would influence the BOD concentration profile (k_{BOD}) of leachate more than it does in the case of k_{COD}. Mathematically, the minus sign of $\sqrt{F}$ indicates that this term is inversely proportional with k_{BOD}. In other words, high food content in MSW is likely to slow down the biological decomposition of refuse in landfills. A study by Barlaz *et al.* (1997) on the toxicity of leachate due to anaerobic decomposition of many refuse types suggested that food waste is highly toxic in the acidic phase. The study also suggested that anaerobic decomposition could be inhibited in landfills with large amounts of food waste. Reactor #10 in

this study contained food waste only. It failed due to excessive accumulation of acid (pH plot shown in Figure 4-35).

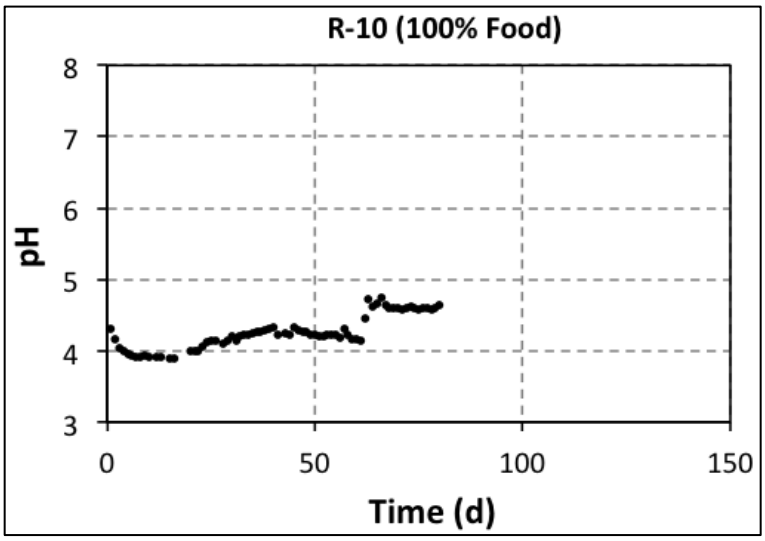

Figure 4-35 Plot of pH vs. Time for Reactor #10

In both models, the paper term (P) has a minus sign and is followed by a temperature-paper (TP) interaction term. To understand how these two terms affect both models, predicted values of k_{COD} and k_{BOD} were calculated by changing P and fixing all other variables in the two models. The same operation was performed for four temperatures (70, 80, 90, and 100 °F). Figures 4-36 and 4-37 show two plots of predicted k value vs. paper. Both k values slightly decrease as the fraction of paper waste increases at 70 °F. When temperature increases, the slope of k-P curve increases. If this behavior of the curves were to be translated into physical sense, it would mean that paper waste decomposes better/faster at higher temperatures.

A similar type of plot was created for Textile (X) and Rainfall Rate (R) and another plot for Yard (Y) and Temperature (T) since they have interaction effects in k_{COD} model and k_{BOD} model, respectively. The two plots are shown in Figures 4-38 and 4-39.

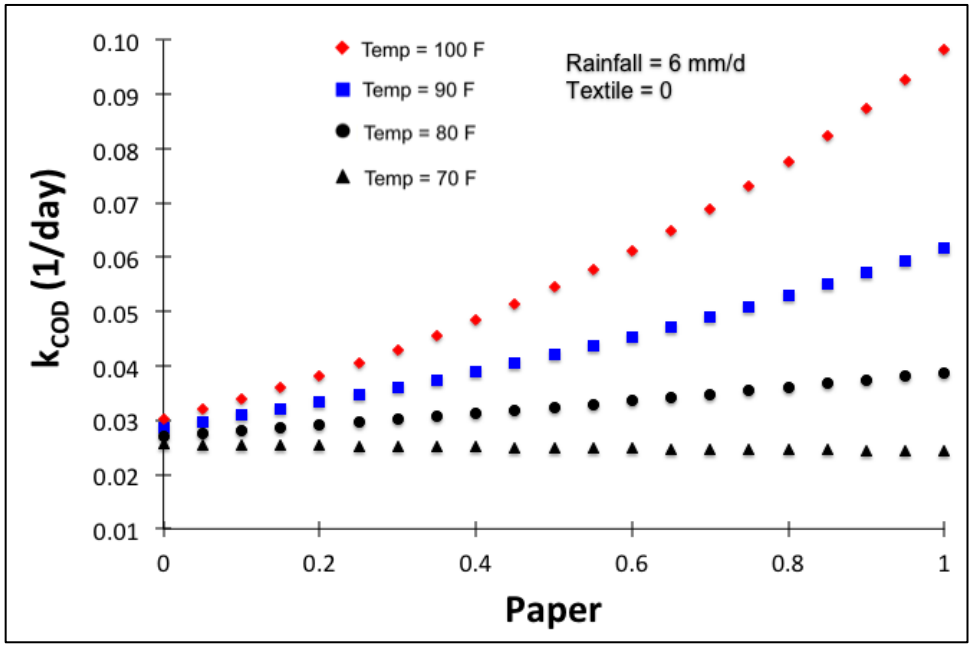

Figure 4-36 Plot of Predicted k_{COD} vs. Paper and Temperature

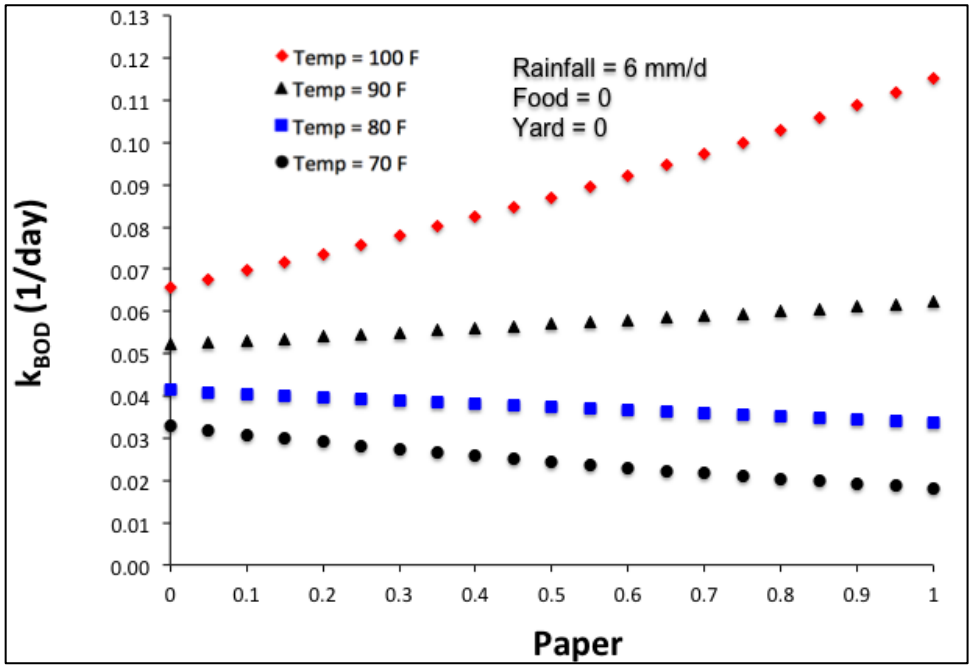

Figure 4-37 Plot of Predicted k_{BOD} vs. Paper and Temperature

It makes sense that textile appears only in the COD model, since a substantial part of the textile was not biodegradable (polyester, for example). The predicted k_{COD} value in Figure 4-38 increases with increasing textile waste at the low rainfall rate (2 mm/day). As rainfall rate increases, k_{COD} is also increasing but the slope of k_{COD}-Textile curve is decreasing. In other words, at high rainfall rates, decomposition of refuse in the reactors slows down when the amount of textile waste increases. In several reactors, textiles were observed to retain leachate. If the textile retained too much leachate, it could cause the waste moisture content to increase beyond optimum. This would lead to a decrease in the waste decomposition rate, and thus a decrease in the rate of COD accumulation in the leachate. The temperature-yard (TY) interaction effect changes the predicted k_{BOD} value significantly as shown in Figure 4-39. The four lines in this plot intersect at the 0.5-yard fraction. It is not clear at this point why the temperature-yard interaction term behaves this way in the model.

Paper and yard/wood wastes contain high amounts of lignin, which could be responsible for resisting decomposition or leaching process in landfills due to its high durability (Barlaz *et al.*, 1997). Lignin is known to have a complex structure that might require higher temperatures to break down or decompose (Brebu & Vasile, 2010).

> Due to its complex composition and structure, the degradation of lignin is strongly influenced by its nature, reaction temperature, heating rate and degradation atmosphere, which also affects the temperature domain of degradation, conversion and product yields. (Brebu & Vasile, 2010)

In order to validate both models, field data that includes information on the waste composition, temperatures, and precipitation rates is required. Both models will be validated in future work.

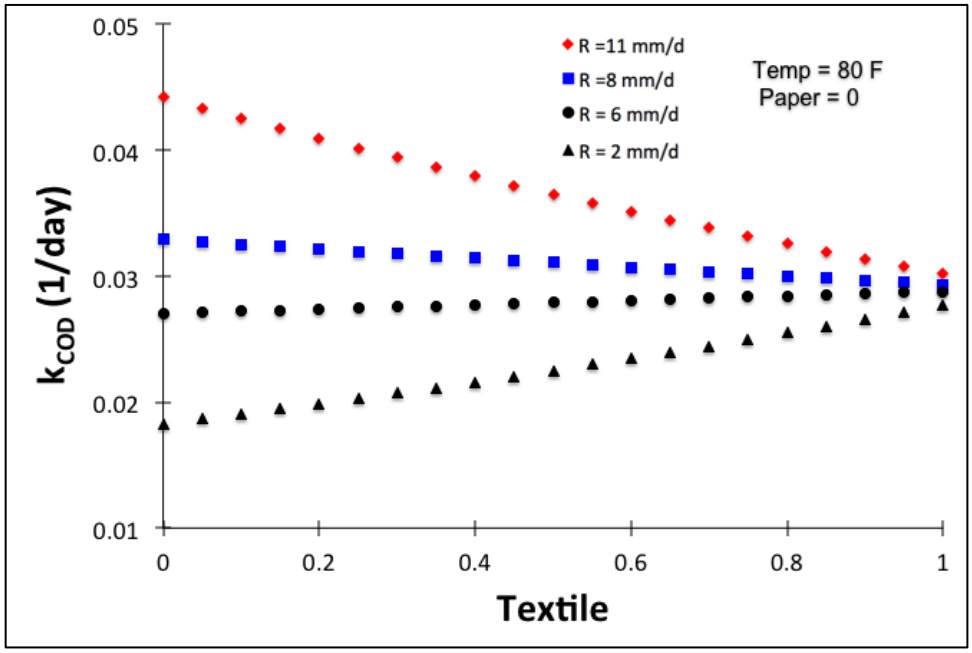

Figure 4-38 Plot of Predicted k_{COD} vs. Textile and Rainfall Rate

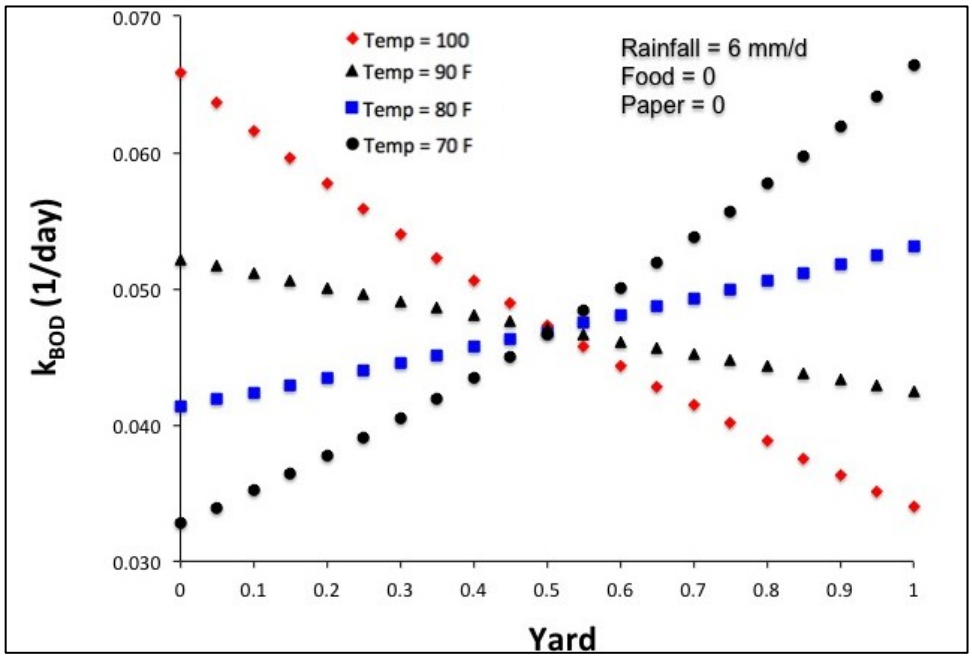

Figure 4-39 Plot of Predicted k_{BOD} vs. Yard and Temperature

Solid waste usually decomposes faster in lab-scale reactor landfills than actual landfills because of the ideal conditions in laboratory experiments (Youcai *et al.*, 2002). Therefore, the k_{BOD} and k_{COD} values calculated using the two models were expected to be larger than actual situations. In an attempt to come up with a scale factor for the k values, BOD and COD data from a field-scale study (Ozkaya *et al.*, 2006) was regenerated as shown in Figure 4-40. The field's k_{BOD} and k_{COD} values were found to be -0.0125 and -0.0135 day^{-1}, respectively. When the two models were used, k_{BOD} and k_{COD} were calculated to be -0.026 and -0.0256 day^{-1}, respectively. Therefore,

$$k_{BOD}\ \text{scale factor} = \frac{k_{BOD(field)}}{k_{BOD(model)}} = \frac{-0.0125}{-0.026} \approx 0.5$$

and

$$k_{COD}\ \text{scale factor} = \frac{k_{COD(field)}}{k_{COD(model)}} = \frac{-0.0135}{-0.0256} \approx 0.5$$

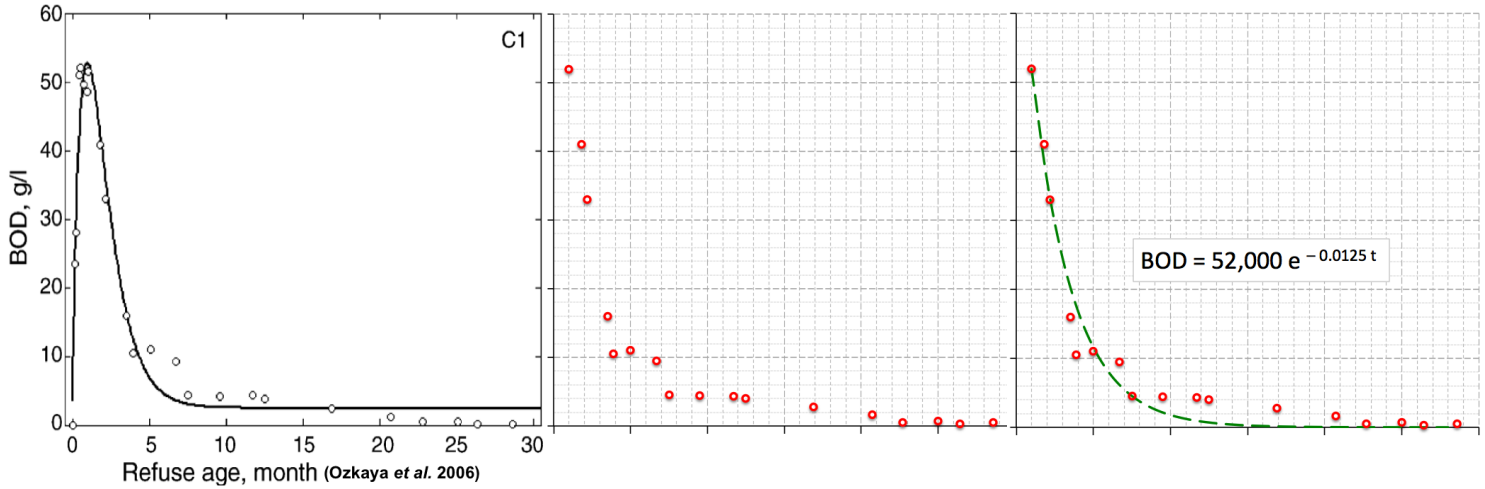

(a)

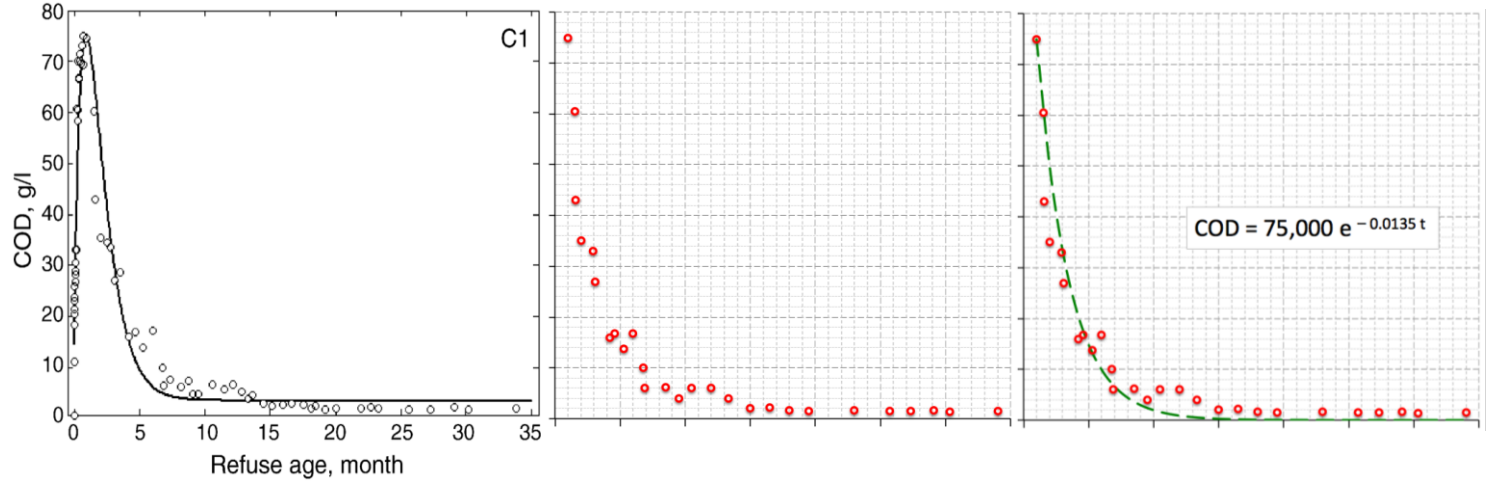

(b)

Figure 4-40 Determining BOD and COD Scale Factor between Lab and Field

Chapter 5

Conclusions and Recommendations

5.1 Conclusions

The main objective of this study was to develop two mathematical relationships that describe the behavior of leachate BOD and COD concentration profiles in terms of rainfall rate, temperature, and composition of waste. Experiments involved the design and operation of 27 lab-scale reactor landfills. Multiple linear regression analysis was utilized to build the two models.

- The approximate peak BOD concentrations in all the reactors ranged between 856 and 46,134 mg/L and peak COD concentrations were between 2,458 and 64,032 mg/L. The time it took a given reactor to reach the peak BOD or COD value varied significantly (6-102 days) among all the reactors. The wide range emphasizes the significance of temperature, rainfall rate, and waste composition (the experimental factors) in the leachate quality studies.
- The 85 °F reactors appeared to have higher waste decomposition rates (higher BOD and COD) than other reactors except when a reactor was also operated under the highest rainfall rate (12 mm/day). This observation suggests that among the three temperatures adopted in this study, 85 °F is probably the closest to being the optimum temperature for microbial growth.
- The 2-mm/day reactors showed longer time (180-200 days) in reaching minimum or stable BOD and COD concentrations and BOD:COD ratio than all other reactors. Low moisture content in those reactors led to slow waste stabilization rates. Many previous researchers reported the same observation.

- Food waste reactors produced the highest BOD (46,134 mg/L) and COD (64,032 mg/L) leachate and textile waste produced the lowest (BOD_{max}=8,960 mg/L and COD_{max}= 16,054 mg/L).
- The two models developed in this study are:

$$k_{COD} = 10^{(-2.015+0.0426\,R+0.0024\,T-1.268\,P+0.0178\,TP+0.258\,X-0.0385\,RX)}$$

and

$$k_{BOD} = 10^{(-2.330+0.0231\,R+0.0101\,T-1.418\,P+0.0166\,TP+1.693\,Y-0.0198\,TY-0.311\,\sqrt{F})}$$

Both models show that increasing rainfall rate and temperature leads to higher BOD and COD content in leachate, which translates into faster waste decomposition. The k_{COD} model suggests that only paper and textile are the types of refuse that contribute to shaping leachate's COD concentration profile. Paper, yard, and food waste components were found to be significant in the k_{BOD} model. The TP interaction term in both models suggests that paper waste decomposes faster at higher temperatures. In future work, the two models will be validated using field data.

5.2 Recommendations

Ideas for future research include the following:

- There are different types of waste with different characteristics within each waste category (yard, paper, textile, and food) studied in this research. For example, yard waste might include leaves, branches, thin grass, and other forms. The biodegradability of each type is most probably different than the others in a landfill. Therefore, it would be a good idea to separate each waste component in this manner to see the effects of temperature, moisture content, and other influential factors on the decomposition rate of each form.
- Analysis of BOD and COD content in leachate can be accompanied with methane generation rates for a better understanding of the relationship between the rate/extent of

waste decomposition and the change in weather conditions (precipitation rate and temperature) and waste composition in a landfill.

- Since lab experiments involve relatively small portions of waste, it is likely that the rate of waste decomposition would be much faster than it would be in actual landfills. Hence, it is important to find a way to relate lab results with actual situations. When a proper dataset becomes available for validating the two models in this study, a scaling factor can be calculated using k values from both lab experiments and actual landfills. The same method can be followed to study other leachate constituents.
- To better simulate actual landfills, rainfall can be added to the reactors at intervals (once a week, for example) other than daily.
- Similar experiment can be conducted with temperatures beyond the range tested (>100 °F and/or <70 °F). This would, for example, apply for the Arabian Gulf countries, where temperatures stay well above 100 °F from June to August.
- Similar work can be conducted with bioreactors, which involve leachate recirculation.
- A comparative study can be conducted where water is added on a per-volume of waste basis, rather than per-inches of rainfall basis. This would reduce leaching of microbes and nutrients.

Appendix A

Plots of Exponential Curve Fitting

BOD Curves

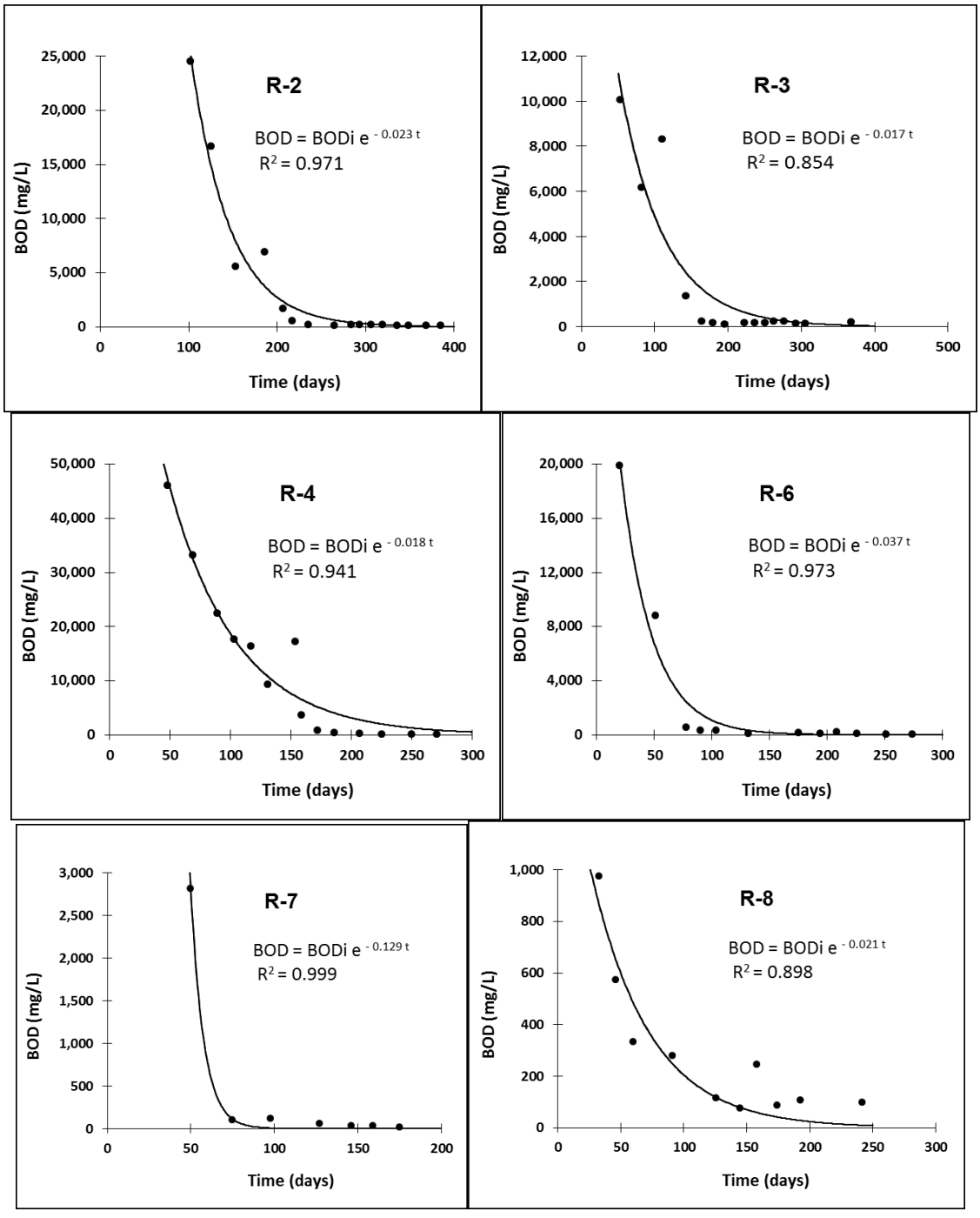
R-2
BOD = BODi e - 0.023 t
R2 = 0.971
BOD (mg/L)
Time (days)
R-3
BOD = BODi e - 0.017 t
R2 = 0.854
BOD (mg/L)
Time (days)
R-4
BOD = BODi e - 0.018 t
R2 = 0.941
BOD (mg/L)
Time (days)
R-6
BOD = BODi e - 0.037 t
R2 = 0.973
BOD (mg/L)
Time (days)
R-7
BOD = BODi e - 0.129 t
R2 = 0.999
BOD (mg/L)
Time (days)
R-8
BOD = BODi e - 0.021 t
R2 = 0.898
BOD (mg/L)
Time (days)

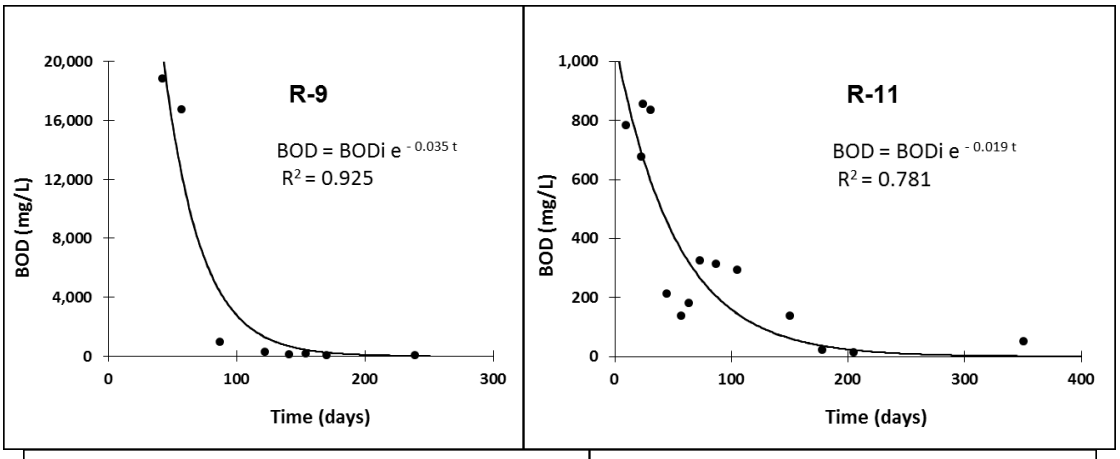
R-9
BOD = BODi e - 0.035 t
R2 = 0.925
BOD (mg/L)
Time (days)
R-11
BOD = BODi e - 0.019 t
R2 = 0.781
BOD (mg/L)
Time (days)

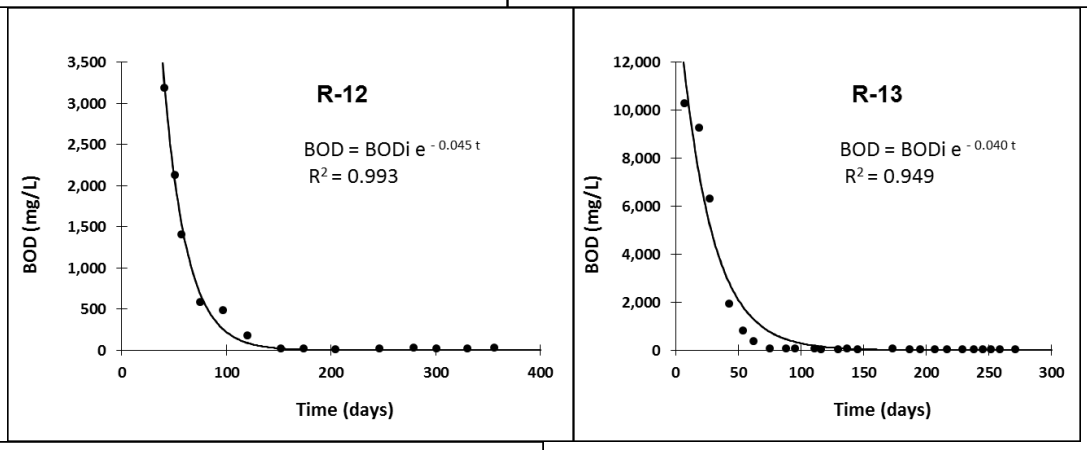
R-12
BOD = BODi e - 0.045 t
R2 = 0.993
BOD (mg/L)
Time (days)
R-13
BOD = BODi e - 0.040 t
R2 = 0.949
BOD (mg/L)
Time (days)

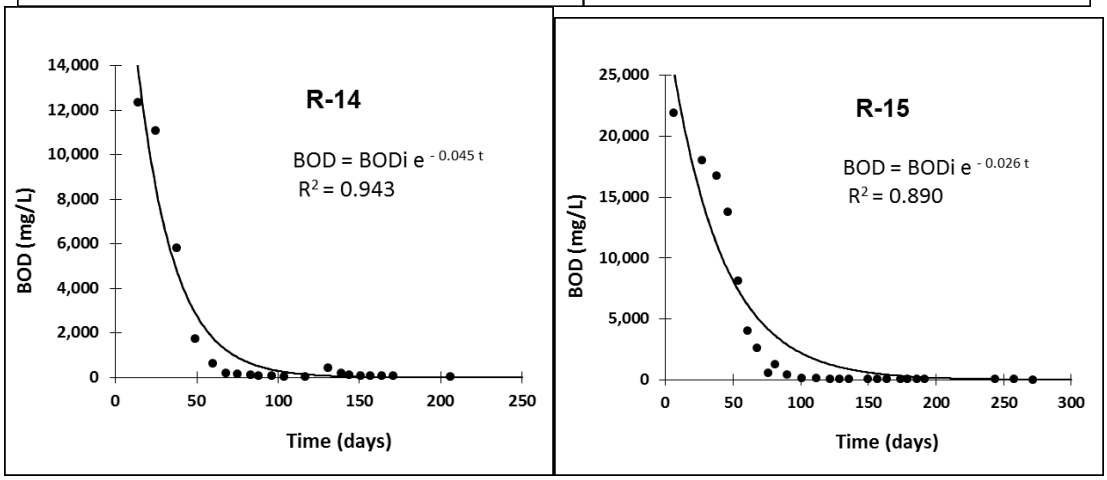
R-14
BOD = BODi e - 0.045 t
R2 = 0.943
BOD (mg/L)
Time (days)
R-15
BOD = BODi e - 0.026 t
R2 = 0.890
BOD (mg/L)
Time (days)

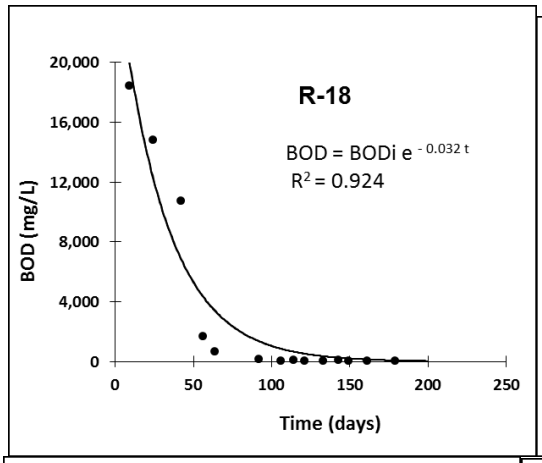
R-18
BOD = BODi e - 0.032 t
R2 = 0.924
BOD (mg/L)
Time (days)

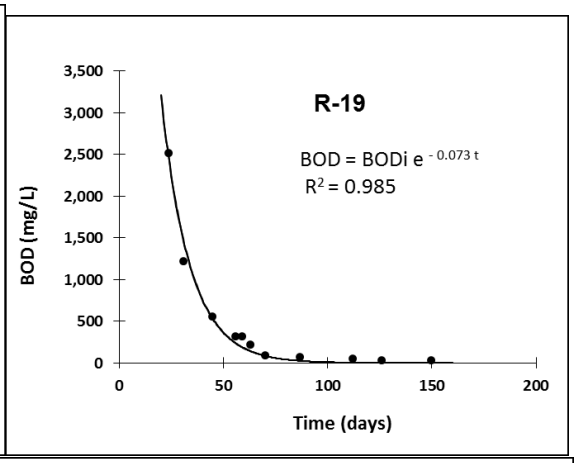
R-19
BOD = BODi e - 0.073 t
R2 = 0.985
BOD (mg/L)
Time (days)

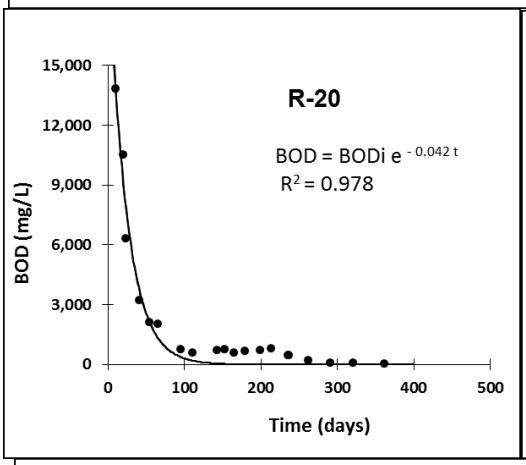
R-20
BOD = BODi e - 0.042 t
R2 = 0.978
BOD (mg/L)
Time (days)

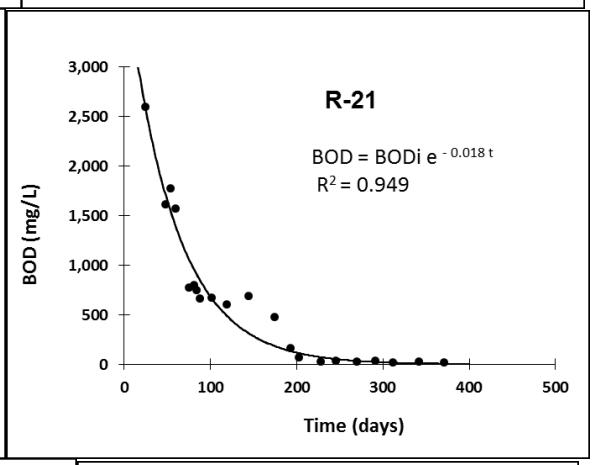
R-21
BOD = BODi e - 0.018 t
R2 = 0.949
BOD (mg/L)
Time (days)

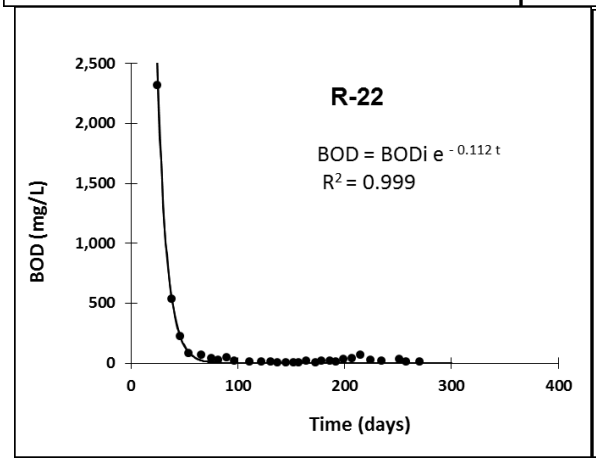
R-22
BOD = BODi e - 0.112 t
R2 = 0.999
BOD (mg/L)
Time (days)

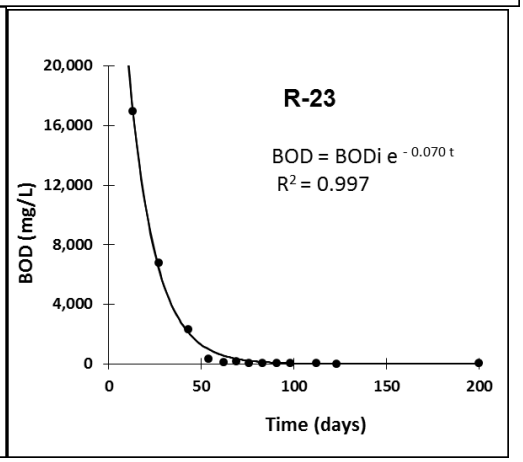
R-23
BOD = BODi e - 0.070 t
R2 = 0.997
BOD (mg/L)
Time (days)

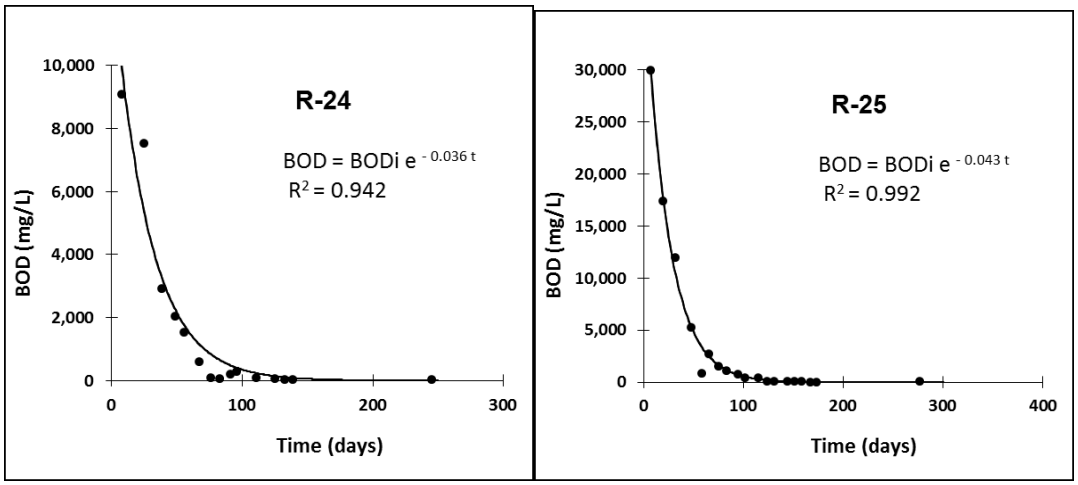
R-24
BOD = BODi e - 0.036 t
R2 = 0.942
BOD (mg/L)
Time (days)
R-25
BOD = BODi e - 0.043 t
R2 = 0.992
BOD (mg/L)
Time (days)

COD Curves

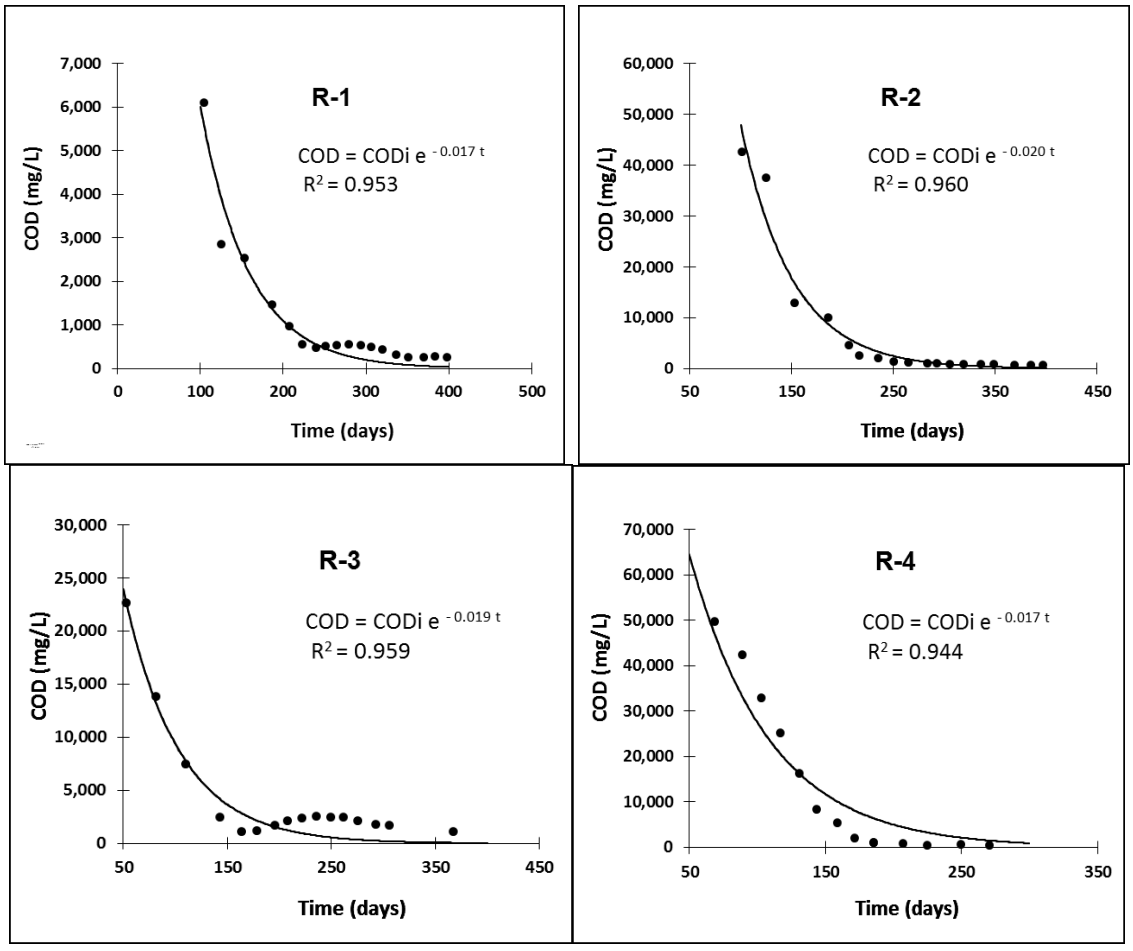
R-1
COD = CODi e - 0.017 t
R2 = 0.953
COD (mg/L)
Time (days)
R-2
COD = CODi e - 0.020 t
R2 = 0.960
COD (mg/L)
Time (days)
R-3
COD = CODi e - 0.019 t
R2 = 0.959
COD (mg/L)
Time (days)
R-4
COD = CODi e - 0.017 t
R2 = 0.944
COD (mg/L)
Time (days)

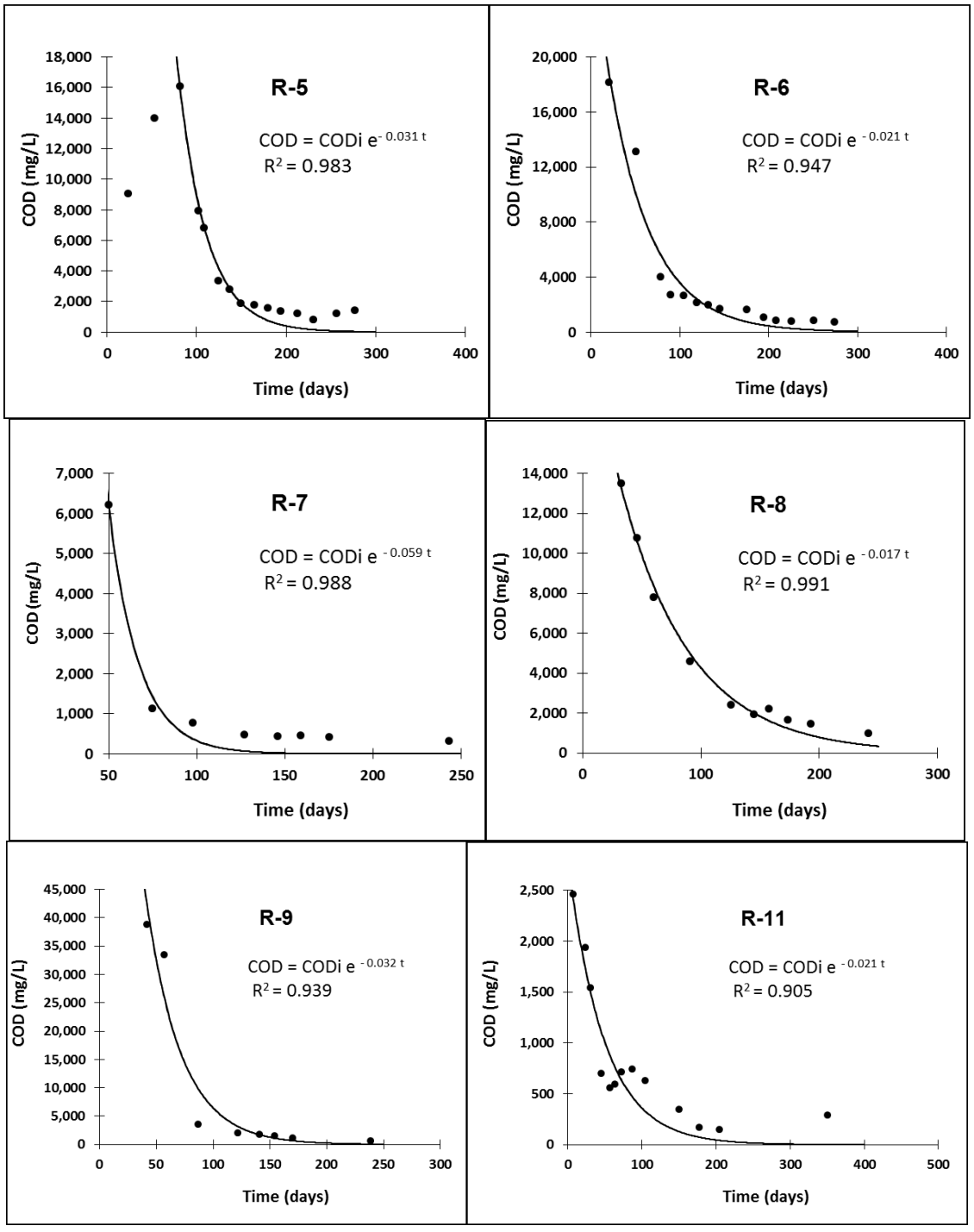
R-5
COD = CODi e- 0.031 t
R2 = 0.983
COD (mg/L)
Time (days)
R-6
COD = CODi e - 0.021 t
R2 = 0.947
COD (mg/L)
Time (days)
R-7
COD = CODi e - 0.059 t
R2 = 0.988
COD (mg/L)
Time (days)
R-8
COD = CODi e - 0.017 t
R2 = 0.991
COD (mg/L)
Time (days)
R-9
COD = CODi e - 0.032 t
R2 = 0.939
COD (mg/L)
Time (days)
R-11
COD = CODi e - 0.021 t
R2 = 0.905
COD (mg/L)
Time (days)

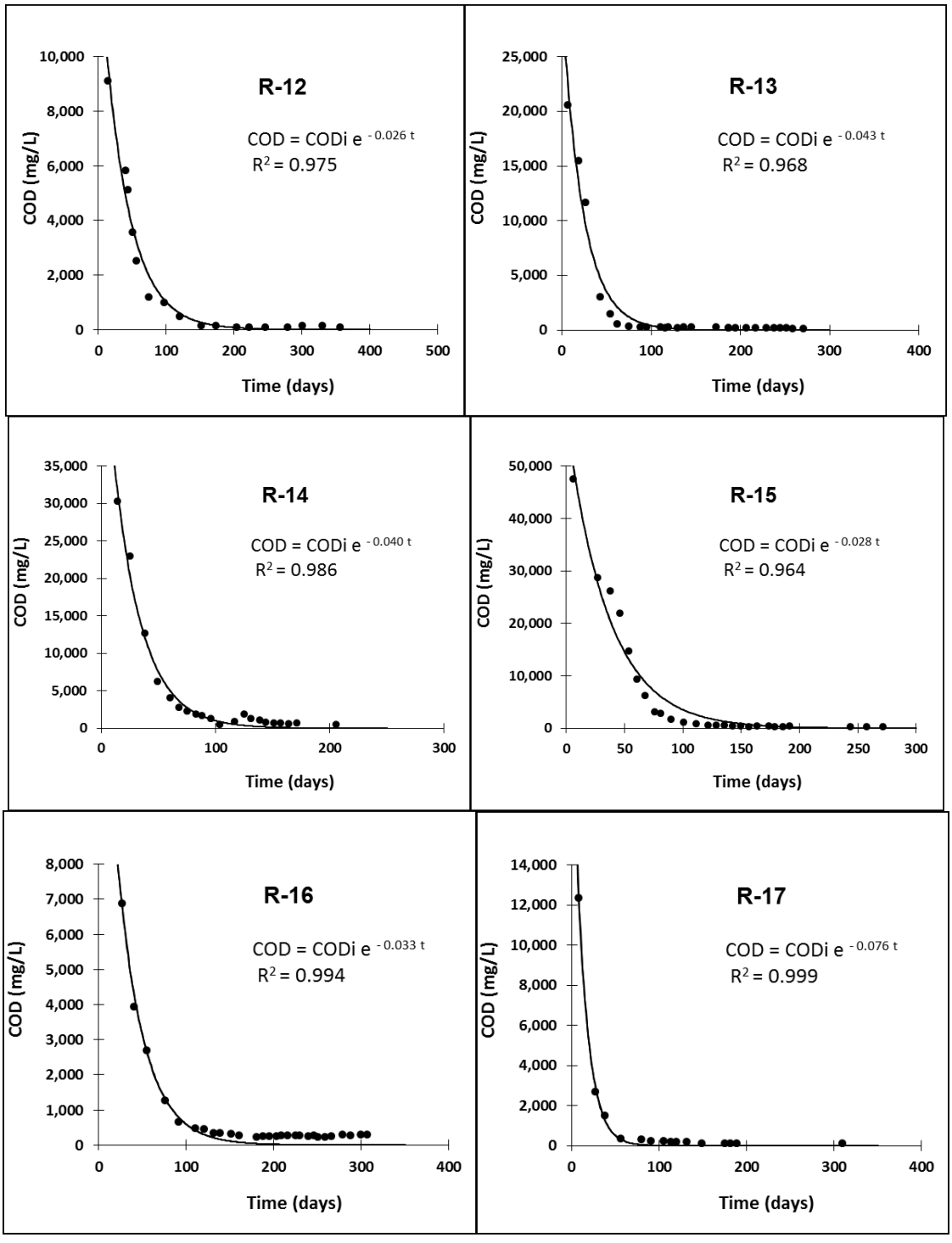
R-12
COD = CODi e - 0.026 t
R2 = 0.975
COD (mg/L)
Time (days)
R-13
COD = CODi e - 0.043 t
R2 = 0.968
COD (mg/L)
Time (days)
R-14
COD = CODi e - 0.040 t
R2 = 0.986
COD (mg/L)
Time (days)
R-15
COD = CODi e - 0.028 t
R2 = 0.964
COD (mg/L)
Time (days)
R-16
COD = CODi e - 0.033 t
R2 = 0.994
COD (mg/L)
Time (days)
R-17
COD = CODi e - 0.076 t
R2 = 0.999
COD (mg/L)
Time (days)

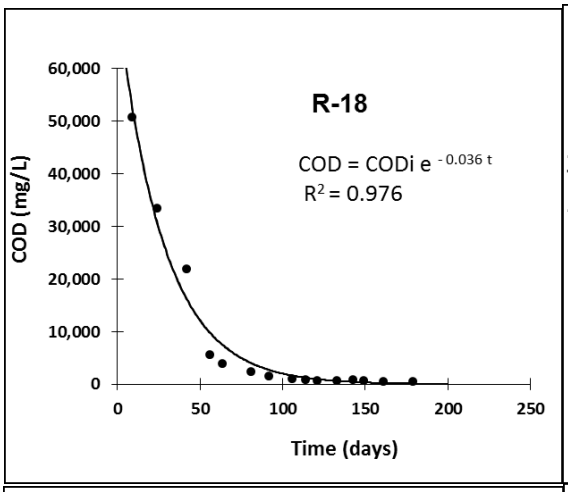
R-18
COD = CODi e - 0.036 t
R2 = 0.976
COD (mg/L)
Time (days)
60,000
50,000
40,000
30,000
20,000
10,000
0
0
50
100
150
200
250

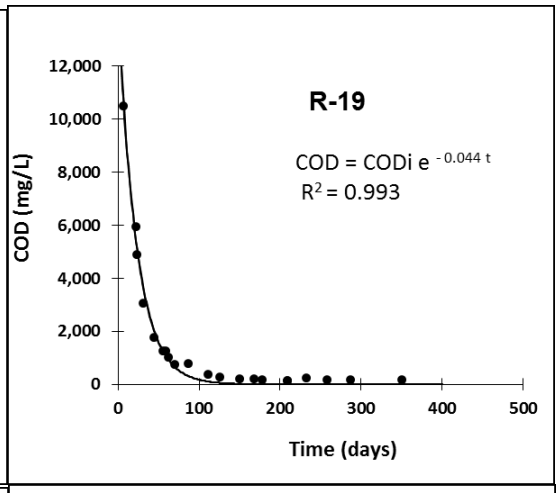
R-19
COD = CODi e - 0.044 t
R2 = 0.993
COD (mg/L)
Time (days)
12,000
10,000
8,000
6,000
4,000
2,000
0
0
100
200
300
400
500

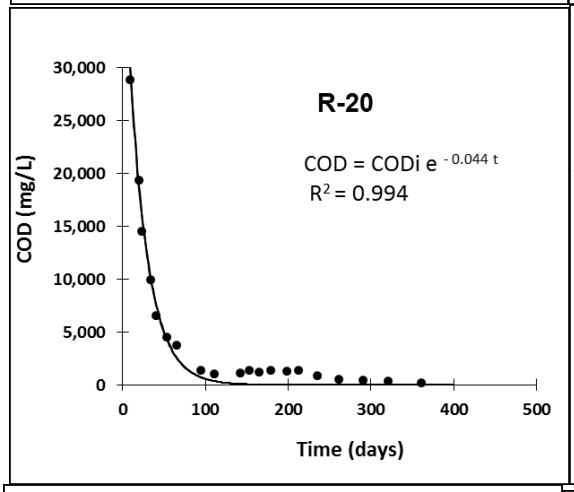
R-20
COD = CODi e - 0.044 t
R2 = 0.994
COD (mg/L)
Time (days)
30,000
25,000
20,000
15,000
10,000
5,000
0
0
100
200
300
400
500

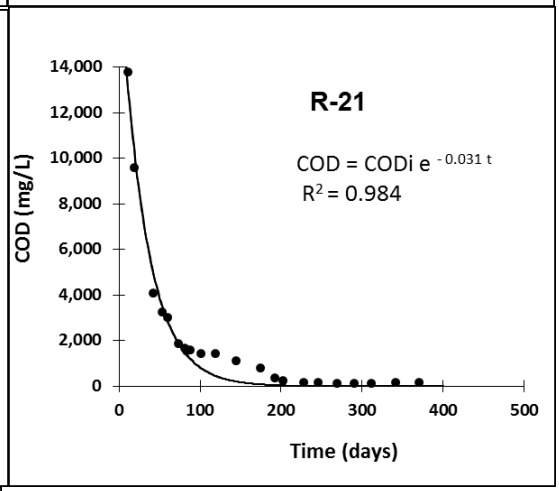
R-21
COD = CODi e - 0.031 t
R2 = 0.984
COD (mg/L)
Time (days)
14,000
12,000
10,000
8,000
6,000
4,000
2,000
0
0
100
200
300
400
500

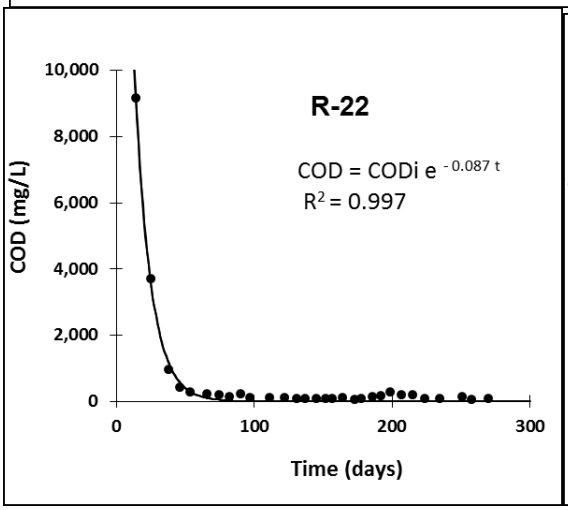
R-22
COD = CODi e - 0.087 t
R2 = 0.997
COD (mg/L)
Time (days)
10,000
8,000
6,000
4,000
2,000
0
0
100
200
300

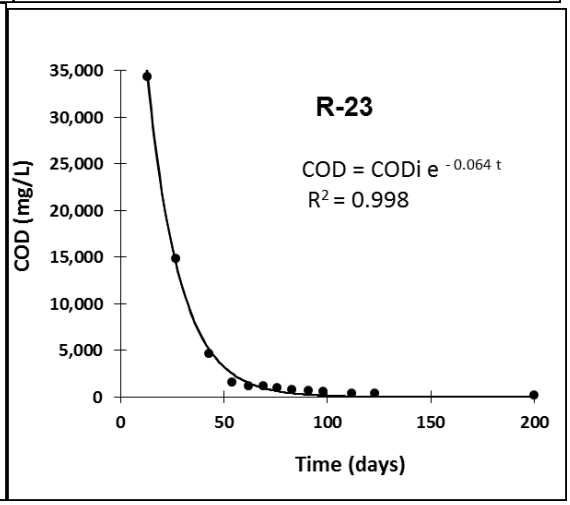
R-23
COD = CODi e - 0.064 t
R2 = 0.998
COD (mg/L)
Time (days)
35,000
30,000
25,000
20,000
15,000
10,000
5,000
0
0
50
100
150
200

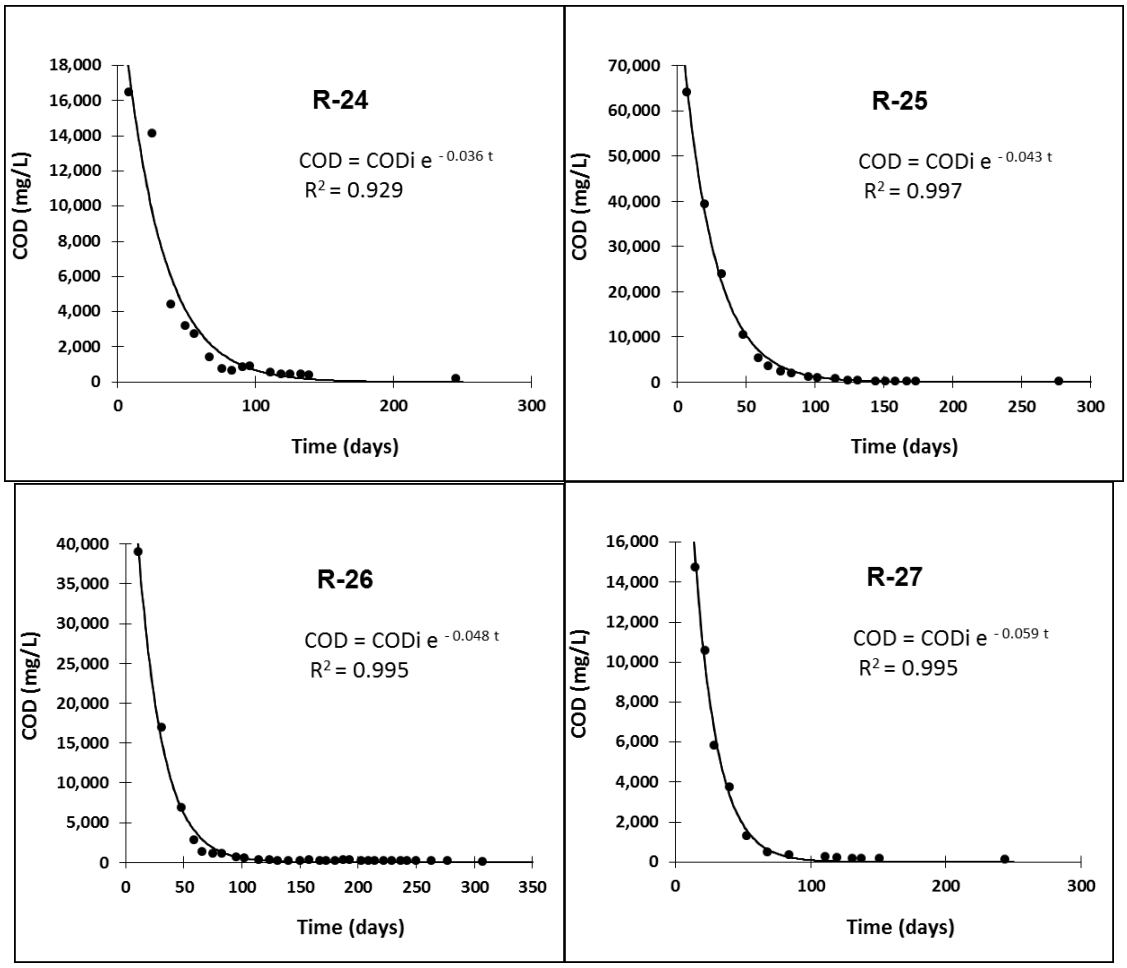
R-24
COD = CODi e - 0.036 t
R2 = 0.929
COD (mg/L)
Time (days)
R-25
COD = CODi e - 0.043 t
R2 = 0.997
COD (mg/L)
Time (days)
R-26
COD = CODi e - 0.048 t
R2 = 0.995
COD (mg/L)
Time (days)
R-27
COD = CODi e - 0.059 t
R2 = 0.995
COD (mg/L)
Time (days)

Appendix B

Residual Plots for Several Transformations and Hypothesis Tests

Square Root k_{COD} → R, T, F, P, Y, X

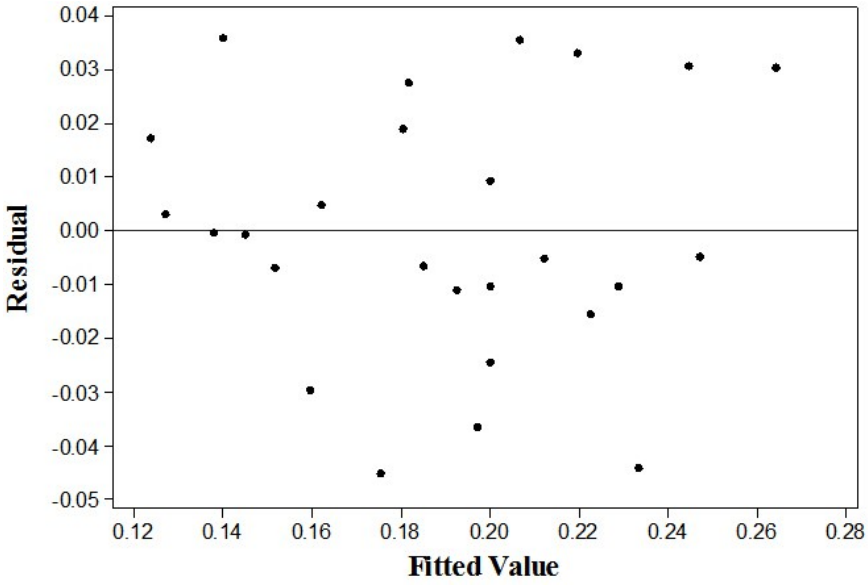

Residuals vs. Fitted Values

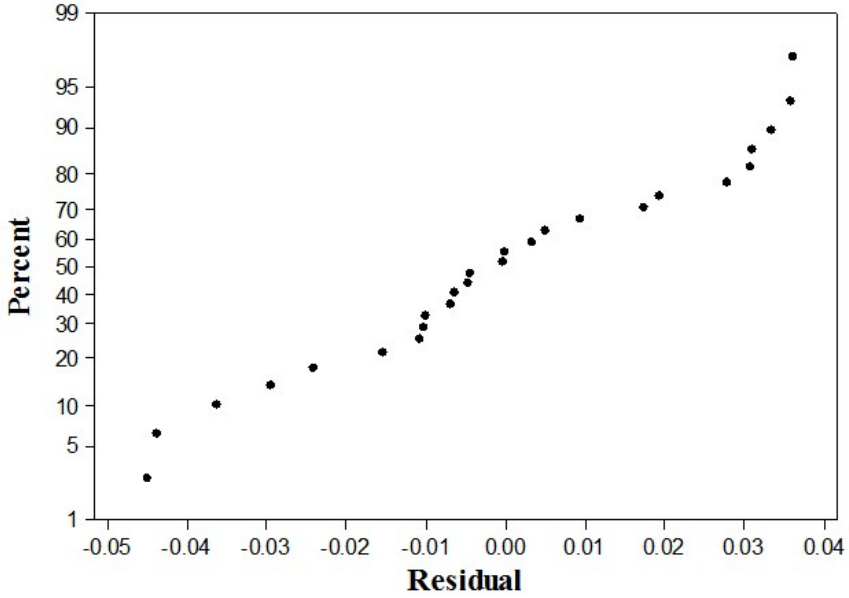

Normal Probability Plot

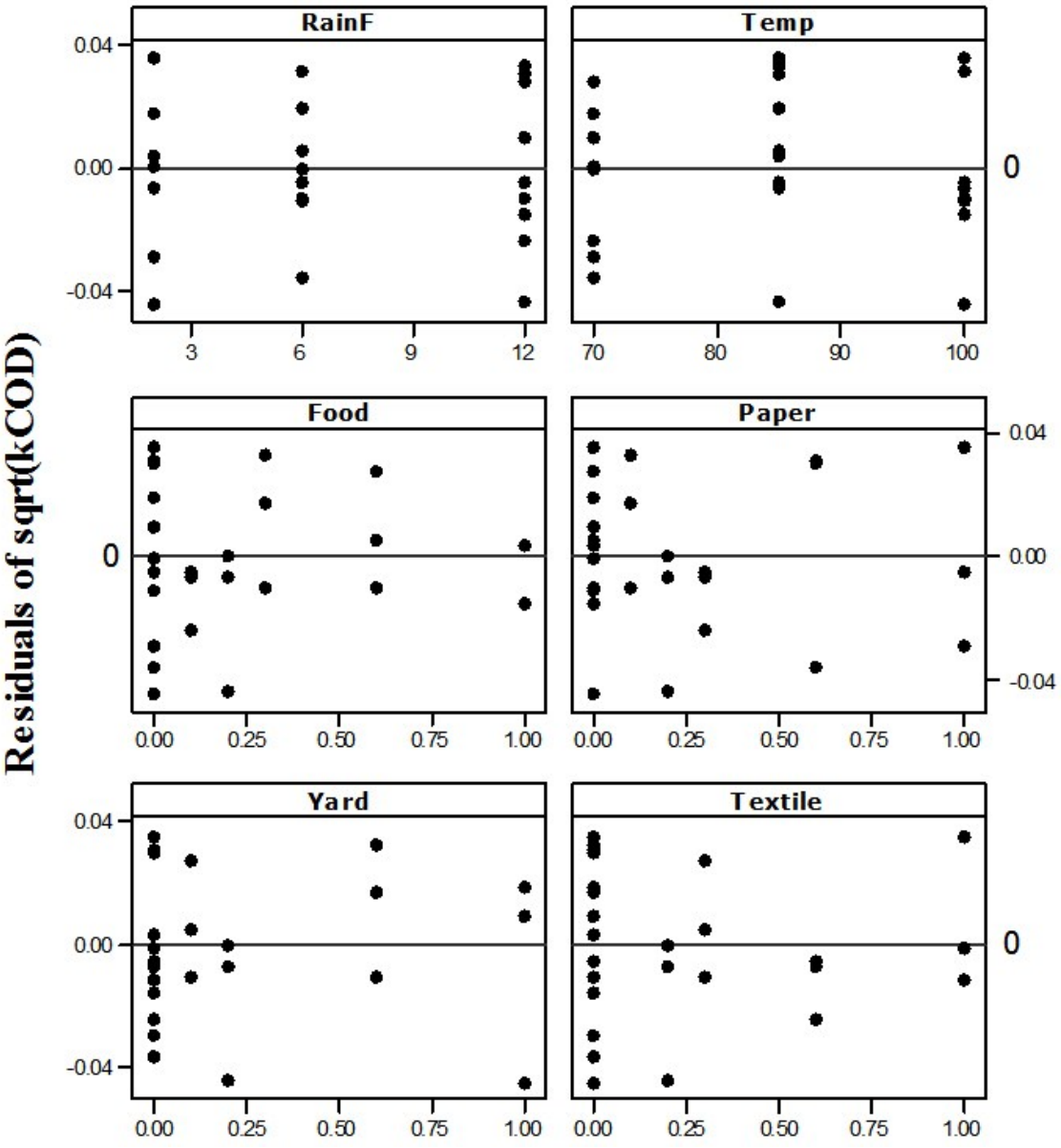

Plots of Residuals vs. Predictor Variables

$Log_{10}(k_{COD})$ → R, T, F, P, Y, X

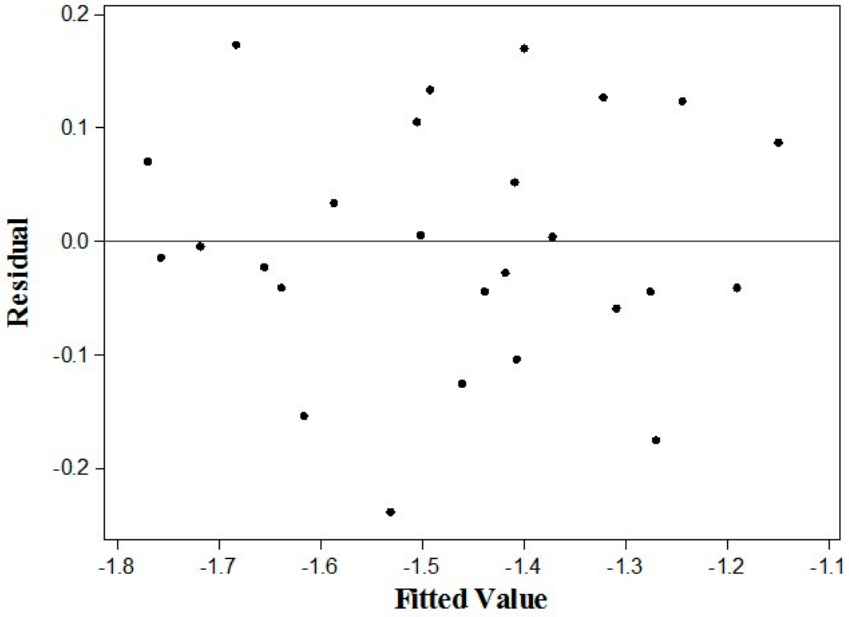

Residuals vs. Fitted Values

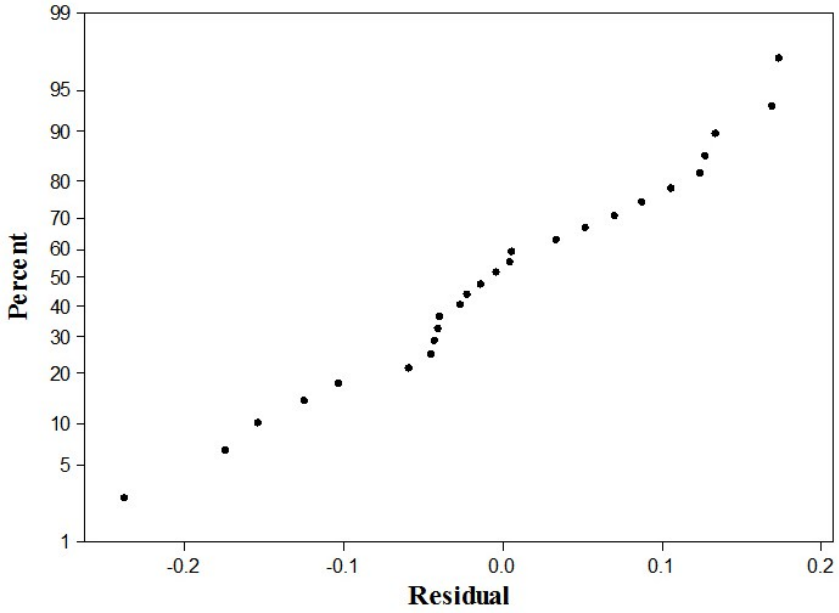

Normal Probability Plot

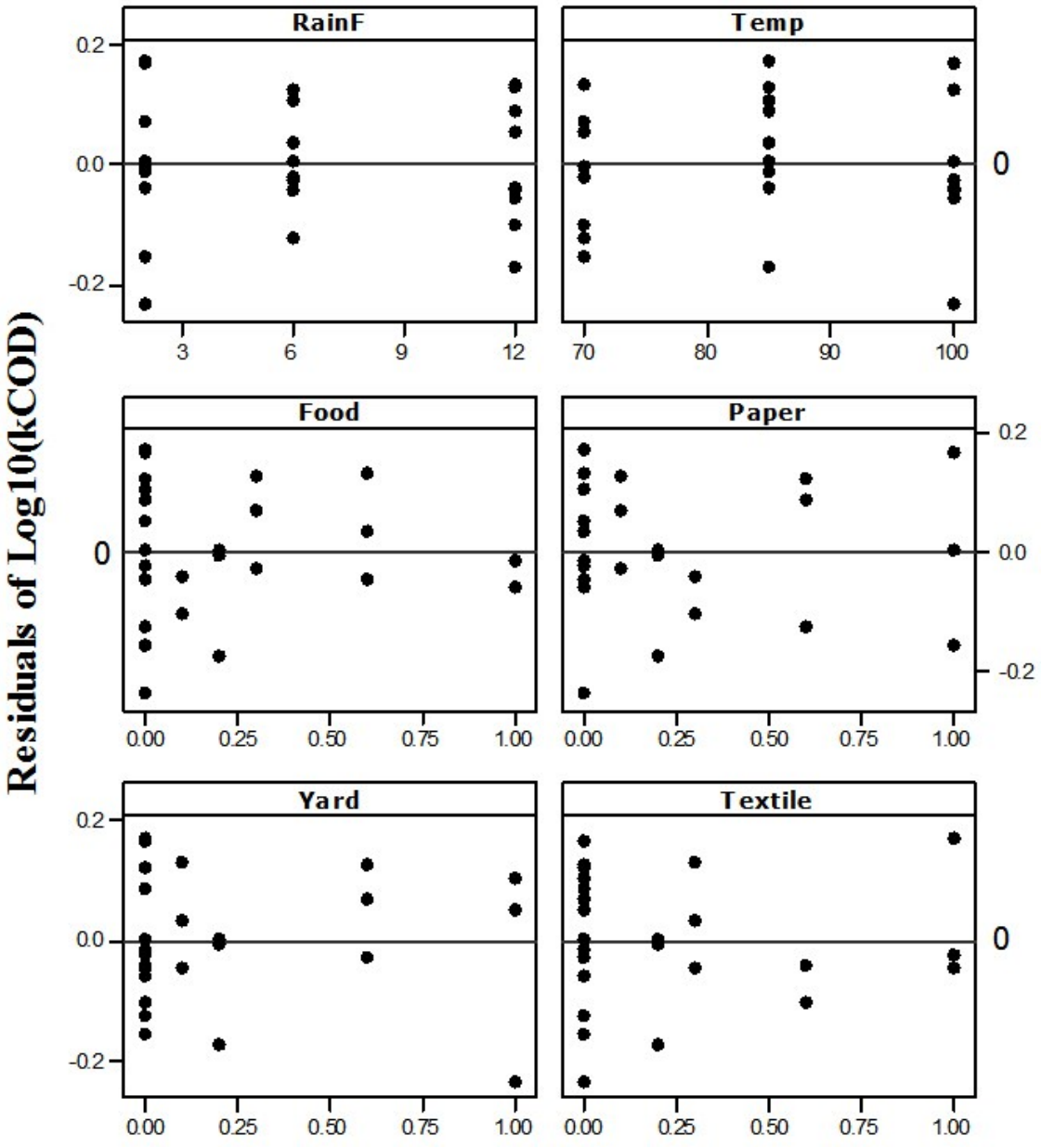

Plots of Residuals vs. Predictor Variables

Hypothesis Tests for the k_{COD} Transformed Model:

A- Modified Levene Test is a tool to test whether the residuals have a constant variance. It divides the 26 residuals, at their median value, into two groups of 13 observations each; d_1 and d_2. Variances $(\sigma_{d_1}, \sigma_{d_2})$ of the two groups are then tested to check whether they are equal.

1- F-test

- Hypothesis:

$$H_0 : \sigma_{d_1} = \sigma_{d_2}$$

$$H_1 : \sigma_{d_1} \neq \sigma_{d_2}$$

- Decision Rule:

If the p-value from the F-test is < 0.1, then reject H_0.

Table B-1 shows SAS output of the Modified Levene Test (also called Brown and Forsythe test). The F-test p-value (denoted Pr > F) was 0.4564 which was > 0.1, so we failed to reject H_0.

- Conclusion:

Variances of d_1 and d_2 were equal.

2- T-test is performed to check whether the means of d_1 and d_2 populations are equal.

- Hypothesis:

$$H_0 : error\ variance\ is\ constant$$

$$H_1 : error\ variance\ is\ not\ constant$$

- Decision Rule:

If the p-value from the t-test is < 0.1, then reject H_0.

The p-value from Table B-1 (Pooled-Pr > | t |) was 0.6744 > 0.1, so we failed to reject H_0.

- Conclusion:

The model's error variance was constant.

Table B-1 SAS Output of the Modified Levene Test

The TTEST Procedure
Variable: d

group	N	Mean	Std Dev	Std Err	Minimum	Maximum
1	13	0.0911	0.0862	0.0239	0	0.2964
2	13	0.0781	0.0692	0.0192	0	0.1926
Diff (1-2)		0.0130	0.0782	0.0307		

Method	Variances	DF	t Value	Pr > |t|
Pooled	Equal	24	0.43	0.6744
Satterthwaite	Unequal	22.922	0.43	0.6746

Equality of Variances

Method	Num DF	Den DF	F Value	Pr > F
Folded F	12	12	1.55	0.4564

B- The Normality Test is performed to confirm whether the residuals are normally distributed. It is conducted by calculating the correlation coefficient between the residuals (e) and their expected values under normality (enrm).

- Hypothesis:

H_0 : $Normality\ is\ okay$

H_1 : $Normality\ is\ violated$

- Decision Rule:

If the correlation coefficient *p* is < $C(\alpha, n)$, then reject H_0. C is the critical value, α is 0.1 and n is 26. $C(\alpha, n) = (0.1,26) = 0.967$

Table B-2 shows SAS output of the normality test.

p = 0.9837 > 0.967, so we failed to reject H_0.

- Conclusion:

Normality assumption was satisfied.

Table B-2 SAS Output of the Normality Test

	e	enrm
e(Log10kCOD | R T sqF P sqY X)	1.00000	0.98365
enrm	0.98365	1.00000

Normal scores

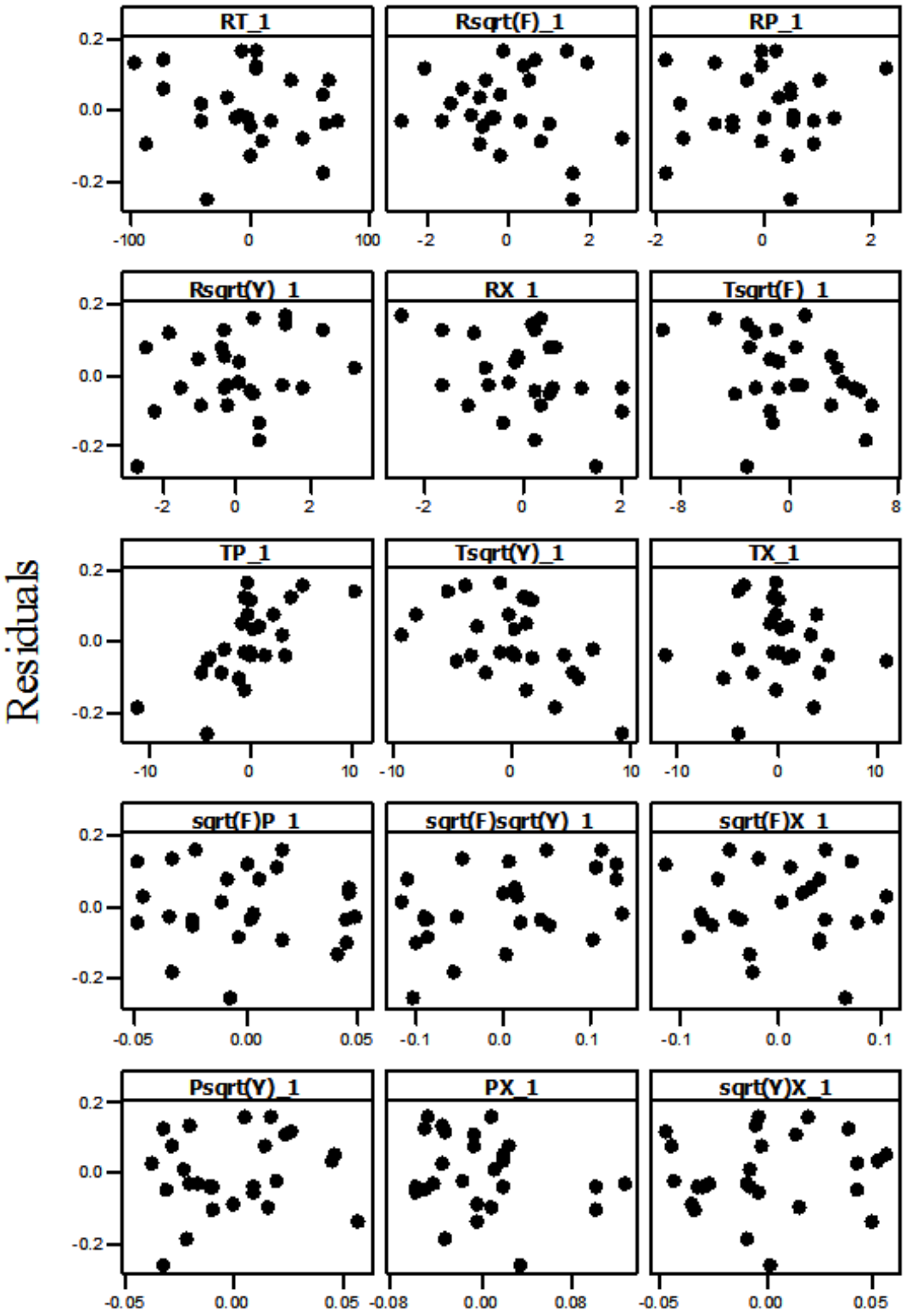

Partial Regression Plots – Transformed k_{COD} Model

Square Root k_{BOD} → R, T, F, P, Y, X

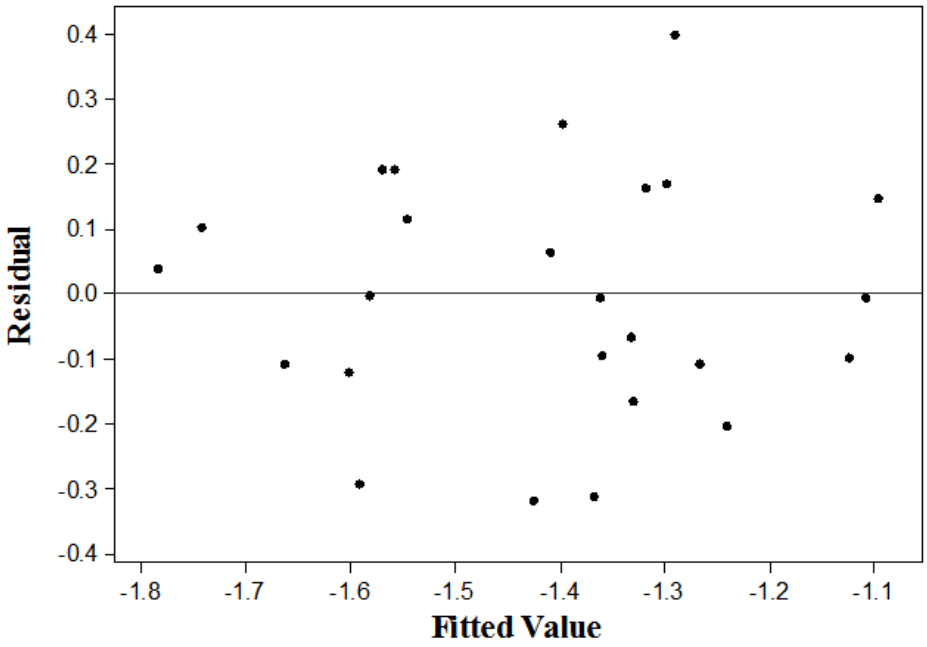

Residuals vs. Fitted Values

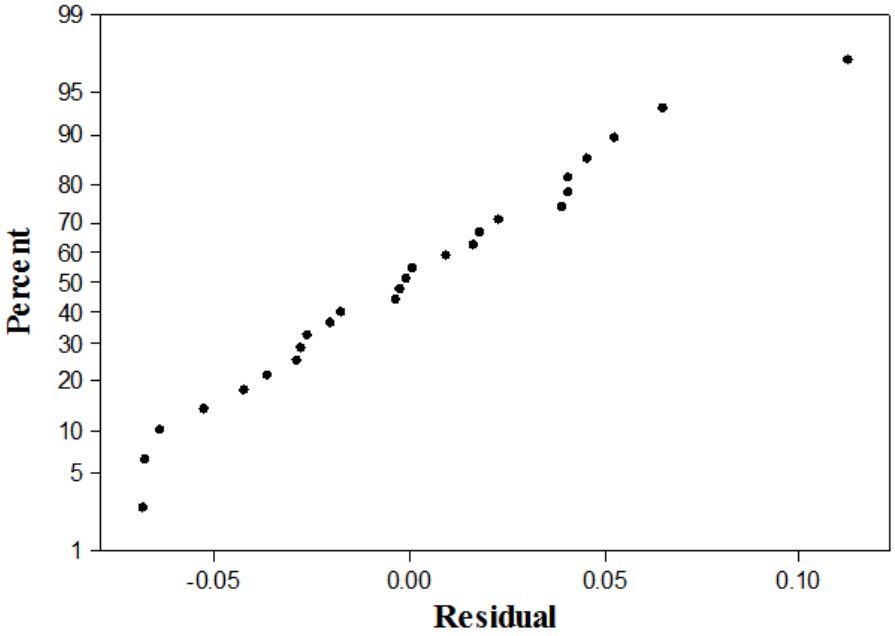

Normal Probability Plot

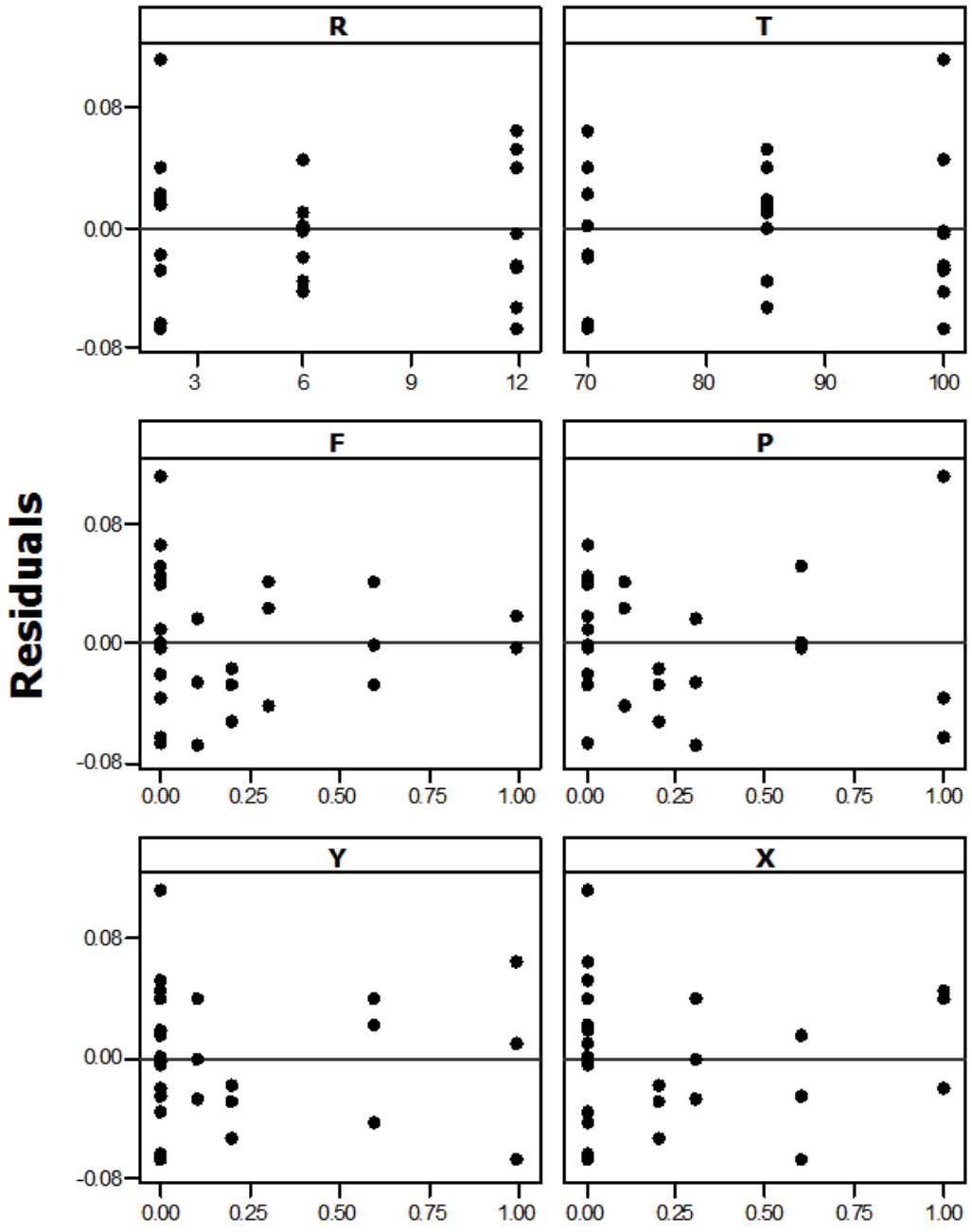

Plots of Residuals vs. Predictor Variables

$Log_{10}(k_{BOD})$ → R, T, F, P, Y, X

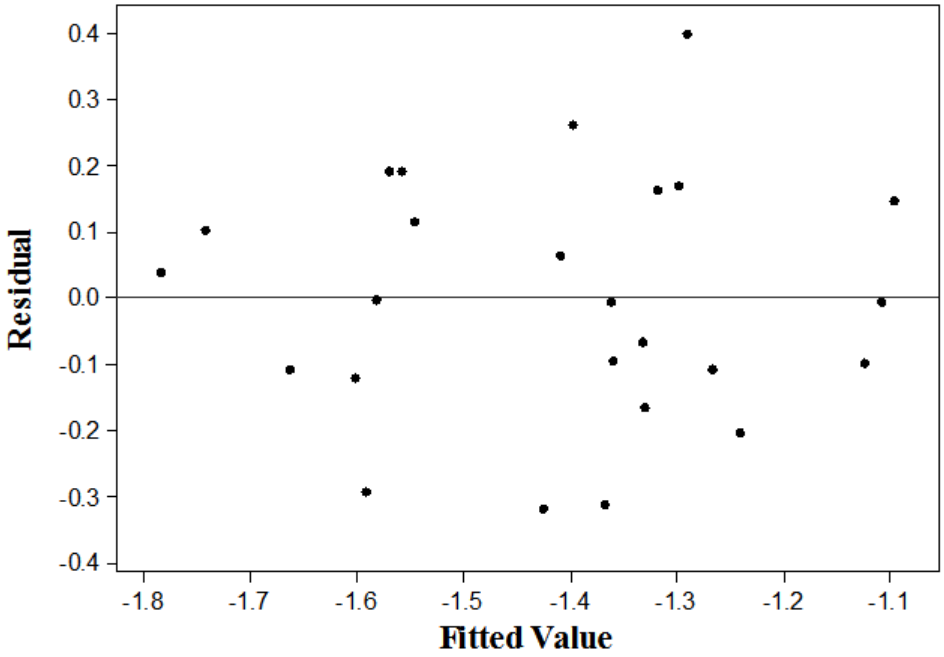

Residuals vs. Fitted Values

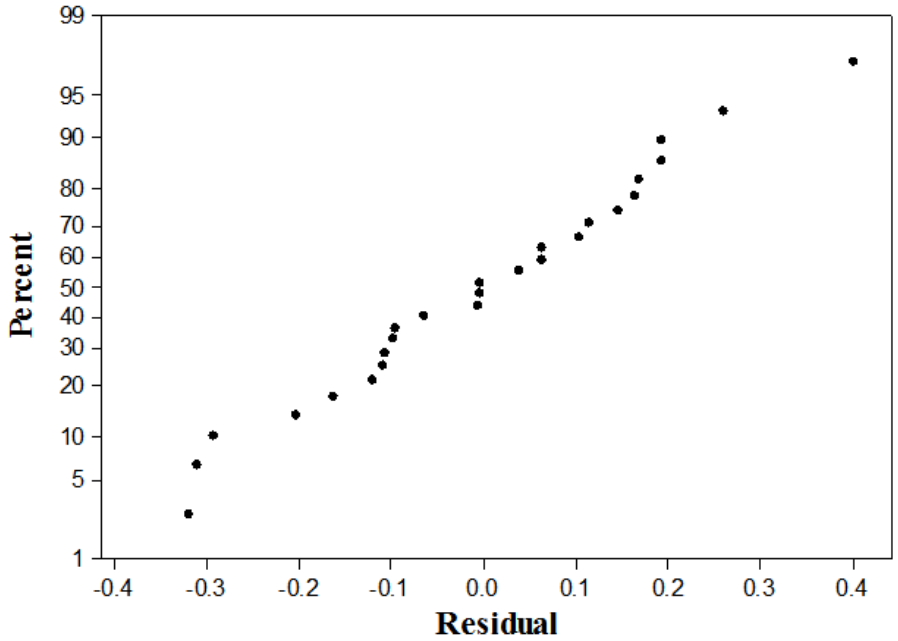

Normal Probability Plot

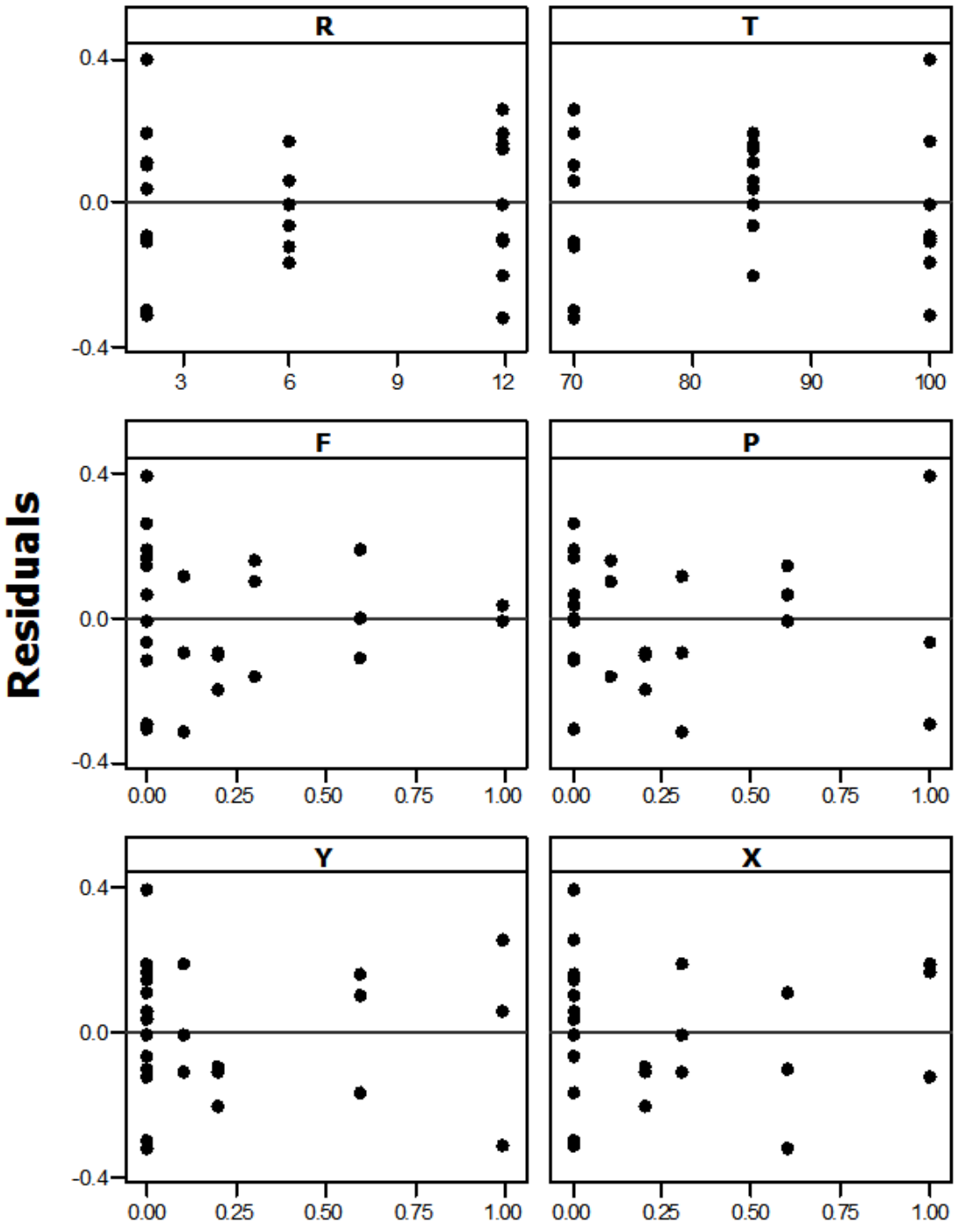

Plots of Residuals vs. Predictor Variables

Hypothesis Tests for the k_{BOD} Transformed Model:

A- Modified Levene Test

1- F-test

- Hypothesis:

$H_0 : \sigma_{d_1} = \sigma_{d_2}$

$H_1 : \sigma_{d_1} \neq \sigma_{d_2}$

- Decision Rule:

If the p-value from the F-test is < 0.1, then reject H_0.

Table B-3 shows SAS output of the Modified Levene Test. The F-test p-value (denoted Pr > F) was 0.8554 which was > 0.1, so we failed to reject H_0.

- Conclusion:

Variances of d_1 and d_2 were equal.

2- T-test is performed to check whether the means of d_1 and d_2 populations are equal.

- Hypothesis:

$H_0 : error\ variance\ is\ constant$

$H_1 : error\ variance\ is\ not\ constant$

- Decision Rule:

If the p-value from the t-test is < 0.1, then reject H_0.

The p-value from Table B-3 (Pooled-Pr > | t |) was 0.9101 > 0.1, so we failed to reject H_0.

- Conclusion:

The model's error variance was constant.

Table B-3 SAS Output of the Modified Levene Test

The TTEST Procedure
Variable: d

group	N	Mean	Std Dev	Std Err	Minimum	Maximum
1	13	0.1322	0.1127	0.0312	0	0.3545
2	13	0.1374	0.1189	0.0330	0	0.3977
Diff (1-2)		-0.00518	0.1158	0.0454		

Method	Variances	DF	t Value	Pr > |t|
Pooled	Equal	24	-0.11	0.9101
Satterthwaite	Unequal	23.931	-0.11	0.9101

Equality of Variances

Method	Num DF	Den DF	F Value	Pr > F
Folded F	12	12	1.11	0.8554

B- The Normality Test

- Hypothesis:

H_0 : $Normality\ is\ okay$

H_1 : $Normality\ is\ violated$

- Decision Rule:

If the correlation coefficient *p* is < $C(\alpha, n)$, then reject H_0. C is the critical value, α is 0.1 and n is 26. $C(\alpha, n) = (0.1{,}26) = 0.967$

Table B-4 shows SAS output of the normality test.

p = 0.9896 > 0.967, so we failed to reject H_0.

- Conclusion:

Normality assumption is satisfied.

Table B-4 SAS Output of the Normality Test

	e	enrm
e(Log10kBOD | R T sqF P Y sqX)	1.00000	0.98961
enrm	0.98961	1.00000

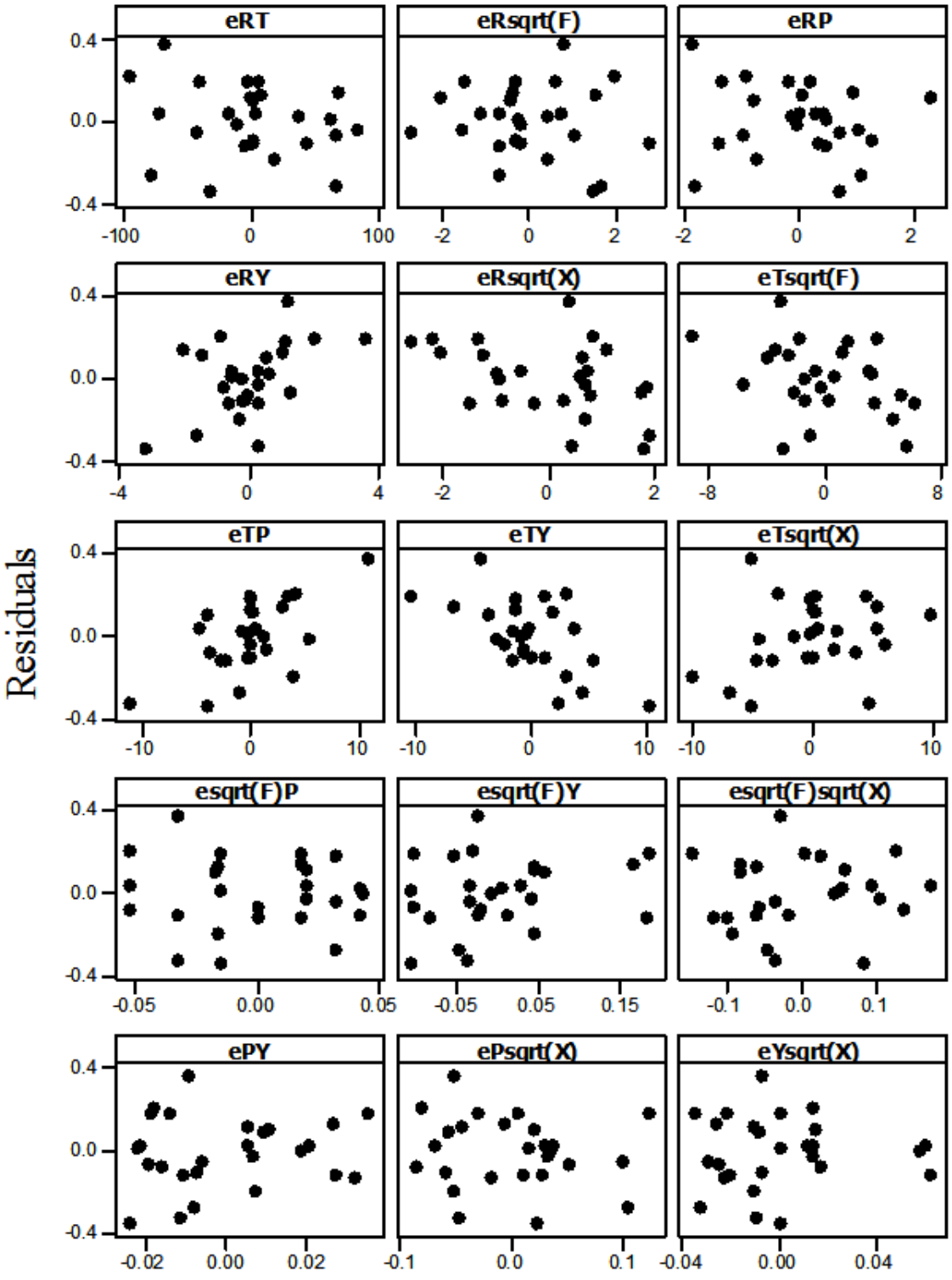

Partial Regression Plots – Transformed k_{BOD} Model

References

1. Al-Yaqout, A. F., & Hamoda, M. F. (2003). Evaluation of landfill leachate in arid climate-a case study. *Environ Int, 29*(5), 593-600.
2. Armstrong, M., & Rowe, R. (1999). *Effect of landfill operations on the quality of municipal solid waste leachate*.
3. Aziz, S. Q., Aziz, H. A., Yusoff, M. S., Bashir, M. J., & Umar, M. (2010). Leachate characterization in semi-aerobic and anaerobic sanitary landfills: a comparative study. *J Environ Manage, 91*(12), 2608-2614.
4. Barlaz, M. A. (2006). Forest products decomposition in municipal solid waste landfills. *Waste Management, 26*(4), 321-333.
5. Barlaz, M. A., Eleazer, W. E., Odle, W. S., Qian, X., & Wang, Y. S. (1997). Biodegradative analysis of municipal solid waste in laboratory-scale landfills. *Environmental Protection Agency, Cincinnati, OH*.
6. Barlaz, M. A., Ham, R. K., Schaefer, D. M., & Isaacson, R. (1990). Methane production from municipal refuse: a review of enhancement techniques and microbial dynamics. *Critical Reviews in Environmental Science and Technology, 19*(6), 557-584.
7. Brebu, M., & Vasile, C. (2010). Thermal degradation of lignin—A review. *Cellulose Chemistry & Technology, 44*(9), 353.
8. Chain, E. S. K. (1977). Stability of organic matter in leachates. *Water Research, 11*(225-232).
9. Chen, K. Y., and Bowerman, F. R. (1974). Recycling and disposal of solid wastes: industrial, agricultural, domestic: Ann Arbor Science Publishers.
10. Chen, P. H. (1996). Assessment of leachates from sanitary landfills: Impact of age, rainfall, and treatment. *Environment International, 22*(2), 225-237.

11. Christensen, T. H. (2011). *Solid Waste Technology & Management* (Vol. 2): John Wiley and Sons.

12. Clesceri, L. S., Greenberg, A.E., Eaton, A.D. (1999). *Standard Methods for Examination of Water & Wastewater*: Amer Public Health Assn.

13. Daskalopoulos, E., Badr, O., & Probert, S. (1998). Municipal solid waste: a prediction methodology for the generation rate and composition in the European Union countries and the United States of America. *Resources, conservation and recycling, 24*(2), 155-166.

14. Demetracopoulos, A. C., Sehayek, L., & Erdogan, H. (1986). Modeling Leachate Production from Municipal Landfills. *Journal of Environmental Engineering, 112*(5), 849-849.

15. El-Fadel, M., Bou-Zeid, E., Chahine, W., & Alayli, B. (2002). Temporal variation of leachate quality from pre-sorted and baled municipal solid waste with high organic and moisture content. *Waste Management, 22*(3), 269-282.

16. Eleazer, W. E., Odle III, W. S., Wang, Y. S., & Barlaz, M. A. (1997). Biodegradability of municipal solid waste components in laboratory-scale landfills. *Environmental Science & Technology, 31*(3), 911-917.

17. EPA. (1997). EPA's COMPOSITE MODEL FOR LEACHATE MIGRATION WITH TRANSFORMATION PRODUCTS: USER'S GUIDE. *U. S. E. P. Agency.*

18. EPA. (2008). MSW in the U.S.: Facts and Figures. *O. o. S. W. United States Environmental Protection Agency.*

19. EPA. (2011). Municipal Solid Waste Generation, Recycling, and Disposal in the United States: Facts and Figures for 2010. *USEPA.*

20. Fan, H. J., Shu, H. Y., Yang, H. S., & Chen, W. C. (2006). Characteristics of landfill leachates in central Taiwan. *Sci Total Environ, 361*(1-3), 25-37.

21. Farquhar, G. (1989). Leachate. Production and characterization. *Canadian Journal of Civil Engineering/Revue Canadienne de Genie Civil, 16*(3), 317-325.

22. Fellner, J., & Brunner, P. H. (2010). Modeling of leachate generation from MSW landfills by a 2-dimensional 2-domain approach. *Waste Manag, 30*(11), 2084-2095.

23. Fuller, W., Alesii, B., & Carter, G. (1979). Behavior of municipal solid waste leachate. I. Composition variations. *Journal of Environmental Science & Health Part A, 14*(6), 461-485.

24. Gau, S., Chang, P., & Chang, F. (1991). *A study on the procedure of leachate treatment by Fenton method*.

25. Gau, S.-H., & Chow, J.-D. (1998). Landfill leachate characteristics and modeling of municipal solid wastes combined with incinerated residuals. *J Hazard Mater, 58*(1-3), 249-259.

26. Gönüllü, M. T. (1994). Analytical Modelling Of Organic Contaminants In Leachate. *Waste Management & Research, 12*(2), 141-150.

27. Grellier, S., Robain, H., Bellier, G., & Skhiri, N. (2006). Influence of temperature on the electrical conductivity of leachate from municipal solid waste. *J Hazard Mater, 137*(1), 612-617.

28. James, J. N., & Arnold, A. E. (1991). Experimental and mathematical modeling of moisture transport in landfills. *Chemical Engineering Communications, 100*(1), 95-111.

29. Johannessen, L. M. (1999). Guidance note on leachate management for municipal solid waste landfills. *T. W. Bank.*

30. Jung, J. Y., Lee, S. M., Shin, P. K., & Chung, Y. C. (2000). Effect of pH on phase separated anaerobic digestion. *Biotechnology and Bioprocess Engineering, 5*(6), 456-459.

31. Kemper, J. M., & Smith, R. B. (1981). Leachate Production by Landfilled Processed Municipal Wastes.

32. Kjeldsen, P., Barlaz, M. A., Rooker, A. P., Baun, A., Ledin, A., & Christensen, T. H. (2002). Present and long-term composition of MSW landfill leachate: a review. *Critical Reviews in Environmental Science and Technology, 32*(4), 297-336.

33. Kouzeli-Katsiri, A., Bosdogianni, A., & Christoulas, D. (1999). Prediction of Leachate Quality from Sanitary Landfills. *Journal of Environmental Engineering, 125*(10), 950-950.

34. Kulikowska, D., & Klimiuk, E. (2008). The effect of landfill age on municipal leachate composition. *Bioresour Technol, 99*(13), 5981-5985.

35. Kutner, M., Nachtsheim, C., Neter, J., & Li, W. (2005). Applied Linear Statistical Models. McGraw-Hill. *New York*.

36. Lu, C. S., Eichenberger, B., & Stearns, R. (1985). Leachate from municipal landfills: production and management.

37. Lu, C. S. J., Morrison, R., & Stearns, R. (1981). *Leachate Production and Management From Municipal Landfills: Summary and Research.* Paper presented at the Land Disposal: Municipal Soild Waste - The 7th Annual Research Symposium

38. Lu, J. C. S., Stearns, R. J., Eichenberger, B., Service, U. S. N. T. I., & Laboratory, M. E. R. (1984). *Production and management of leachate from municipal landfills: summary and assessment*: Municipal Environmental Research Laboratory, Office of Research and Development, US Environmental Protection Agency.

39. Ludwig, C., Hellweg, S., & Stucki, S. (2002). *Municipal Solid Waste Management: Strategies and Technologies for Sustainable Solutions*: Springer.

40. McBean, E. A., Rovers, F. A., & Farquhar, G. J. (1995). *Solid Waste Landfill Engineering and Design*: Prentice Hall PTR.

41. McGinley, P. M., & Kmet, P. (1984). *Formation, characteristics, treatment and disposal of leachate from municipal solid waste landfills*: Bureau of Solid Waste Management.

42. Metcalf, & Eddy. (2004). *Wastewater Engineering: Treatment and Reuse*: McGraw-Hill.

43. Miller, W. L., Townsend, T., Earle, J., Lee, H., & Reinhart, D. R. (1994). *Leachate recycle and the augmentation of biological decomposition at municipal solid waste landfills.* Paper presented at the Second Annual Research Symposium, Florida Center for Solid and Hazardous Waste Management, Tampa.

44. Ozkaya, B., Demir, A., & Bilgili, M. S. (2006). Mathematical simulation and long-term monitoring of leachate components from two different landfill cells. *J Hazard Mater, 135*(1-3), 32-39.

45. Palmisano, A. C., & Barlaz, M. A. (1996). *Microbiology of Solid Waste*: CRC Press.

46. Pidwirny, M. (2010). Introduction to the Hydrosphere. *Fundamentals of Physical Geography*. British Columbia: Michael Pidwirny.

47. Pohland, F. G., Harper, S. R., & Laboratory, H. W. E. R. (1985). *Critical review and summary of leachate and gas production from landfills*: Solid and Hazardous Waste Research Division, Office of Research and Development, US Environmental Protection Agency.

48. Ponsá, S., Ferrer, I., Vázquez, F., & Font, X. (2008). Optimization of the hydrolytic–acidogenic anaerobic digestion stage (55° C) of sewage sludge: Influence of pH and solid content. *Water Research, 42*(14), 3972-3980.

49. Qasim, S. R., & Chiang, W. (1994). *Sanitary Landfill Leachate: Generation, Control and Treatment*: CRC Press.

50. Reinhart, D. R., & Al-Yousfi, B. (1996). The Impact of Leachate Recirculation On Municipal Solid Waste Landfill Operating Characteristics. *Waste Management & Research, 14*(4), 337-346.

51. Reinhart, D. R., & Grosh, C. J. (1998). Analysis of Florida MSW Landfill Leachate Quality.

52. Reinhart, D. R., & Townsend, T. G. (1998). *Landfill bioreactor design and operation*: CRC Press.

53. Rowe, R. K. (1991). Contaminant Impact Assessment and the Contaminating Lifespan of Landfills. *Canadian Journal of Civil Engineering, 18*(2), 244-253.

54. Rowe, R. K. (1995). Leachate Characteristics For MSW Landfills. *G. R. Center.*

55. Senior, E. (1995). *Microbiology of landfill sites*: CRC Press.

56. Sulfita, J., Gerba, C., Ham, R., Palmisano, A., Rathje, W., & Robinson, J. (1992). The world's largest landfill—a multidisciplinary investigation. *Environ Sci Technol, 26*, 1486-1495.

57. UNEP. (2011). UNEP 2010 Annual Report *U. N. E. Programme.*

58. Warith, M. (2002). Bioreactor landfills: experimental and field results. *Waste Management, 22*(1), 7-17.

59. Weitz, K. A., Thorneloe, S. A., Nishtala, S. R., Yarkosky, S., & Zannes, M. (2002). The impact of municipal solid waste management on greenhouse gas emissions in the United States. *Journal of the Air & Waste Management Association (1995), 52*(9), 1000-1011.

60. Wigh, R. J. (1979). Boone County Field Site Interim Report. *U. S. EPA.*

61. Youcai, Z., Luochun, W., Renhua, H., Dimin, X., & Guowei, G. (2002). A comparison of refuse attenuation in laboratory and field scale lysimeters. *Waste Management (New York, N.Y.), 22*(1), 29-35.

62. Zanetti, M. C. (2008). Aerobic Biostabilization of Old MSW Landfills. *American J. of Engineering and Applied Sciences, 1*(4), 393-398.

Biographical Information

Said Altouqi received both his Bachelor's and Master's degrees in Civil Engineering in 2005 and 2008, respectively, from Sultan Qaboos University in Muscat, Oman. He joined The University of Texas at Arlington in 2008 to pursue his Ph.D. in Civil Engineering. His Bachelor's final year project investigated the distribution of trace elements and hydrocarbons in seawater that was caused by offshore crude oil spills in The Gulf of Oman. His Master's thesis focused on studying the regional quality of groundwater resources in Muscat and the effects of landfills and septic tanks on those resources. His research interests are modeling groundwater quality and leachate quality in landfills.